

FACILITY FORM 802

N66 31932

(ACCESSION NUMBER)

163

(PAGES)

CR-76471

(NASA CR OR TMX OR AD NUMBER)

(THRU)

1

(CODE)

03

(CATEGORY)

Designers and manufacturers of advanced control systems and components

WESTON HYDRAULICS LIMITED

SUBSIDIARY OF BORG-WARNER CORPORATION

GPO PRICE \$ _____

CFSTI PRICE(S) \$ _____

Hard copy (HC) 3-25

Microfiche (MF) 1.00

ff 653 July 65

fluid power
products

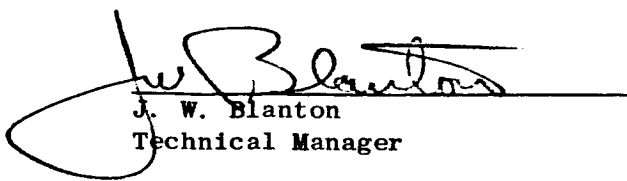


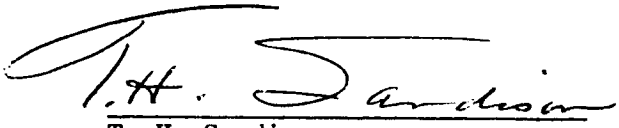
Weston Hydraulics Limited



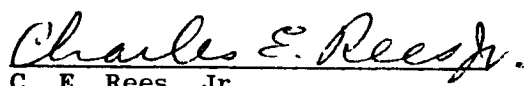
TECHNICAL SUMMARY REPORT
PNEUMATIC DIGITAL ACTUATOR
FOR
THRUST VECTOR CONTROL
PREPARED BY:
WESTON HYDRAULICS, LTD.
VAN NUYS, CALIFORNIA
SERVO CONTROLS GROUP
NASA CONTRACT NO. NAS 8-11388

PREPARED FOR
GEORGE C. MARSHALL
SPACE FLIGHT CENTER
HUNTSVILLE, ALABAMA


J. W. Blanton
Technical Manager


T. H. Sandison
Contract Administrator


E. J. Davidson
Program Manager


C. E. Rees, Jr.
Chief Engineer

October 25, 1965



TABLE OF CONTENTS

SECTION	
1.	SUMMARY AND CONCLUSIONS
2.	RECOMMENDATIONS
3.	INTRODUCTION - BACKGROUND
4.	CONCEPT
5.	ANALYSIS
6.	COMPONENT DESCRIPTION
7.	TEST RESULTS
8.	WEIGHT COMPARISON WITH ANALOG
9.	RELIABILITY COMPARISON WITH ANALOG, REDUNDANT
10.	PHOTOGRAPHS
 APPENDIX I	
PER CENT INPUT (OPEN LOOP) FOR VELOCITY SATURATION	
 APPENDIX II	
LOW PRESSURE INSTABILITY	

Weston Hydraulics Limited



FOREWORD

This final report describes the development study of a Pneumatic Digital Actuator for Thrust Vector Control (TVC) of a deep space vehicle. The included work was performed at Weston Hydraulics, Ltd., Van Nuys, California under the NASA Contract No. NAS 8-11388.

The program at Weston was managed by Mr. E. Davidson and Mr. J. Blanton. The person responsible for the concept and the analysis was Mr. K. Ramchandani. Mr. R. Barnes, Mr. G. Willis and Mr. G. Avisov contributed to the design of the hardware while Mr. R. Perry supervised the testing. The reliability comparisons were made by Mr. J. Cannon. The analog computer study was conducted at the Borg Warner Research Center in Des Plaines, Illinois.



1. SUMMARY AND CONCLUSION:

In general, the pneumatic digital actuation system, as conceived and designed by Weston Hydraulics under the subject contract, performed satisfactorily thus affirming the conclusions set forth in the analytical analysis. In spite of the originality and uniqueness of the design, no major modifications were necessary to obtain the degree of success achieved. The most noteworthy accomplishment being the stability of the pneumatic system, which was made possible by incorporation of a damping network referred to as "dynamic pressure feedback" (D.P.F.). The lack of a completely satisfactory digital command input source prevented operation under simulated actual flight modes but component testing and subsequent testing of the entire system assured its capabilities.

It should be noted that the subject actuation system was designed primarily as a test unit using a "bread board" approach. This was done to provide a means of being able to readily incorporate any necessary modifications without jeopardizing the entire project. Considerable weight and reliability improvements will be achieved in any flight destined design.

The scope of work, i.e. to determine analytically if a digital actuation system for T.V.C. is feasible, and then develop a prototype actuator to prove the theory, has been accomplished. In view of this, Weston is quite confident that it can produce highly reliable and capable pneumatic digital actuation systems for rocket engine gimbaling.



2. RECOMMENDATIONS:

- (i) Further investigation of stepper motors in search of a more powerful motor with small frame size.
- (ii) Commanding the adders directly from the encoder signal, without the use of pilot valves.
- (iii) Telemetering through long distance pulse techniques.
- (iv) Redundant nozzles and code pattern on both sides of the binary disk. In the event that one system fails, the other will still provide the signal. This will also yield better balance on the binary disk.
- (v) Actual testing with H_2 at cryogenic temperatures. This would require minor design modifications such as seals, pivots, material selection, etc. See Section 7.7 for correlation between various fluid media.



3.

INTRODUCTION:

This report describes the analysis and development of a digital-analog actuation system designed, fabricated and tested at Weston Hydraulics, Limited. The scope of work required construction of a digital actuation system to be used for engine gimbaling. The position servoactuator system would be required to control a resonant load typical of rocket engines exhibiting a natural frequency as low as 8 cycles per second. The attitude control requirements dictate the actuation system response capability to be of the order of 5 cycles per second. This high response requirement coupled with the low load resonance frequency presents serious stability problems for the closed loop actuation system. In the past, several hydraulic flight control equipment manufacturing companies have coped with this problem by devising frequency sensitive networks or by feedback of load acceleration or pressure to damp the engine vibrations. All of the past work on this problem has dealt with incompressible hydraulic systems.

In addition to the severe response requirements, Weston was asked to consider the operation of the system in extremely low temperature ambients. The low temperature of -260°F ruled out the possibility of any existing practical fluid. NASA further indicated that the fuel for the rocket would be liquid hydrogen and oxygen and that gaseous hydrogen will be available on board if suitable for the actuation system. Weston's task, therefore, was to build a digitally commanded actuation system using gaseous hydrogen as the working fluid. The operating pressure was selected to be approximately 1600 psi.

Weston's initial efforts were to establish basic system requirements inasmuch as the only specification requirement was the frequency response criteria. Also, one of the initial concerns was the definition of the digital inputs that the system would receive.



3. INTRODUCTION: (Continued)

Preliminary meetings with NASA indicated that during the development stage of the digital system, the nature of the inputs need not be defined. This was because electrical parallel to serial digital translation and visa versa is relatively simple and could be accomplished in the guidance computer with very little additional complexity. It was up to Weston, therefore, to select any digital command input that they wished in order to devise a system that would provide reliability, efficiency, good performance, and the economy of the fluid power. In October 1964, Weston generated a set of basic requirements and later confirmed these with NASA as being reasonable for the system.

One of the factors established during the early phases of the program was that a digital actuator by itself cannot be used to position the undamped resonant engine load. The nature of digital systems being on-off would generate step inputs which would cause the load to oscillate violently. It was therefore decided that the engine would be positioned by an analog servo. The inputs to the analog servo would be from some type of a digital actuator. It was also decided that it would be necessary to incorporate a frequency sensitive network in the analog servo which would prevent the oscillations of the engine when a rapid command was given to the system. The analog servo would also act as a mechanical filter for the digital actuator.

The program was initiated by an evaluation of the nature of the frequency sensitive network required to achieve the necessary system damping. In doing so, a linear servoanalysis of the analog servo (hereafter termed the power servo) was conducted. After considerable thought, a suitable network was devised. Weston then conceived a new concept for the digital actuator. This approach showed a great deal of promise in providing ultimate reliability, simplicity



3. INTRODUCTION: (Continued)

and ruggedness. There were certain phases of this concept which had to be experimented with and perfected before it could be finally used in the prototype system. An experimental model of this concept, the pneumatic encoder, was constructed. The results from this experimental model were successful and encouraged it being incorporated in the final system.

A computer study of the power servo was performed which included simulation of all of the non-linearities of the pneumatic servo-mechanism. This study was conducted at the Borg-Warner Research Center in Des Plaines, Illinois, on a space 150 amplifier computer. The results of the computer study very closely approximated that of the linear servoanalysis.

Finally, components to prove the theory and the concept were built. The Weston Digital Actuation System for TVC application consists of a stepper motor, a parallel binary encoder, pilot valves, a parallel binary digital actuator (adder piston version) and the power servo.

Early in 1965, Weston made two basic decisions which affected the technical direction of the study program. These decisions were based on rapid completion of the program with the funds allocated to finish the task:

1. A prime purpose of the contract, by Weston interpretation, is to determine if digitally commanded actuation systems can be used for TVC applications. The reliability and power economy are major considerations, while actual operation under cryogenic conditions is secondary. Therefore, Weston's objectives should include the generation of concepts capable of successful implementation at extremely low temperatures. The prototype components would not, however, be designed to operate at cryogenic temperatures, and cryogenic operation would not be considered as a necessary part of the test program. A consider-



3. INTRODUCTION: (Continued)

ation would be given in the design to the selection of functional components capable of adaptation to cryogenic operation.

2. The system generated by the study program is operated with a pneumatic fluid system because of the eventual application as a cryogenic system. However, the power fluid, gaseous H_2 at $-260^\circ F$, which is understood to be on-board working fluid, represents a substantial test and handling hazard. Weston, therefore, has sized the system to operate to the dynamic performance requirements specified by the contract using room temperature air as the working fluid. This has the primary advantage, from a test evaluation standpoint, of low cost and ready availability at the necessary upstream pressure 1600 psi at both Weston and NASA facilities. Correlation data between air and hydrogen performance will be provided, and the design modifications necessary to convert the system to gaseous hydrogen operation will be suggested. (See Section 7.7)



4. CONCEPT:

4.1 General:

Basically, the digital actuator is a device which accepts digital information and transforms this information to high powered displacement for moving a machine tool or an aircraft control surface or any other application requiring accurate position control. In other words, a digital actuator is a physical decoder of electrical digital signals. The digital signals may be of the following form:

1. Pulse amplitude modulation
2. Pulse sum modulation
3. Pulse width modulation
4. Pulse code modulation
5. Straight binary
6. Gray code

The first four signal types form digital serial information and type numbers five and six form parallel digital information. The last two are also known as the full binary word. A device like a stepper motor, which may be considered as a form of a digital actuator, accepts pulses and causes the rotor to take up discrete positions. For example, one pulse would make the rotor rotate through 15° , two pulses through 30° , three pulses through 45° , etc. Another form of the actuator can work from parallel binary signals. The adder piston type digital actuator consists of multiple series adding pistons, the strokes of which are arranged in binary increasing fashion. Each adder piston is either pressurized or vented depending on the direction of motion desired. The total output position obtained is the algebraic summation of the strokes of the individual adder pistons. The fluid flow to each adder piston is controlled by a separate valve. A bias force opposing the adders is provided by maintaining fluid supply pressure on the unbalanced area of the output piston rod to collapse the adders when so commanded. The bias force also serves to continuously



4. CONCEPT: (Continued)

4.1 General: (Continued)

maintain the entire stack of pistons against a ground reference point of the actuator. The total number of output positions achievable from such an actuator is 2^n where n is the number of inputs, the number of operating valves, and the number of adder pistons.

A principle for fluid digital actuators working from pulse or serial information has also been considered. The basic principle of the pulse sum information system is as follows: The system will meter discrete amounts of fluid to the actuator for each pulse received. It may be noted that the output accuracy of such a system is greatly dependent upon the extent to which leakage, slippage, and losses are minimized. Normal accuracy requirements would demand some form of loop closure, adding to the complexity of the system. The pulse width modulation system works on the principle that either an orifice (between pressure and load) is kept open for the duration of the pulse or a small piston is recycled continuously to force through slugs of oil for the duration of the pulse. In the former case, the operation suffers from nonrepeatability because of variations in fluid characteristics with temperature and usage effects; while in the second case the recycling capability within the valve not only adds to the design complexity but results in slow time response.

A quick review of the parallel and serial type of fluid digital actuators described above would indicate the following:

1. The adder piston type digital actuator is highly accurate. In fact, the positional accuracy is comparable to that of gage blocks. This type of actuator is not pressure sensitive because the piston motions are unrestricted until they hit



4. CONCEPT: (Continued)

4.1 General: (Continued)

stops or other adders. This type of actuator is also insensitive to contamination, temperature changes, fluid bulk modulus changes, and fluid viscosity changes. Since the actuator employs no feedback, there is no instability problem. The components used are quite simple and very rugged, hence the reliability is very high.

2. Disadvantages of the adder piston type digital actuator are that it requires multiple valves, and if these valves are energized electrically, it requires multiple solenoids and multiple solenoid drivers. The use of multiple wires running from the control computer or electronics to the actuator may not be a problem in machine tool controls; however, for an application such as rocket engine gimballing, these wires would be required to run the length of the vehicle and this length, coupled with a number of connections, would reduce the overall reliability of the system.
3. The system, which operates from serial information, either pulse sum or pulse width modulation would require only two wires. However, such a system is susceptible to pressure, temperature, and viscosity changes and therefore suffers from repeatability and accuracy considerations.

Weston selected the input to the power servo to be from a digital actuator of the adder pistons type. The reason for this decision was that only such a system would provide the desired accuracy and predictable performance in varying ambients.



4. CONCEPT: (Continued)

4.2 Encoder:

In the past, Weston and other companies have designed adder piston type digital actuators using solenoid valves to direct the fluid flow to individual adders. However, the objection of requiring multiple wiring, components, etc. for this particular application prompted Weston to think of a new approach which would eliminate such deficiencies. For the system to be digital and yet use only two or three wires, the input had to be some kind of serial digital information. Also, since the input was electrical, the best practical transition from electric to fluid power appeared to be a stepper motor. The missing link between incremental motions and binary intelligence was an encoder.

Shaft angle encoders, used extensively in digital electrical servos to transform the shaft position to electrical binary signals, offered an acceptable solution. A stepper motor could drive some form of a coded disk and if the output of the disk could be a pressure signal which could actuate the adders either directly or through small pilot valves, the system would be complete. The first approach was to build a disk which would contain a coded pattern consisting of raised areas and recessed areas in an arrangement to generate binary intelligence. The information would be transmitted in the following form. A set of nozzles would face the disk. Depending on the position of the disk, these nozzles would either face a raised area or a recessed area. These nozzles would be fed from a high pressure air supply through a primary orifice. If the nozzle is positioned with a raised surface and the clearance between the nozzle and the surface is small, then the pressure within the nozzle chamber would be approximately the supply pressure because there is reduced flow through the nozzle. When the nozzle faces a recessed area, there is an increased flow because of reduction of the resistance and the pressure inside the nozzle chamber would drop to a lower value.



4. CONCEPT: (Continued)

4.2 Encoder: (Continued)

This change in pressure could be used as a signal to actuate a small valve which in turn would direct the flow into the adders or the nozzle pressure signal itself could be used to fill or vent the adder.

After considerable evaluation, it was decided to configure the encoder in the following manner: (See Figure 4.2.1)

1. Reduce the output travel of the stepper motor (15° per pulse) by gearing down its output to obtain rotation of the binary disk corresponding to 10° per pulse. The binary code would be on the driven gear.
2. Incorporate raised or recessed area patterns at different radii from the center of the binary disk. A different bit channel of the binary code would be located at each radii.
3. Install a set of stationary nozzles on a flat plate facing the coded pattern of the binary disk. These nozzles would be on corresponding radii to the various channels on the binary disk. The number of bit channels is limited only by the physical size of the disk and nozzles and manufacturing techniques necessary to produce them.
4. In order to insure a balance of pressure on the binary disk, it would contain the pattern and the nozzles on both faces.
5. The binary disk would be supported on a spherical bearing so that it could be self-aligning. Air bearing pads would be provided in the two stationary plates so that the binary disk would float parallel to the stationary plates.



4. CONCEPT: (Continued)

4.2 Encoder: (Continued)

6. Both the binary disk and the stationary plates would be well polished. The clearance between the disc and the flat plates would be maintained as small as practical. (Approximately .0005 per side)

Based on the above basic decisions, it was decided to build an experimental model of the encoder to determine the pressure changes as the nozzle faced a raised or recessed area, the load on the stepper motor, the response rate, etc. First of all it was necessary to determine if a stepper motor was available to meet the response rates required for the application. Since the encoder and the digital actuator would drive the power servo, it was necessary that the response rate of the encoder and the digital actuator should be 4 to 5 times faster than the power servo. Assuming that at least a 2 or 3 pulse input would correspond to the desired output motion for frequency response tests, since the system time constant is specified as approximately 100 milliseconds, the motor should go through 2 or 3 increments in a period of 1/10 of 100 milliseconds. The motor requirement of 3 increments in 10 milliseconds corresponds to a motor capable of running at approximately 300 pulses a second. A search for such a motor determined that stepper motors in excess of 500 pulses per second were available. The torque capability of such motors ranged from 1 to 5 oz.-inches. Initially, it was assumed that the pressure forces on the flat surfaces of the binary disk would reflect negligible torque to the stepper motor. The only torque imposed on the motor would be its own inertial torque and the reflected inertial torque of the binary disk. Preliminary analysis showed that the total gear inertial load at the response rates under consideration would be approximately 1 oz.-inch. The stepper motor was a variable reluctance--3 phase motor with a standard step angle of 15°. The motor was capable of providing 1.5 oz.-inch of torque at response rates in excess of 400 pulses



4. CONCEPT: (Continued)

4.2 Encoder: (Continued)

per second. The input power required for the motor is 10 watts. With the potential cryogenic application for the system, Weston consulted IMC Magnetics regarding the low temperature operation of the stepper motor. At this request, IMC Magnetics immersed the stepper motor under question in liquid nitrogen and tested same. The results were very encouraging, i.e. the motor responded at the peak pulse rate satisfactorily.

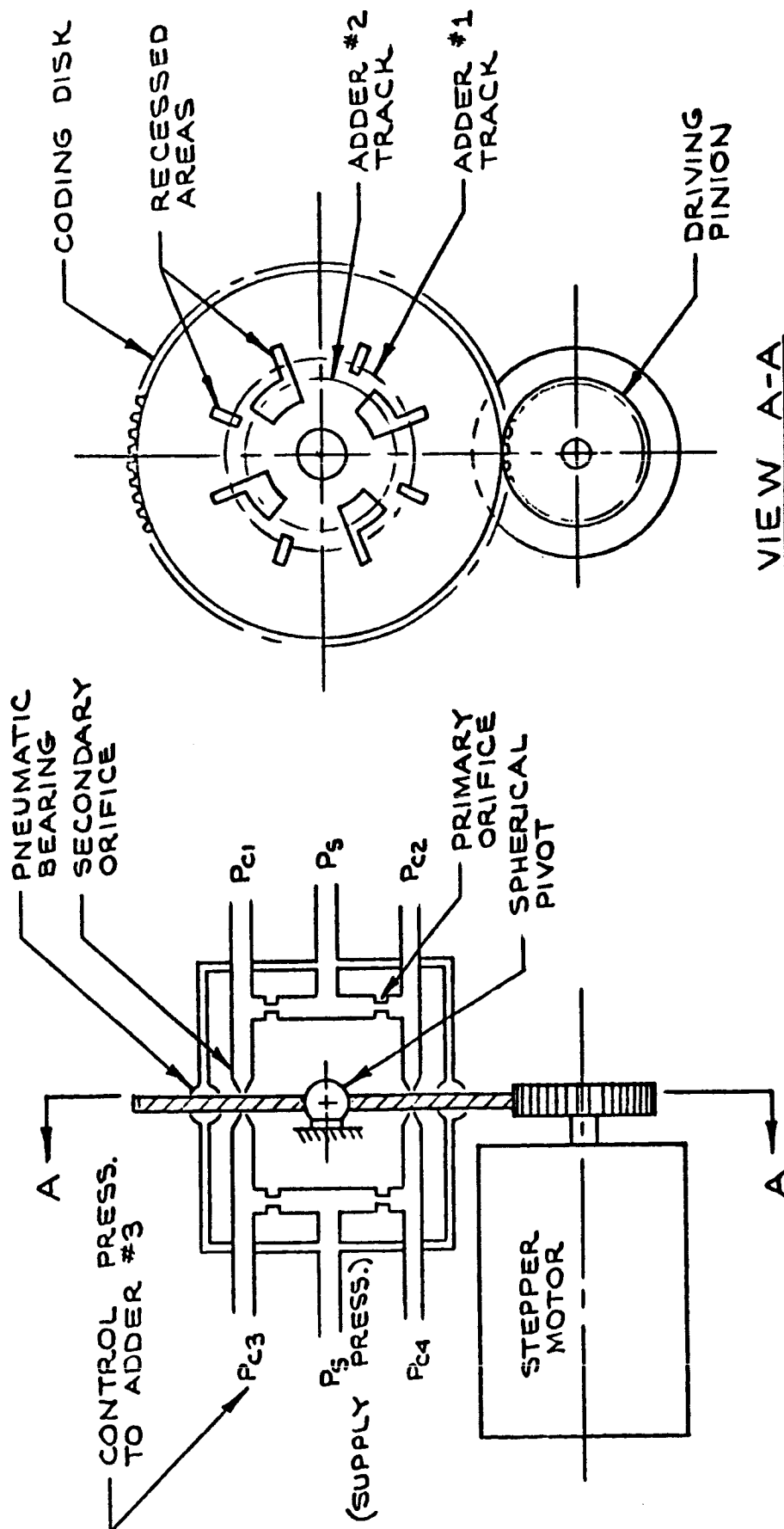
An experimental model of the encoder was built in early 1965 to determine the few unknowns. Test results on the encoder were encouraging. The overall response from the moment of the application of pulse to the pressure change in the output lines was in the order of 4 or 5 milliseconds. This included the time constant of the stepper motor and the pressure build up time constant in the lines. One of the problems experienced in testing was that the flow forces, in spite of appearing on the flat faces of the binary disc and being fairly well balanced on the two sides, were significant enough to load the stepper motor. Originally, it was planned to feed the encoder with common system supply pressure of 1600 psi. However, investigations showed that the stepper motor stalled or did not provide enough response in excess of 800 psi. It was, therefore, decided to feed the encoder with approximately 650 psi supply pressure. By varying the primary orifice and the nozzle orifice, the pressure change in the output lines was observed to be as much as 500 psi. The pressure rise and the fall time also was a function of the primary and nozzle orifices. Optimum orifice sizes were established which provided the pressure signal of approximately 1/2 the supply pressure and symmetrical rise and fall time constants.



4. CONCEPT: (Continued)

4.2 Encoder: (Continued)

Figure 4.2.1 shows the schematic of the encoder. The experimental encoder contained 4 orifices, 2 on each side of the encoder disk. There were four air bearing pads on each side of the disk. The total air flow through the encoder at 600 psi was approximately .038 pounds per second (30 SCFM). Figure 4.2.2 shows the torque on the stepper motor with different supply pressures. Figure 4.2.3 shows pressure response curves with the optimum primary and nozzle orifices.



SKETCH OF PNEUMATIC ENCODER

FIG. 4.2.1

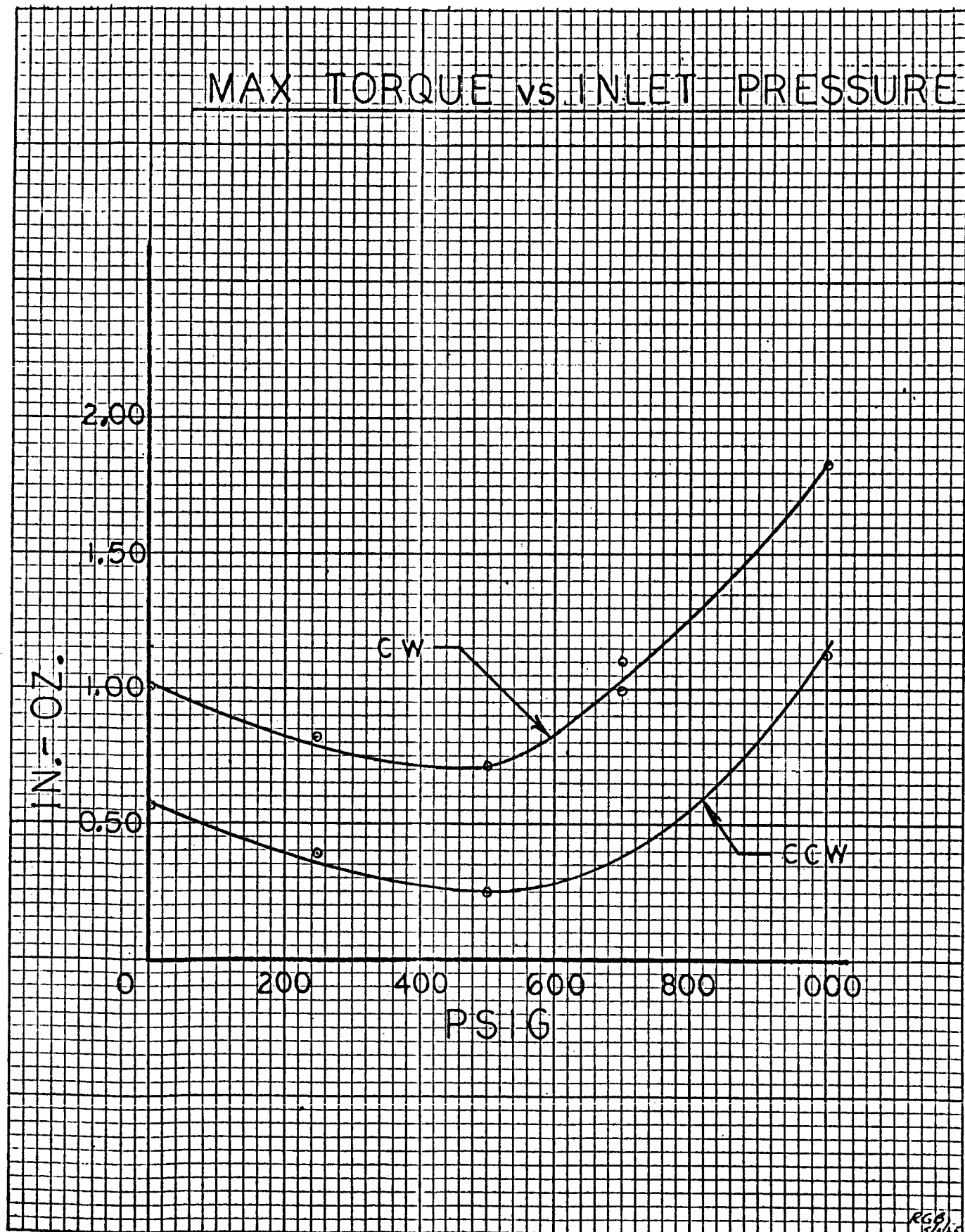
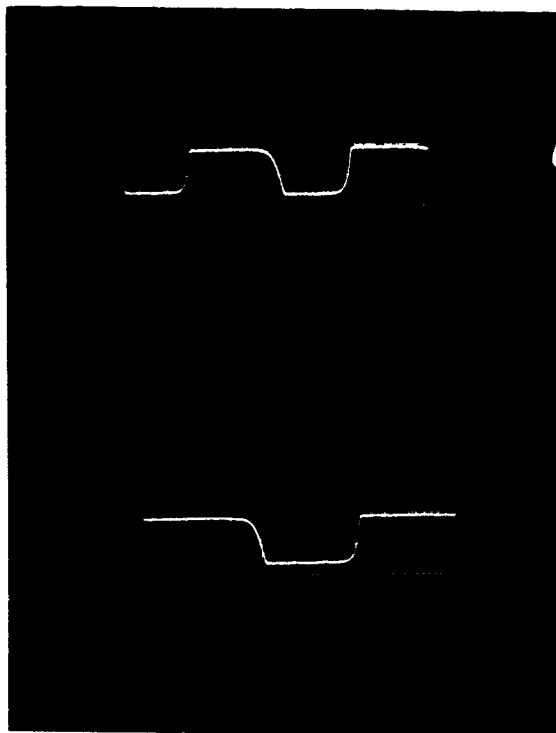


FIG. 4.2.2

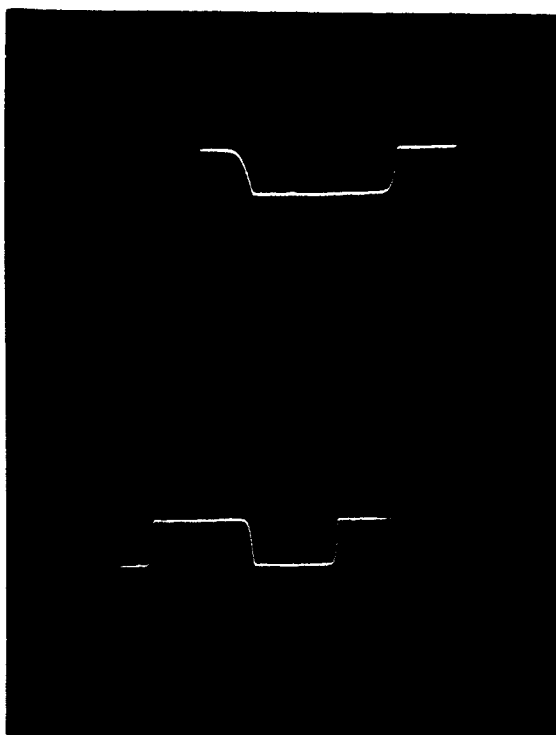


B 20 MILLISEC/CM.
300 PPS

PHOTO 103
ADDER No. 3

A 20 MILLISEC/CM.
200 PPS

S W E E P



B 20 MILLISEC/CM
300 PPS

PHOTO 104
ADDER No. 4

A 50 MILLISEC/CM
200 PPS

FIG. 4.2.3



4. CONCEPT: (Continued)

4.3 Parallel Binary Digital Actuator (P.B.D.A.):

The operation of the parallel binary digital actuator was briefly described in the Section 4.1. Figure 4.3.1 shows the straight binary code. Figure 4.3.2 shows a 7 bit digital actuator. From the figure it will be observed that the first piston is denoted as the one bit piston, the stroke of which is one unit. The next piston has a stroke of 2 units and the third piston has a stroke of 4 units. This particular actuator includes solenoid valves which pressurize or vent the adders. The total output stroke is the algebraic sum of the adder piston strokes. In Figure 4.3.3 pistons number 1 and 2 are extended giving a total output stroke of 3 units. It may be noted that the figures show an actuator which is only one sided; in other words, the output moves in only one direction. The actuator could be made to swing in plus or minus direction about neutral by using the complementary binary code. This function could be achieved by pressurizing the largest adder piston would have a valve which is normally open. The other adder pistons would have valves which are normally closed.

Inspection of the binary code shows that for ramp inputs the one bit piston shuttles back and forth for every decimal integer increase. The two bit piston shuttles for every two integer increase and so on. The pattern of the binary code indicates that if the input to a digital actuator is a slow ramp or a slow sinusoidal wave such that the actuator is made to go through each decimal integer, then the shuttling of the pistons back and forth to give the net desired position would demand more fluid power than a single piston to move up to the command position. The larger flow demand is further increased if a complementary binary code is used. Observation of the complementary binary code in Figure 4.3.1 shows that in going from +1 decimal



4. CONCEPT: (Continued)

4.3 Parallel Binary Digital Actuator (P.B.D.A.) (Continued)

value to -1 decimal value through zero, the largest four bit adder piston collapses while the two smaller pistons extend. Thus, for small increments around null, in particular, increments of the value of plus or minus one cause all the adder pistons to change their state demanding a large amount of fluid power.

NASA's prime consideration of this system is that it should demand the least possible operating power, and practically zero coasting power. A code such as complementary binary, therefore, appears very uneconomical. Weston, therefore, decided to build an actuator which essentially consisted of two adder stacks for plus or minus directions. This approach would result in a larger number of adders than if the complementary binary code be employed. However, the power saving advantage is greater hence this approach was selected. The two adder stacks would be housed in one bore. The overall length would be slightly larger than if the complementary binary code were used. For example, a 32 bit digital actuation function could be accomplished with 5 adder pistons having strokes of 1, 2, 4, 8, 16 units. The straight binary code for plus minus direction approach would require 8 adders, 4 for each direction having strokes of 1, 2, 4, and 16 units. It may be noted that in this approach the zero is common, hence the actuator could take 15 positions in the positive and 15 positions in the negative direction. Therefore, the actuator could take up a total of 31 positions.

The Figure 4.3.4 shows the code selected for the prototype digital actuator. The adder ports and the adders are identified as A, B, C, D, E, F, G, H. Adders A and B are one unit adders, C and D are two unit adders, E and F are four unit adders, with G and H being 8 unit adders. Because the encoder signal is fed to the adders through pilot valves, i.e. each pilot valve either



4. CONCEPT: (Continued)

4.3 Parallel Binary Digital Actuator (P.B.D.A.): (Continued)

pressurizes or vents its corresponding adder, these valves could be normally open or normally closed valves. Figure 4.3.5 and Figure 4.3.6 show the operation of the encoder signal with the normally closed and normally opened valves and their corresponding adders. For reasons to be explained later, pilot valves A, C, E, and G are normally closed valves while pilot valves B, D, F and H are normally opened valves. When the encoder is in zero position, i.e. all the nozzles are across a raised area, the control pressure to all the pilot valves is approximately equal to supply pressure to the encoder (650 psi). With the application of this high signal pressure to the normally closed pilot valves, they open. Therefore, adders A, C, E, and G are pressurized with pilot valve supply pressure (1600 psi), and they extend. The situation is reversed for adders B, D, F and H. As a result of the application of the high control pressure from the encoder to their corresponding normally open pilot valves, they are collapsed. The reason for going to normally closed and normally opened valves now becomes apparent. If the supply pressure to the encoder is lost for some reason, the pilot valves would assume their normal mode. This would generate a command to the adders identical to that at encoder zero position except that it is opposite. That is, under pressurized zero position, the adders that would extend would now retract and the adders that would retract under power conditions would extend under no power conditions. In this loss of encoder pressure condition, the actuator would return to neutral, regardless of the code disk position.

Referring to the top row in Figure 4.3.4, which states the number of adders commanded, it may be noted that to move from neutral position to +1 position to +2 position requires only two adders to change their state. Moving from +2 to +3 requires

CODE COMPARISON

STRAIGHT
BINARY CODE

COMPLEMENTARY
BINARY CODE

DEC.	4 BITS = 2 ²	2 BITS = 2 ¹	1 BIT = 2 ⁰
0	0	0	0
1	0	0	1
2	0	1	0
3	0	1	1
4	1	0	0
5	1	0	1
6	1	1	0
7	1	1	1

DEC.	4 BITS = 2 ²	2 BITS = 2 ¹	1 BIT = 2 ⁰
-4	0	0	0
-3	0	0	1
-2	0	1	0
-1	0	1	1
0	1	0	0
+1	1	0	1
+2	1	1	0
+3	1	1	1

0 = RETRACTED
1 = EXTENDED

FIG. 4.3.1

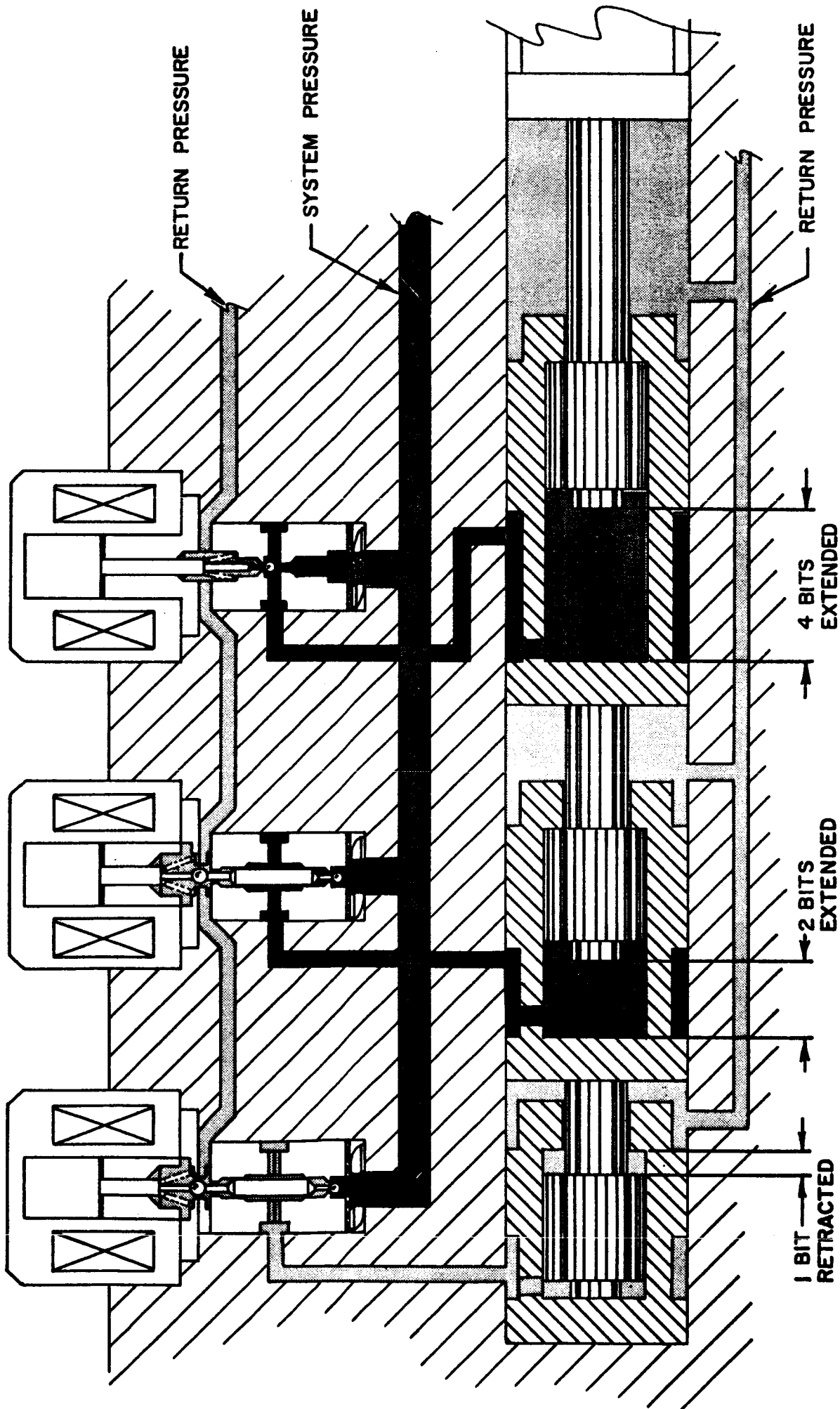


FIG. 4.3.2

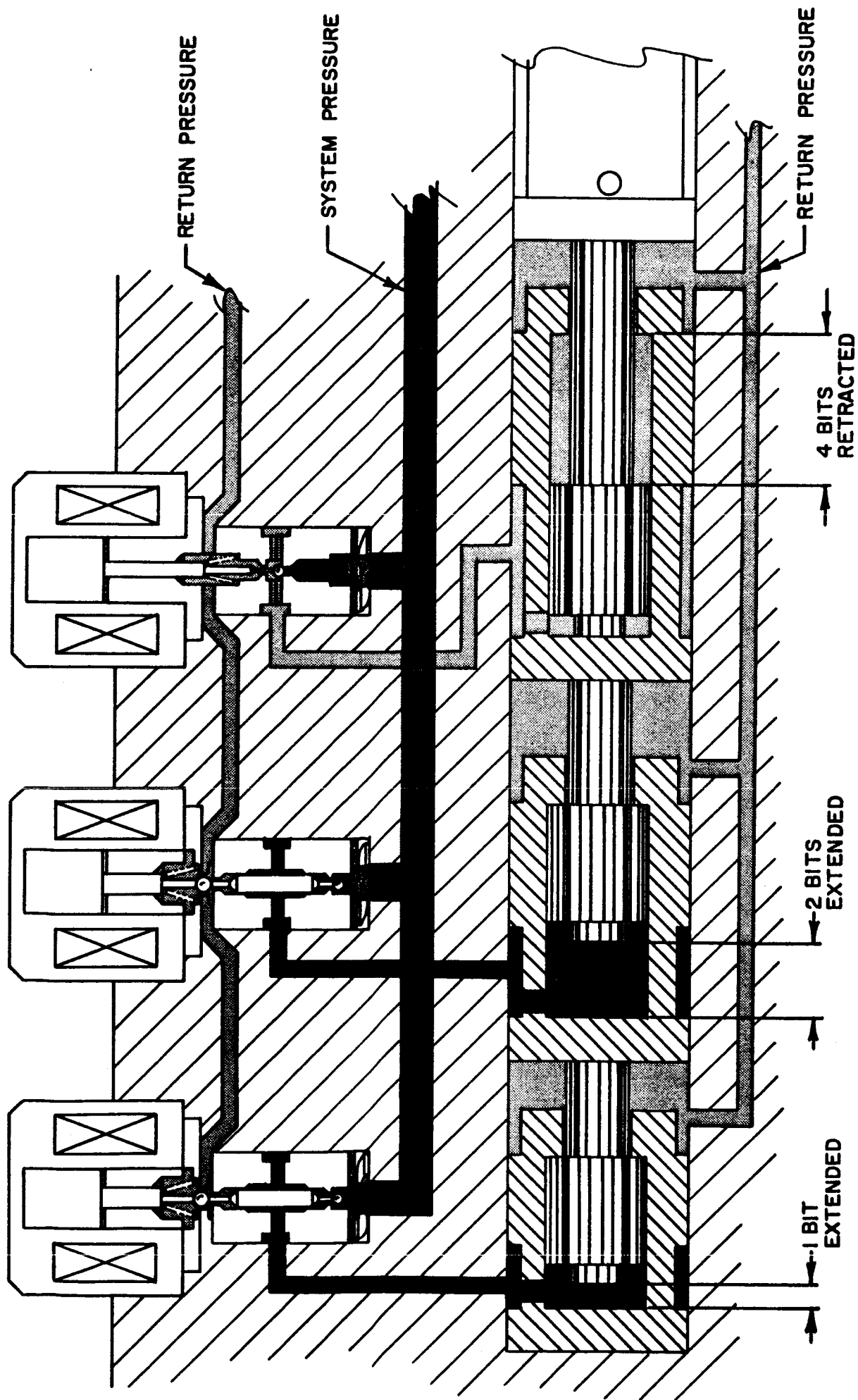


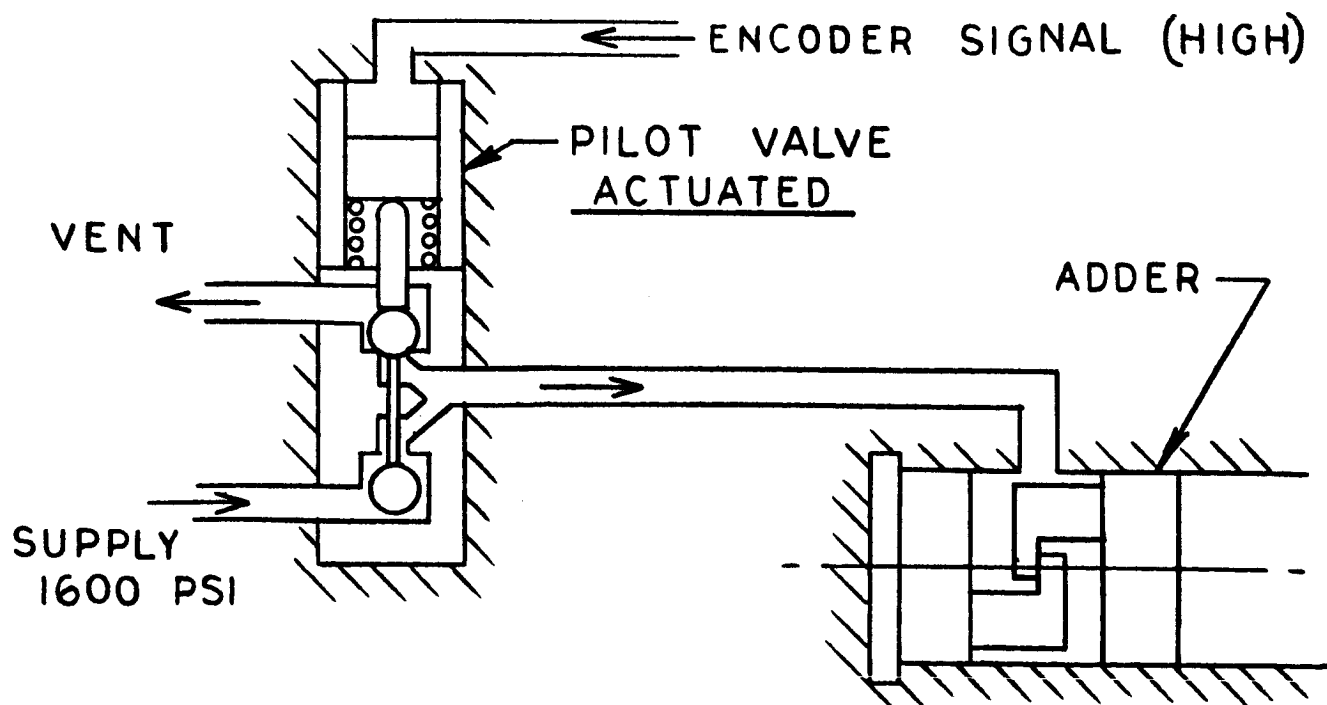
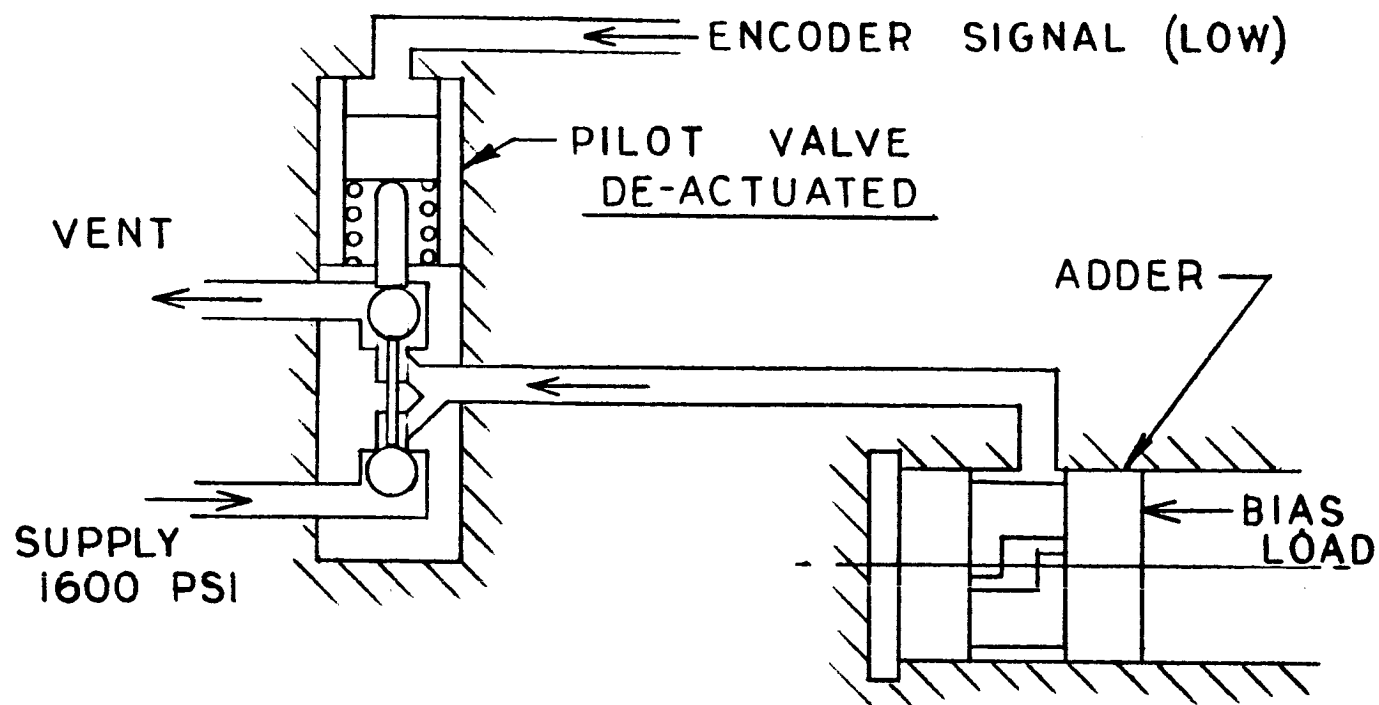
FIG. 4.3.3

[illegible]

LEGEND:

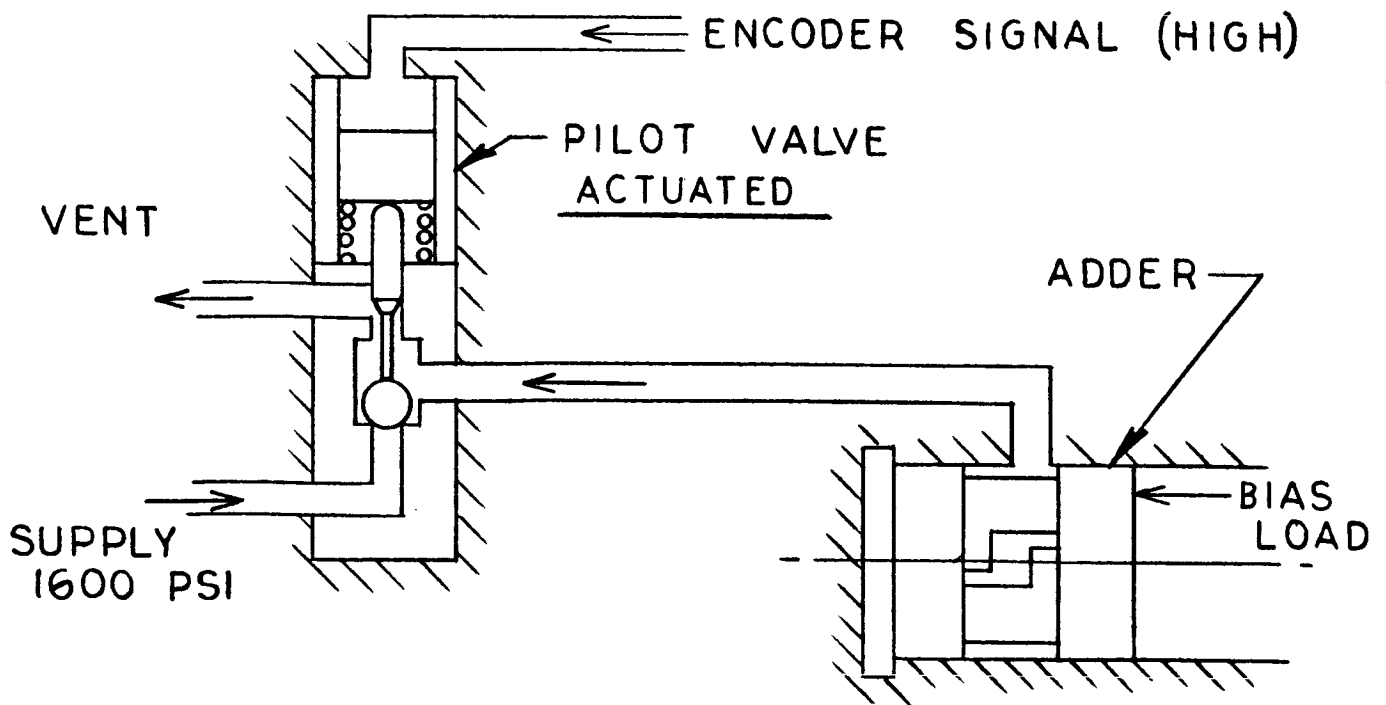
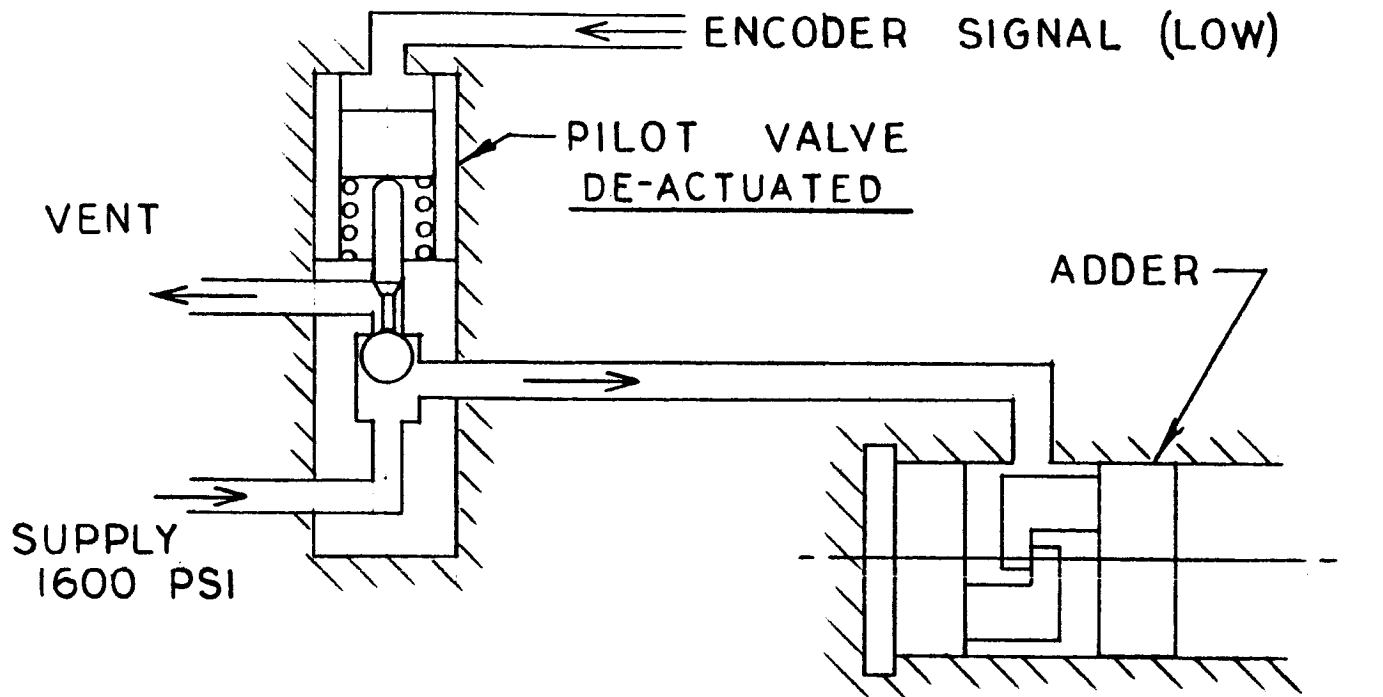
☐ ADDER DE-PRESSURIZED

ADDER PRESSURIZED



PILOT VALVE - NORMALLY CLOSED

FIG. 4.3.5



PILOT VALVE - NORMALLY OPEN

FIG. 4.3.6.



4. CONCEPT: (Continued)

4.3 Parallel Binary Digital Actuator (P.B.D.A.): (Continued)

only one adder change. The advantage of this code then becomes obvious. Up to the seventh position, the maximum number of adders commanded at any one time is three. This occurs while moving from the +3 position to the +4 position. Retrograde, an inherent problem in digital actuators, has been reduced to a minimum.

Since TVC is most used around neutral position, normally 10% to 15% of the maximum input, the two sided straight binary code approach offers a considerable saving of fluid power. It was stated above that whether the encoder supply pressure is on or off, the adder stack still would retain neutral position. The switch over from one condition to the other merely requires the collapsed adders to extend, and the extended adders to collapse. This function is automatically accomplished because of the phasing of the pilot valves. This then satisfies one of the prime requirements of the contract, namely, that the entire system will not demand any fluid power during coasting. During idle periods, the supply pressure to the encoder could be shut off by means of a separate solenoid valve with the TVC retaining neutral position. The pilot valves and the adders would still be pressurized; therefore, there would be a pneumatic force holding the adder stack, but the system as such will not demand any fluid power, except for slight leakage.

4.4 Power Servo:

The power servo is a conventional mechanical feedback servo-mechanism. The input to the power servo is from the motion of the adder stack. The summing link connects the adder stack input, the main ram output, and the summing point. The input to the control valve spool from the summing point is through a bungee (which is a missing link and can pick up the over travel of the summing point beyond the point when the spool hits the stops).



4. CONCEPT: (Continued)

4.4 Power Servo: (Continued)

The system employs a dynamic pressure feedback network. This network is incorporated to damp the open loop natural frequency comprising of the structure, the load and the pneumatic spring in the actuator. Because the load is practically undamped, artificial damping has to be introduced to achieve stability. The operation of the dynamic pressure feedback network is similar to the D.P.F. servovalve. Basically, it feeds the derivative of load pressure back to the control valve. This feedback enables the servo to be softer or less stiff at high frequencies, but retain full stiffness at steady state or low frequencies. The D.P.F. network consists of two spring centered pistons, one of which having an orifice across it. The network is connected across the cylinder lines. The motion of the piston containing the orifice is fed back to the control valve as shown schematically in Figure 4.4.1.



FIG. 4.4.1

Weston Hydraulics Limited



5. SYSTEM ANALYSIS:

5.1 Problem Statement and General Requirements:

5.1.1 Basic:

Design a Digital Actuation System

- (i) Output Stroke = ± 1.5 In.
- (ii) Frequency Response and Transient Response as shown in Figures 5.1.2 and 5.1.3.

5.1.2 Additional Information:

5.1.2.1 Load:

The actuator is to drive a resonant load consisting of

M_E = Equivalent Mass referred to the actuator

$$= 3.337 \frac{\text{in.} \cdot \text{lb.}}{\text{sec}^2}$$

$$K_E = \text{Load Spring} = 40,000 \frac{\text{lbs}}{\text{in.}}$$

5.1.2.2 Structure Compliance:

The equivalent spring rate of the structure (supporting the actuator) along the actuation axis is given by

$$K_S = \text{Structure Spring} = 10,418 \frac{\text{lbs}}{\text{in.}}$$

5.1.2.3 Supply:

The actuation system would eventually be operated with gaseous hydrogen at 1600 psi and -260°F .

For demonstration of feasibility, air at 1600 psi and room temperature is substituted as the working fluid.

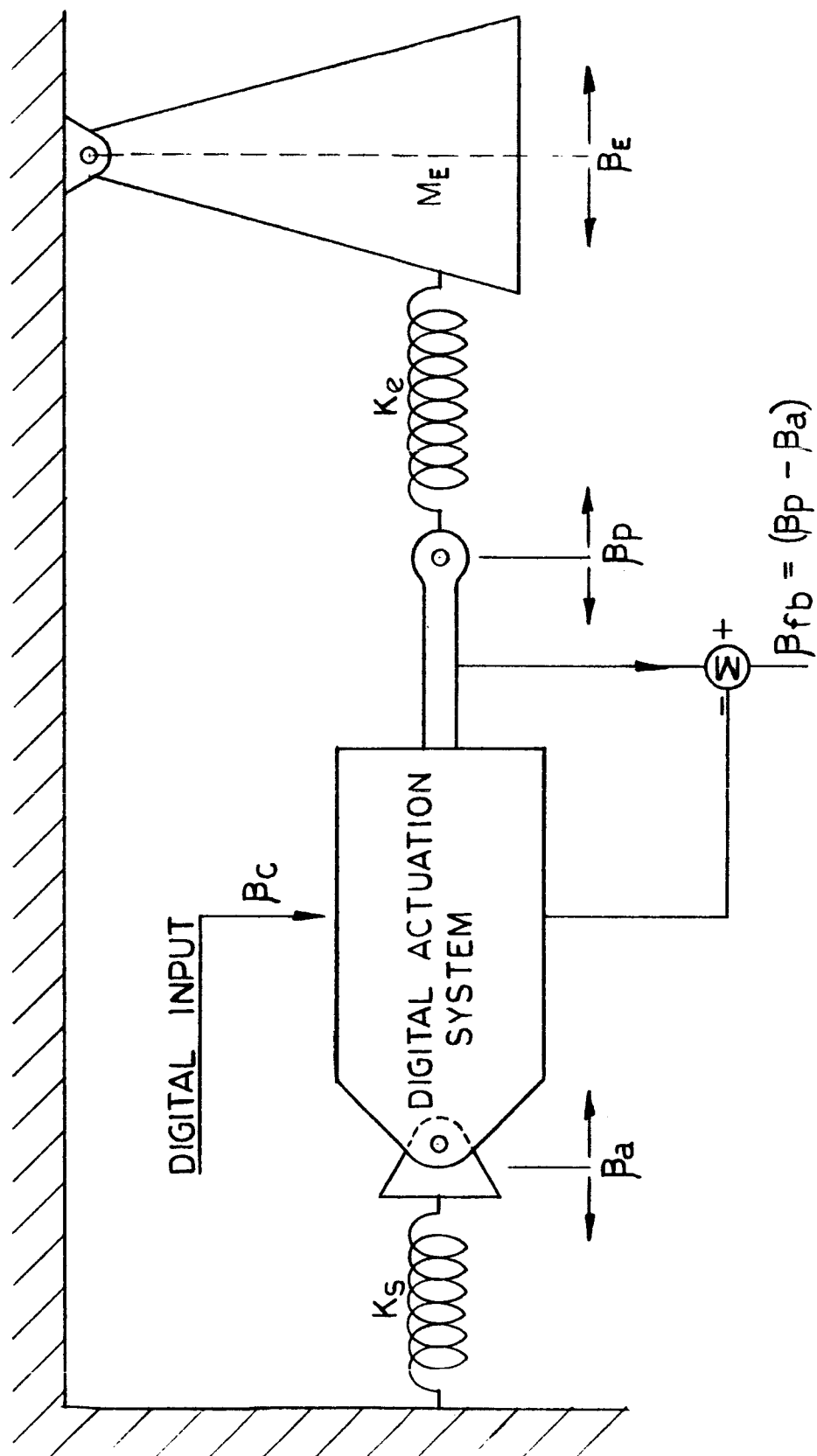
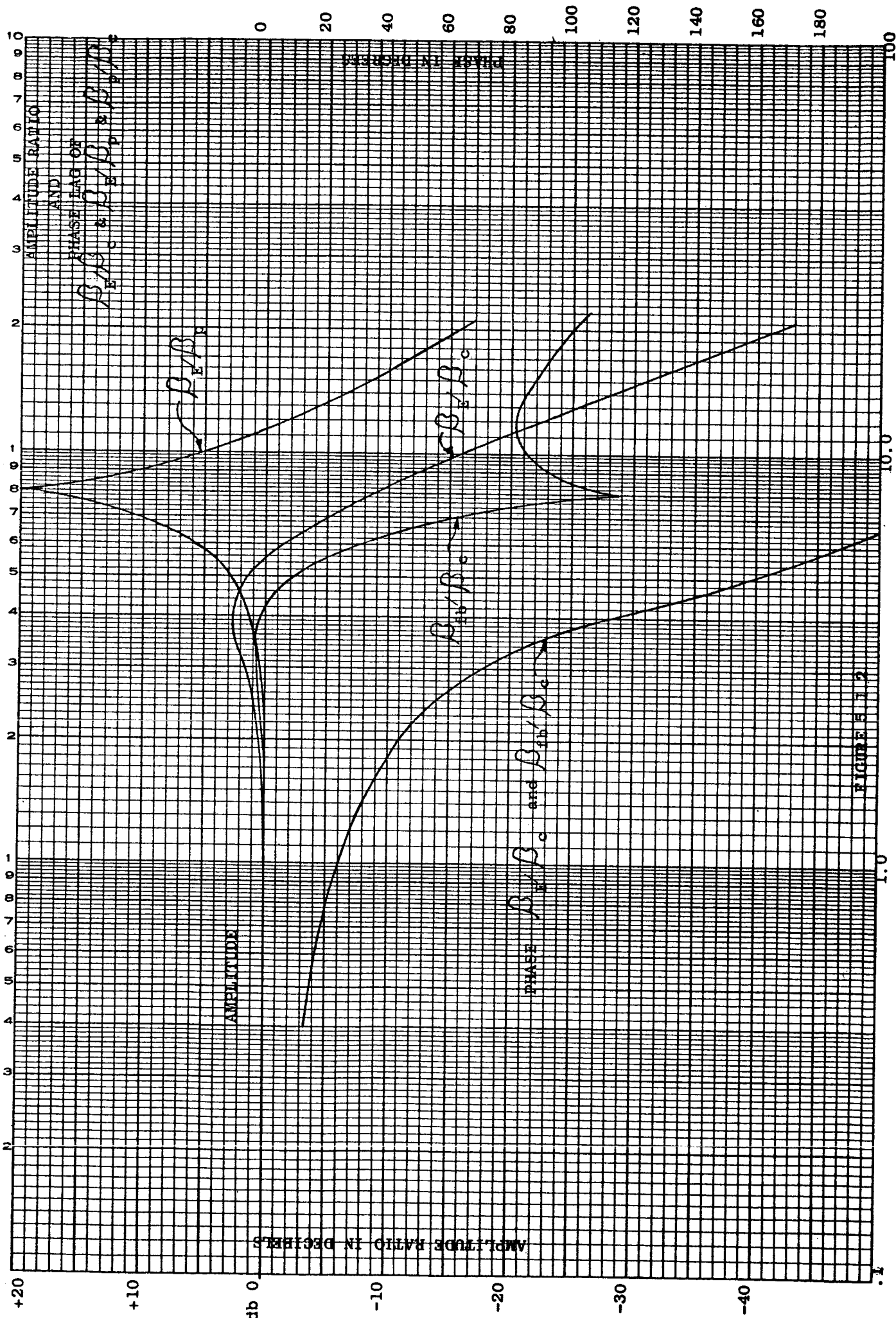


FIG. 5.11.



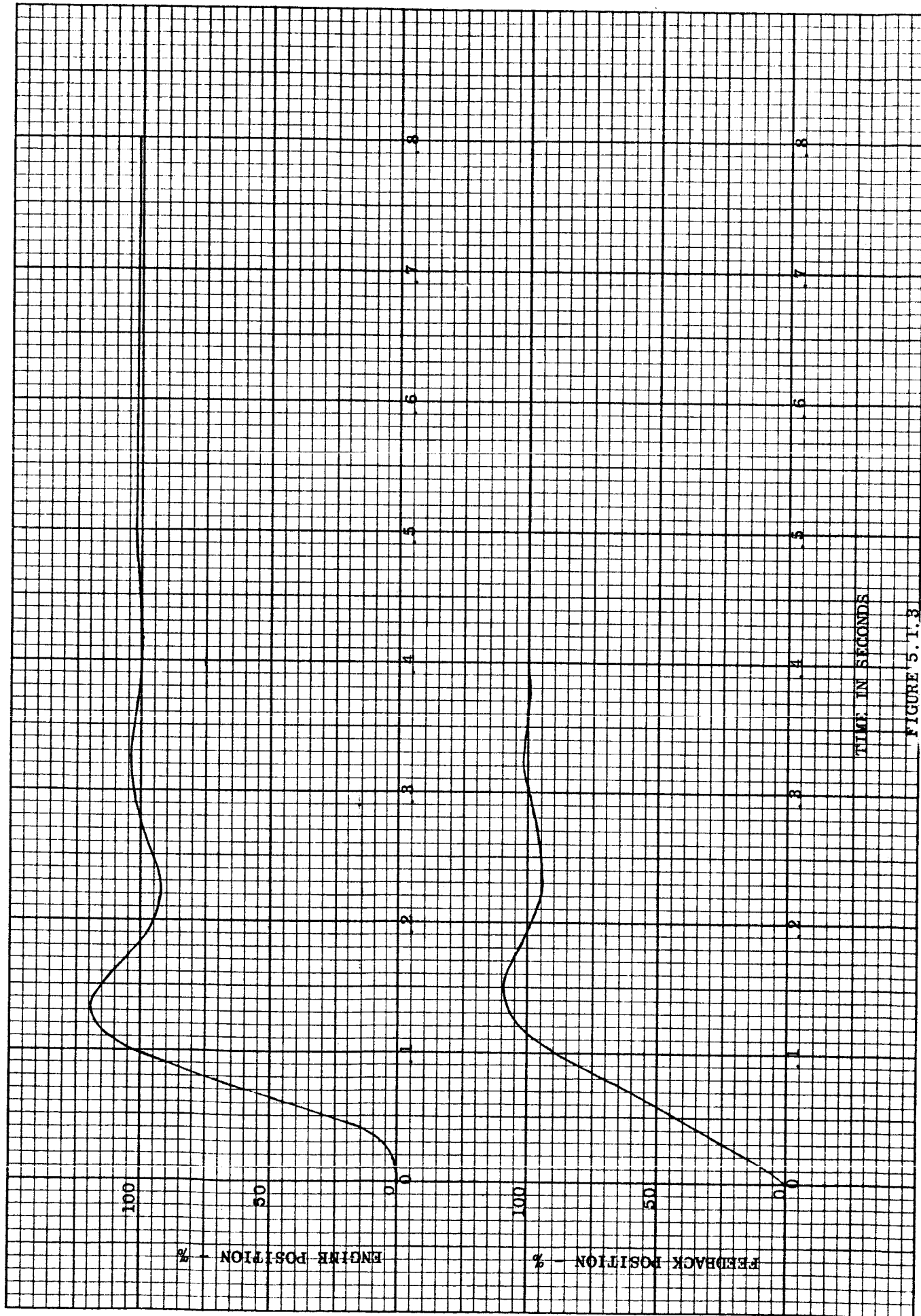


FIGURE 5.1.3



5. SYSTEM ANALYSIS: (Continued)

5.2 Other Specification:

5.2.1 System Components:

The Digital Actuation System is described in Section 4. It consists of following subsystems.

- a) Function Generator
- b) A/D Converter
- c) Controller
- d) Stepper Motor
- e) Gear
- f) Encoder
- g) Lines and Pilot Valve
- h) Parallel Binary Digital Actuator
- i) Power Servo
- j) Instrument Servo (Mechanical Oscillator)

In order to make a complete system, the subsystems were assigned definite specifications. These specifications were considered as design goals. Enough leeway was provided to account for unpredictable behavior.

5.2.2 Subsystems Specifications:

The general philosophies in setting up the subsystem specification were

- (i) The power servo would be designed to meet the frequency response specified by NASA.
- (ii) The encoder and the digital actuator would have to be 3-4 times faster response than the power servo so that at low frequencies the over all response would be that of the power servo.

Weston Hydraulics Limited



5. SYSTEM ANALYSIS: (Continued)

5.2 Other Specification: (Continued)

5.2.2 Subsystems Specifications: (Continued)

5.2.2.1 Signal Generator: (Signal Source)

A standard low frequency signal generator. (Such as Hewlett Packard 202 A)

Frequency Range: 0.008 - 1200 cps

Output Waveforms: Sinusoidal, Square, and Triangular

Output Voltage: 30 V p - p Across 4000 Ω load

Output Impedance: 40 Ω

Power: 115 V, 150 Watts

5.2.2.2 Analog to Digital Converter:

The function of the A/D converter is to convert analog inputs into pulse output. The output pulses should be available on two wires, one controlling the clockwise rotation of the stepper motor and the other controlling the counter-clock-wise rotation. Figure 5.2.1 shows the input-output characteristics.

Input	20 V p - p
Frequency	0 - 100 cps
Source Impedance	40 Ω
Desired Input Impedance	Greater Than 4 K Ω
Output Pulse (Minimum)	+10 V, 1 μ sec. wide
Load Impedance	2000 Ω
Desired Output Impedance	Less than 2000 Ω
Maximum Output	15 C.W/Pulses 15 C.C.W/Pulses 30 Total Maximum
Scale Factor	15 Pulses/10 Volts
Maximum Output	
Pulse Rate	5000 pps
Time Lag (Input-Output)	Less than 200 μ sec.

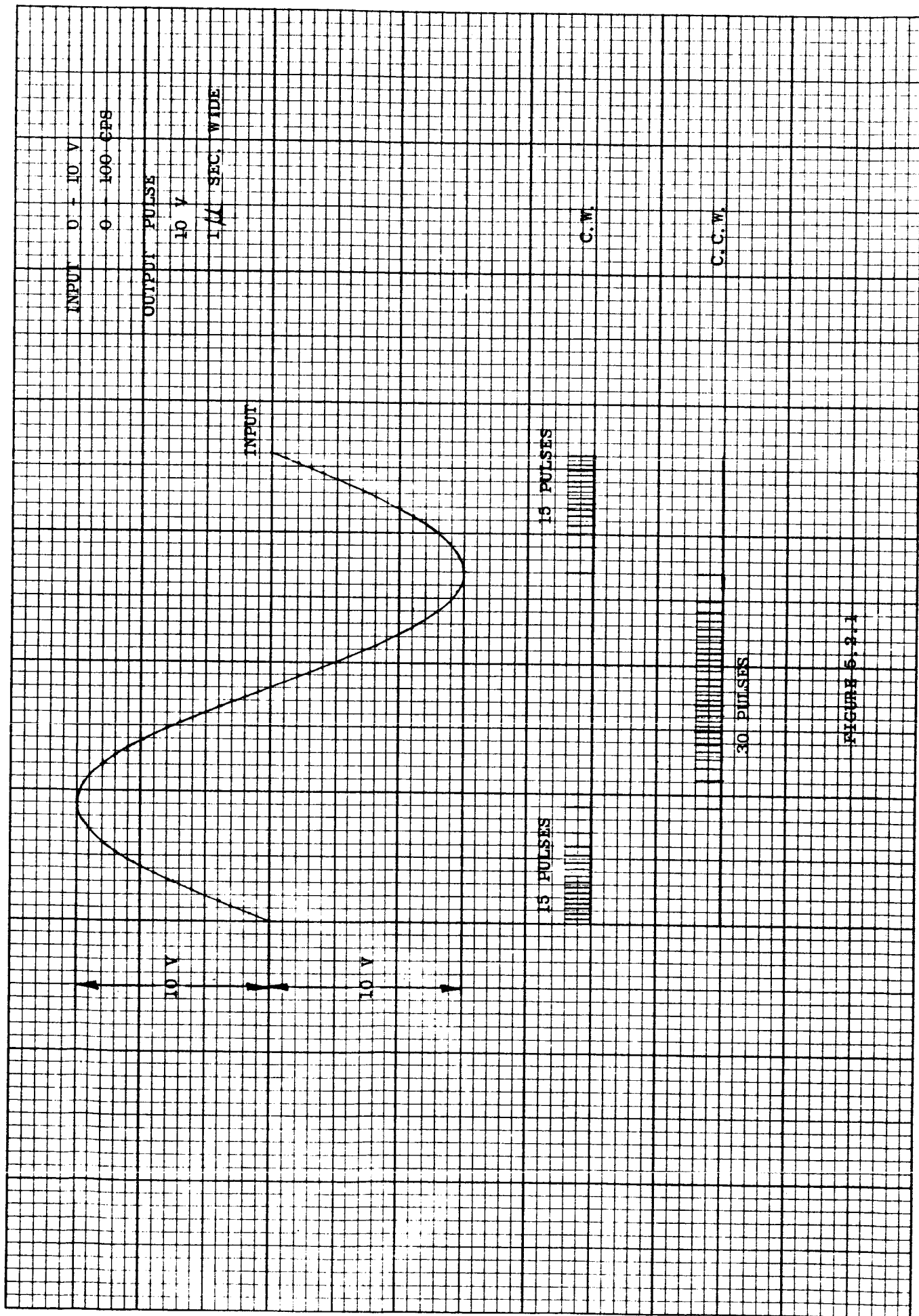


FIGURE 5-2-1

Weston Hydraulics Limited



5. SYSTEM ANALYSIS: (Continued)

5.2 Other Specification: (Continued)

5.2.2 Subsystems Specifications: (Continued)

5.2.2.3 Controller:

The function of the stepper motor controller is similar to that of a servoamplifier in an analog system.

In the stepper servo, the controller sequentially energizes the windings of the stepper motor in response to input command pulse. The controller herein specified is capable of driving the stepper motor of Section 5.2.2.4.

Input

Pulses	10 V (Min.) 1 μ sec. (Min.) wide
Source Impedance	200 Ω
Supply	28 V D.C.
Output	28 V D.C. @ .7 Amp. Max. Into Motor Windings
Motor Winding Load	75 - 80 Ω

5.2.2.4 Stepper Motor:

The stepper motor should be as fast as possible with a running torque capability of approximately 2 oz.-inch. The motor should exhibit no resonance throughout the pulse range.

Type	Variable Reluctance
Phases	Three (3)
Response	0 - 600 Pulses Per Second
Stall Torque	3 oz.-inch (Min.)
Step Angle	15°

Weston Hydraulics Limited



5. SYSTEM ANALYSIS: (Continued)

5.2 Other Specification: (Continued)

5.2.2 Subsystems Specifications: (Continued)

5.2.2.5 Gear:

$$\text{Ratio } \frac{\text{Output}}{\text{Input}} = \frac{10^\circ}{15^\circ} = \frac{2}{3}$$

5.2.2.6 Parallel Binary Encoder (P.B.E.):

The encoder is a physical "Incremental Position to Binary Pressure Output Converter".

Positions	Total 31 including one zero position
Step Angle	10°
Supply Pressure	700 psi
Output Pressure	1/2 Supply Pressure
Change-Signal	
Running Torque	Less than 2 oz.-inch
Output code	Binary
Time Response	1 millisecond

5.2.2.7 Parallel Binary Digital Actuator (P.B.D.A.):

Stroke	± 0.5 inch
Resolution	$\frac{1}{31}$
Number of Adders	8
Travel Per Bit Move	0.0323 inch
Supply Pressure	1600 psi
Output Force	50 pounds
Response/Bit Move	1 - 2 milliseconds

Weston Hydraulics Limited



5. SYSTEM ANALYSIS: (Continued)

5.2 Other Specification: (Continued)

5.2.2 Subsystems Specifications: (Continued)

5.2.2.8 Power Servo:

The power servo should provide the response defined in Figure 5.1.2 and 5.1.3.

Input Stroke	± 0.5 from P.B.D.A.
Output Stroke	± 1.5 inch
Supply Pressure	1600 psi - Air At Room Temp.
Control Valve Stroke	± 0.1 inch

5.2.2.9 Instrument Servo (Mechanical Oscillator):

The analog to digital converter, specified in Section 5.2.2.2 is specialized electronic equipment. Weston's efforts to obtain this equipment would have required an unduly large expenditure and development effort.

Since the digital actuator in reality would receive digital inputs (pulses) and the need for Analog to Digital conversion is purely for test purposes, Weston, in the interest of economy and simplicity, decided to drive the encoder by a mechanical oscillator. In the final test program, therefore, the stepper motor will not be energized, instead its shaft will be driven by an instrument servomechanism. The time lag of the stepper motor would be simulated in the servomechanism, so that the over all frequency response information would be similar to that as if the stepper motor were energized. The input to the instrument servo would be from a low frequency sine wave generator.



5. SYSTEM ANALYSIS: (Continued)

5.2 Other Specification: (Continued)

5.2.2 Subsystems Specifications: (Continued)

5.2.2.9 Instrument Servo (Mechanical Oscillator): (Continued)

Specifications for the instrument servo system are as follows:

Input	± 10 Volts peak to peak
Frequency	0 - 10 cps
Output	$\pm 225^\circ$ about zero
Maximum Speed	1250 rpm
Running Torque	2 to 3 oz.-inch
Loop Gain	300 sec^{-1}
Time Constant	3.3 milliseconds

Note that the loop gain and the time constant is established to simulate the time lag of the stepper motor.

5.3 Preliminary Analysis:

5.3.1 Power Servo Loop Gain:

In designing the power servo, the loop gain is established by converting the specified closed loop response into open loop response with the aid of Nichols Charts. Figure 5.3.1 shows the open loop response.

The initial 20 db/decade open loop response intersects the 0 db gain line at 2.9 cps, indicating that the open loop gain is $2\pi \times 2.9 = 18.2 \text{ Sec}^{-1}$. The open loop response also defines the open loop natural frequency.

$$\omega'_{PL} = 6 \text{ cps} \quad \text{with} \quad \xi'_{PL} = 0.85$$

Later on it will be shown that this frequency is governed by the series combination of pneumatic and structure springs and the load mass.

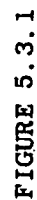


FIGURE 5.3.1



5. SYSTEM ANALYSIS: (Continued)

5.3 Preliminary Analysis: (Continued)

5.3.2 Maximum Piston Rate (Power Servo):

Based on experience with other Thrust Vector Control and flight control actuation systems, the maximum piston rate is selected to be 5.5 inches/second.

5.3.3 Per Cent Input (Open Loop) For Velocity Saturation (Power Servo):

Referring to APPENDIX I, Equation I-7

Per cent input required to velocity saturate the system

$$= \frac{100 \text{ (Maximum Piston Rate)}}{\text{(Open Loop Gain) (Stroke from Neutral)}}$$

$$= \frac{(100) (5.5)}{(18.2) (1.5)}$$

$$= 20\%$$

5.3.4 Simplified Servo Analysis (Power Servo):

The power schematic and simplified servo block diagram (neglecting dynamics) are shown in Figure 5.3.1.2 and 5.3.1.3 respectively.

5.3.4

Simplified Servo Analysis (Power Servo): (Continued)

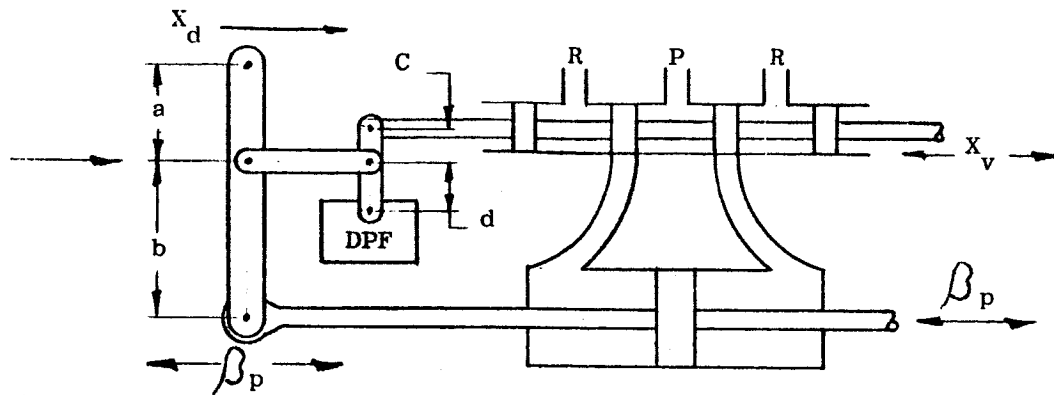


FIGURE 5.3.1.2

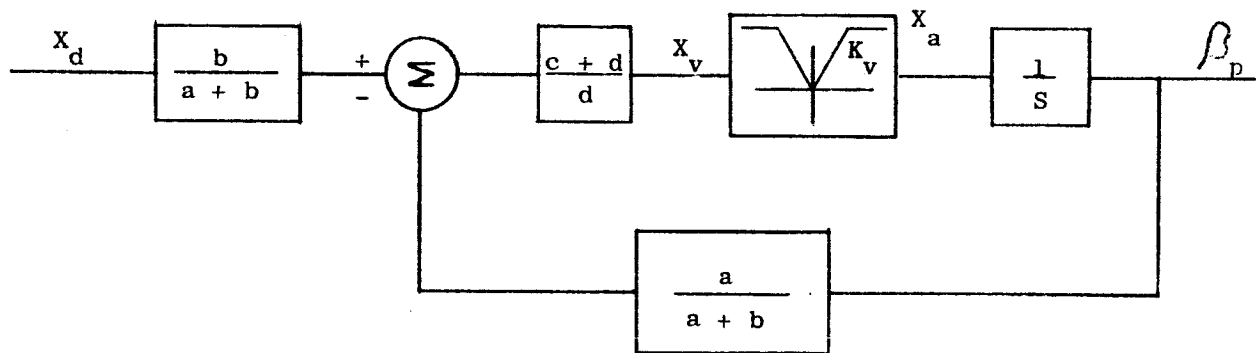


FIGURE 5.3.1.3

X_d = P.B.D.A. Output = ± 0.5

β_p = Power Servo Output = ± 1.5 Inch

X_v = Control Valve Stroke = ± 0.1 Inch

K_v = Forward Loop Gain, Piston Rate in Inches/Sec/Valve Stroke

Writing the transfer function

$$\frac{\beta_p}{X_d} = \frac{\frac{b}{a+b} \cdot \frac{c+d}{d} \cdot \frac{K_v}{s}}{1 + \frac{a}{a+b} \cdot \frac{c+d}{d} \cdot \frac{K_v}{s}}$$

$$= \frac{\frac{b}{a}}{\left(\frac{d}{c+d}\right) \left(\frac{a+b}{a}\right) \left(\frac{1}{K_v}\right) s + 1}$$

Inches/Inches



5. SYSTEM ANALYSIS: (Continued)

5.3 Preliminary Analysis: (Continued)

5.3.4 Simplified Servo Analysis (Power Servo): (Continued)

The steady state gain

$$\frac{\beta_p}{x_d} \text{ Steady State} = \frac{b}{a} = \frac{1.5''}{0.5''}$$

$$\text{Therefore: } \frac{b}{a} = \frac{3}{1} \quad (2)$$

In Section 5.3.1, the loop gain was established as 18.2 sec^{-1} .

Referring to Figure 5.3.1.3, therefore,

$$(K_v) \left(\frac{a}{a+b} \right) \left(\frac{c+d}{d} \right) = 18.2 \quad (3)$$

From equation (2)

$$\frac{a}{a+b} = \frac{1}{3+1} = \frac{1}{4}$$

From design layout $c = .75 \text{ Inch}$ and $d = 2.25 \text{ Inches}$

and substituting for $\frac{a}{a+b}$ in equation (3)

$$K_v = 18.2 \times 4 \times \frac{2.25}{3} = 55 \frac{\text{In/Sec}}{\text{In}} \quad (4)$$

$$\dot{\beta}_p = \text{Maximum Piston Rate} = 5.5 \text{ Inches/Sec.}$$

Therefore

$x_{vm} = \text{Control Valve Slot Length}$

$$= \frac{5.5}{55}$$

$$= 0.10 \text{ Inch}$$



5. SYSTEM ANALYSIS: (Continued)

5.3 Preliminary Analysis: (Continued)

5.3.5 Composite Response of the Stepper Motor -
Encoder and the Digital Actuator:

The power servo frequency response is shown in Figure 5.1.2. Basic system requirements indicate that the frequency response beyond 1 cps is not of much concern.

The digital section preceeding the power servo is designed for 10 cps response as follows. The additional phase shift due to this at 1 cps is 5.6°.

The P.B.D.A. stroke is ± 0.5 inches. In order to provide 10 cps response with 20% input (same as that required to velocity saturate the power servo).

$$\begin{aligned}\text{Maximum velocity of P.B.D.A.} &= 0.2 \times 0.5 (2\pi 10) \\ &= 6.28 \text{ Inches/Second}\end{aligned}$$

The total P.B.D.A. stroke of 1 inch is divided into a total 31 increments; therefore, the travel corresponding to every increment or bit is equal to 0.0322 inches.

The maximum bit rate required for the digital section is

$$\frac{6.28}{0.0322} = 194 \text{ Bits/Second}$$

The time lag from the moment of application of the pulse to the adder stack response therefore is $\frac{1}{194} = 5.2$ milliseconds.

The total time constant of 5.2 milliseconds is distributed between the digital components as follows



5. SYSTEM ANALYSIS: (Continued)

5.3 Preliminary Analysis: (Continued)

5.3.5 Composite Response of the Stepper Motor -
Encoder and the Digital Actuator: (Continued)

	TIME LAG
Stepper Motor (Pulse Rate of 300 Pulses/Sec)	3.3 Millisec.
Lines between Encoder and Pilot Valves	0.45 Millisec.
Pilot Valves	0.45 Millisec.
Adder Response	<u>1.00 Millisec.</u>
Total Time	5.20 Millisec.

5.3.6 Control Valve Sizing:

The following design calculations assume

- (i) Air as the working fluid
- (ii) Supply Pressure = 1600 psi, Return = 0 psi
- (iii) Normal room temperature of 70°F

The flow of air through a sharp edged orifice is

$$W = C_d A_m f \left(P_u, T_u \frac{P_d}{P_u} \right)$$

where W = Flow in lbs/sec

A_m = Metering orifice area in²

P_u = Upstream pressure psi

P_d = Downstream pressure psi

T_u = Absolute temperature in chamber u

k = Ratio of specific heats $\frac{C_p}{C_v}$ (1.4 for air)

R = Gas constant $\frac{\text{in}^2}{\text{sec}^2 \text{ } ^\circ\text{R}}$ = $(2.47 \times 10^5 \text{ for air})$

f = Function of $P_u, \frac{P_u}{P_d}, T_u$



5. SYSTEM ANALYSIS: (Continued)

5.3 Preliminary Analysis: (Continued)

5.3.6 Control Valve Sizing: (Continued)

$$g = \text{Gravity constant } \frac{\text{in}}{\text{sec}^2} = (386)$$

$$C_d = \text{Coefficient of discharge.}$$

f , the function of P_u , T_u and $\frac{P_d}{P_u}$ is dependent on the ratio of $\frac{P_d}{P_u}$

$$W = C_d A_m g \sqrt{\frac{2k}{R(k-1)}} \sqrt{\left(\frac{P_d}{P_u}\right)^{2/k} - \left(\frac{P_d}{P_u}\right)^{(k+1)/k}} \frac{P_u}{\sqrt{T_u}}$$

for

$$\frac{P_d}{P_u} \leq \left(\frac{2}{k+1} \right)^{k/(k-1)} \quad \text{Subsonic Flow} \quad (1)$$

$$W = C_d A_m g \sqrt{\frac{k}{R \left(\frac{k+1}{2} \right)}} \frac{P_u}{\sqrt{T_u}}$$

$$\text{for } \frac{P_d}{P_u} \leq \left(\frac{2}{k+1} \right)^{k/(k-1)} \quad \text{Sonic Flow} \quad (2)$$



5. SYSTEM ANALYSIS: (Continued)

5.3 Preliminary Analysis: (Continued)

5.3.6 Control Valve Sizing: (Continued)

Referring to a four way valve schematic and its equivalent bridge network:

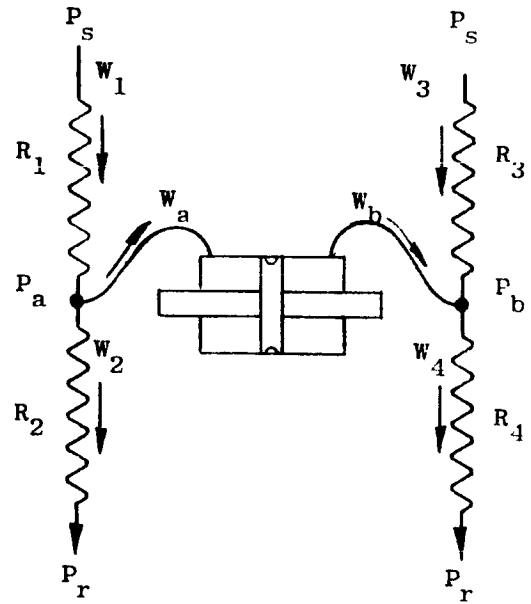
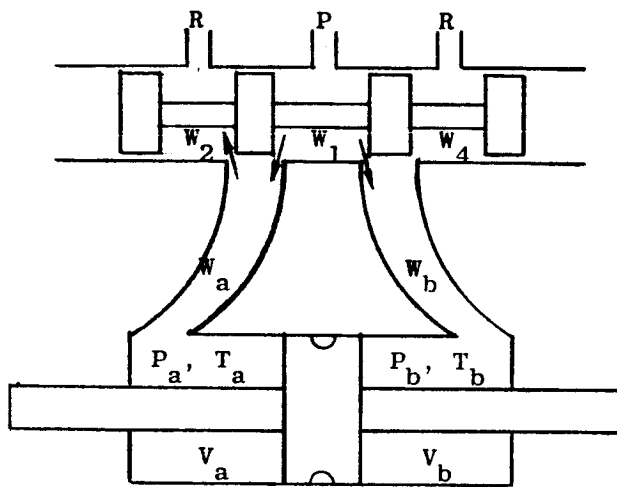


FIGURE 5.3.1.4

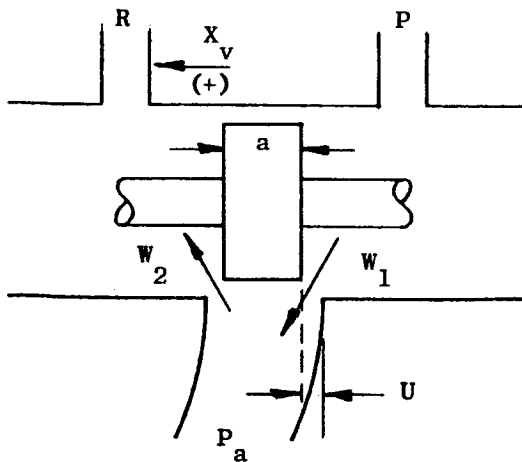


FIGURE 5.3.1.5

- R = Resistance
- W = Weight Flow #/sec
- P = Pressure
- P_s = Supply Pressure
- P_r = Return Pressure
- T = Temperature
- V = Volume
- U = Underlap
- X_v = Valve Travel
- A = Metering Area



5. SYSTEM ANALYSIS: (Continued)

5.3 Preliminary Analysis: (Continued)

5.3.6 Control Valve Sizing: (Continued)

The orifice area, A , is a function of the valve travel X_v .
If the slot width is b , then in neutral position of the spool

$$\begin{aligned} A_1 &= Ub & A_3 &= Ub \\ A_2 &= Ub & A_4 &= Ub \end{aligned}$$

As the spool moves to the left by X_v

$$\begin{aligned} A_1 &= Ub + X_v b & A_3 &= Ub - X_v b \\ A_2 &= Ub - X_v b & A_4 &= Ub + X_v b \end{aligned}$$

Assume that the spool is in neutral position and moved to the left. The weight flow through A , being a function of metering area and P_a , is described by:

$$W_1 = C_d (Ub + X_v b) g \sqrt{\frac{2k}{R(k-1)}} \sqrt{\left(\frac{P_a}{P_s}\right)^{2/k} - \left(\frac{P_a}{P_s}\right)^{(k+1)/k}} \frac{P_s}{T_s}$$

for X_v $a + 2U$

where P_a is dictated by $\frac{P_a}{P_s} \geq \left(\frac{2}{k+1}\right)^{k/(k-1)}$ (3)

$$\text{and } W_1 = C_d (Ub + X_v b) g \sqrt{\frac{k}{R\left(\frac{k+1}{2}\right)^{(k+1)/(k-1)}}} \frac{P_s}{\sqrt{T_s}}$$

$$\text{When } P_a \text{ drops below } \frac{P_a}{P_s} \leq \left(\frac{2}{k+1}\right)^{k/(k-1)} \quad (4)$$



5. SYSTEM ANALYSIS: (Continued)

5.3 Preliminary Analysis: (Continued)

5.3.6 Control Valve Sizing: (Continued)

Since supply pressure is constant, equation (4) indicates constant weight flow for P_a less than the critical pressure. Because the maximum flow occurs at maximum pressure differential, equation (4) also defines the maximum flow possible through A_1 when P_a = Return Pressure and $A_{1m} = (a + 2U) b$ (port fully uncovered) i.e.

$$W_{1 \text{ max.}} = C_d (a + 2U) b g \sqrt{\frac{k}{R \left(\frac{k+1}{2}\right)^{(k+1)/(k-1)}}} \frac{P_s}{\sqrt{T_s}} \quad (5)$$

$$\frac{W_1}{W_{1 \text{ max.}}} = \frac{U + X_v}{(a + 2U)} \sqrt{\frac{2 \left(\frac{k+1}{2}\right)^{(k+1)/(k-1)}}{k-1}} \sqrt{\left(\frac{P_a}{P_s}\right)^{2/k} - \left(\frac{P_a}{P_s}\right)^{(k+1)/k}} \quad (6)$$

The gas flow W_2 is a function of spool travel X_v and pressure P_a and P_r . If the return pressure $P_r = 0$ and T_a is assumed equal to T_s , the flow through A_2 is always sonic and equation (2) gives

$$W_2 = C_d (Ub - X_v b) g \sqrt{\frac{k}{R \left(\frac{k+1}{2}\right)^{(k+1)/(k-1)}}} \frac{P_a}{\sqrt{T_s}} \quad (7)$$

for $X_v \leq U$ and

$= 0$ for $X_v \geq U$



5. SYSTEM ANALYSIS: (Continued)

5.3 Preliminary Analysis: (Continued)

5.3.6 Control Valve Sizing: (Continued)

Maximum flow through metering area $A_2 = (a + 2U)b$ and $P_a = P_s$ is given by

$$W_{2 \text{ max.}} = C_d (a + 2U)b \sqrt{\frac{k}{R \left(\frac{k+1}{2} \right)^{(k+1)/(k-1)}}} \sqrt{\frac{P_a}{T_s}} \quad (8)$$

Dividing (8) by (7)

$$\frac{W_2}{W_{2 \text{ max.}}} = \frac{U - X_v}{a + 2U} \frac{P_a}{P_s} \quad (9)$$

It can be similarly shown that

$$\frac{W_3}{W_{3 \text{ max.}}} = \left(\frac{U - X_v}{a + 2U} \right) \sqrt{\frac{2 \left(\frac{k+1}{2} \right)^{(k+1)/(k-1)}}{k-1}} \sqrt{\left(\frac{P_s}{P_b} \right)^{2/k} - \left(\frac{P_s}{P_b} \right)^{(k+1)/k}}$$

for $X_v \leq U$ and

$$= 0 \text{ for } X_v \geq U \quad (10)$$

and

$$\frac{W_4}{W_{4 \text{ max.}}} = \frac{U + X_v}{a + 2U} \frac{P_b}{P_s} \quad (11)$$



5. SYSTEM ANALYSIS: (Continued)

5.3 Preliminary Analysis: (Continued)

5.3.6 Control Valve Sizing: (Continued)

In equation (6), (7), (10) and (11) if underlap = 0 i.e. $U = 0$

$$\frac{W_1}{W_{1 \text{ max.}}} = \frac{X_v}{a} \sqrt{\frac{2 \left(\frac{k+1}{2} \right)^{(k+1)/(k-1)}}{k-1}} \sqrt{\left(\frac{P_a}{P_s} \right)^{2/k} - \left(\frac{P_a}{P_s} \right)^{(k+1)/k}}$$

$$W_2 = 0$$

$$W_3 = 0$$

$$\frac{W_4}{W_{4 \text{ max.}}} = \frac{X_v}{a} \frac{P_b}{P_s}$$

For air $k = 1.4$

$$\frac{P_d}{P_u} = \left(\frac{2}{k+1} \right)^{k/(k-1)} = 0.528$$

$\frac{W_1}{W_{1 \text{ max.}}}$ and $\frac{W_4}{W_{4 \text{ max.}}}$ are plotted as functions of P_a and P_s as

shown in Figure 5.3.1.6. It may be noted that the maximum flow (no load flow) occurs at $P_a = P_b = 0.80 P_s$. i.e.

With supply of 1600 psi and return of 0 psi, the no load pressure in the two sides of the ram is $0.80 \times 1600 = 1280$.

The maximum no load velocity required = 5.5 Inches/Sec.

$$\text{Actuator Area} = 6.75 \text{ In}^2$$

$$\text{Volumetric Flow} = 5.5 \times 6.75$$

$$= 37 \text{ In}^3/\text{Sec}$$

Density of air at 70°F and 1280 psi = $0.00376 \text{ Lbs}/\text{In}^3$.

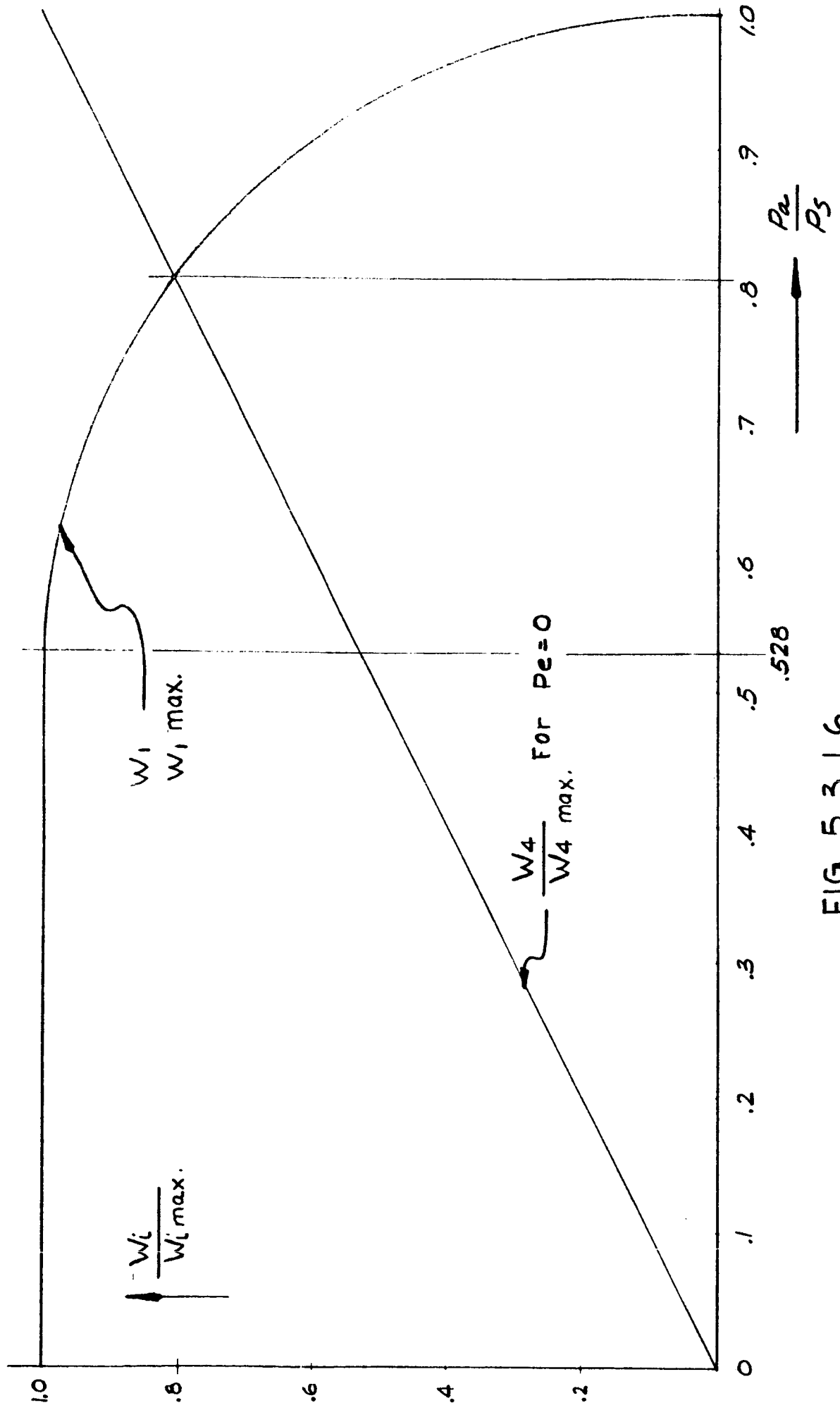


FIG. 5.3.1.6

Weston Hydraulics Limited



5. SYSTEM ANALYSIS: (Continued)

5.3 Preliminary Analysis: (Continued)

5.3.6 Control Valve Sizing: (Continued)

$$\begin{aligned}\text{Maximum weight rate flow} &= 37 \times 0.00376 \\ &= 0.136 \text{ Lbs/Sec}\end{aligned}$$

The metering area required for 0.136 #/Sec flow with upstream pressure of 1600 psi and ram chamber pressure of 1280 psi is 0.007 In.².

$$\text{The control valve stroke} = X_v = 0.100 \text{ In.}$$

$$\text{Therefore, total orifice width} = b_v = \frac{0.007}{0.1} = 0.07 \text{ In.}$$

$$\text{Assuming 4 orifices, the width per slot} = 0.0175 \text{ In.}$$

5.4 Dynamic Analysis (Power Servo):

5.4.1 Nomenclature:

M_E	Load Mass	$3.337 \frac{\text{lb. sec}^2}{\text{in}}$
K_E	Engine Spring	$40,000 \frac{\text{lbs}}{\text{in}}$
K_s	Structure Spring	$10,418 \frac{\text{lbs}}{\text{in}}$
β_e	Engine Motion	In.
β_a	Actuator Barrel Motion	In.
β_c	Equivalent Mechanical Command w.r.t. Barrel	In.
β_{fb}	$\beta_a + \beta_p$ Relative Motion Between Barrel and Piston	In.
a,b,c,d	Link Length	In.
X_d	Digital Actuator Output Stroke	In.



5. SYSTEM ANALYSIS: (Continued)

5.4 Dynamic Analysis: (Continued)

5.4.1 Nomenclature: (Continued)

X_f	D.P.F. Piston Motion	In.
X_l	Summing Point Motion	In.
X_v	Control Valve Motion	In.
b_v	Control Valve Metering Width	In.
W_a	Weight Flow Into Ram Chamber (a)	Lbs/Sec
W_b	Weight Flow Into Ram Chamber (b)	Lbs/Sec
U	Valve Underlap	In.
C_d	Coefficient of Discharge	
k	Ratio of Specific Heats	$\frac{C_p}{C_v}$
R	Air Gas Constant	$2.47 \times 10^5 \frac{\text{in}^2}{\text{sec}^2 \text{ } ^\circ\text{R}}$
P_s	Supply Pressure	psi
g	Gravity Constant	$386 \frac{\text{in}^2}{\text{sec}^2}$
$f_v (X)$	Function of X_v	
P_i	Initial Pressure on Two Sides	psi
P_a	Pressure in Chamber (a)	psi
P_b	Pressure in Chamber (b)	psi
A	Effective Actuation Area	In. ²



5. SYSTEM ANALYSIS: (Continued)

5.4 Dynamic Analysis: (Continued)

5.4.1 Nomenclature: (Continued)

k_1	$\frac{\partial W}{\partial X_v}$	$\frac{\#}{\text{sec-in}}$
k_2	$\frac{\partial W}{\partial P}$	$\frac{\text{in}^2}{\text{sec}}$
T_i	Initial Temperature	$^{\circ}\text{R}$
T_a	Temperature in Chamber (a)	$^{\circ}\text{R}$
T_b	Temperature in Chamber (b)	$^{\circ}\text{R}$
V_a	Volume of Chamber (a)	In^3
V_b	Volume of Chamber (b)	In^3
C_1	Control Valve Gain	$\frac{\text{in}^3/\text{sec}}{\text{in}}$
C_2	Loss of Valve Flow Per Unit Load Pressure (Reciprocal of Valve Output Impedance)	$\frac{\text{in}^5}{\text{lb.}}$
C_3	Pneumatic Compliance	$\frac{\text{in}^5}{\text{lb.}}$
A_1, A_2	D.P.F. Piston Area	In^2
K_1, K_2	D.P.F. Spring Rate (Total On Two Sides Of Each Piston)	Lbs/In
W_{1N}, W_{2N}, W_{3N}	Weight Flows In The D.P.F. Network	Lb/Sec
ρ_c	Density of Air At Intermediate Point In D.P.F. Network	Lbs/In^3
P_c	Intermediate Pressure In The D.P.F. Network	psi
A_o	D.P.F. Orifice Area	In^2



5. SYSTEM ANALYSIS: (Continued)

5.4 Dynamic Analysis: (Continued)

5.4.1 Nomenclature: (Continued)

K_o	Constant of Proportionality For The D.P.F. Orifice	$\frac{1}{\text{sec}}$
T	D.P.F. Time Constant	Sec.
ω_e	$\sqrt{\frac{K_E}{M_E}}$ Engine Resonance Frequency	Rad/Sec.
ω_L	$\frac{1}{\sqrt{\frac{M_E}{K_S} + \frac{M_E}{K_E}}}$ Structure and Load Spring Resonance Frequency	Rad/Sec
ω_{PL}	$\frac{1}{\sqrt{\omega_L^2 + \frac{C_3 M_E}{A^2}}}$ Structure + Load + Pneumatic Spring Resonance Frequency (Without D.P.F.)	Rad/Sec
ζ_{PL}	Damping Factor of ω_{PL} Without D.P.F.	
ω'_{PL}	Pneumatic + Structure + Load Spring Natural Frequency With D.P.F.	Rad/Sec
ζ'_{PL}	Damping Factor Of ω'_{PL} With D.P.F.	
ζ_L	Load Damping Factor	

5. SYSTEM ANALYSIS: (Continued)

5.4 Dynamic Analysis: (Continued)

5.4.2 Equations:

The power servo schematic is shown in Figure 5.4.2.1.

5.4.2.1 Equivalent Structure - Load Spring

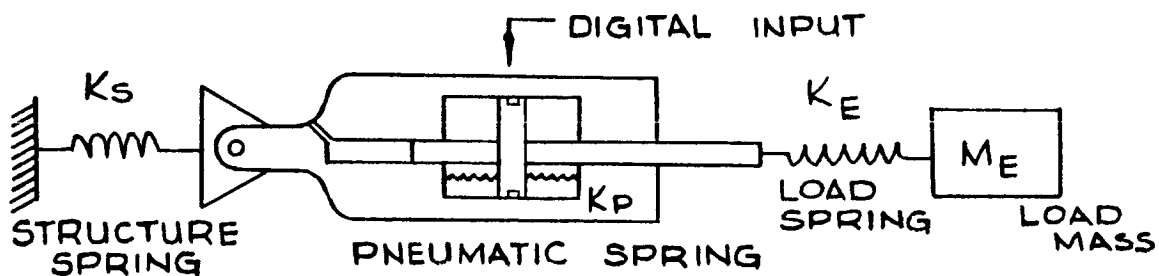


FIGURE 5.4.2.1

System springs and equivalent diagram.

Basically, there are three springs in the system. The structure spring and the load spring are combined into a single spring for a simpler analysis

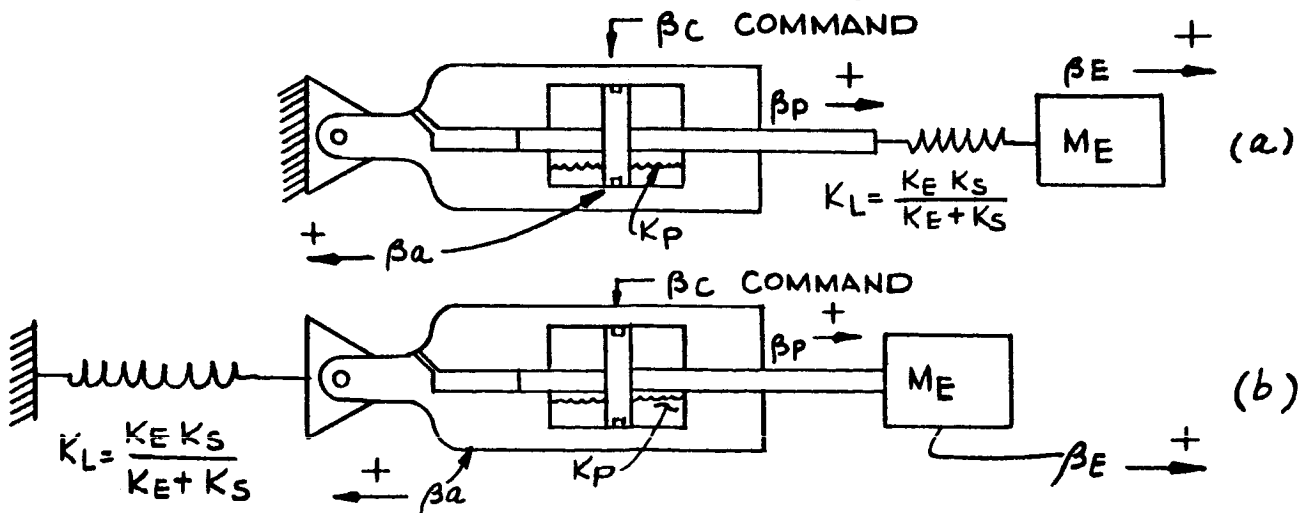


FIGURE 5.4.2.2

System springs with structure and load spring combined into one spring.



5. SYSTEM ANALYSIS: (Continued)

5.4 Dynamic Analysis: (Continued)

5.4.2 Equations: (Continued)

5.4.2.1 (Continued)

The two configurations shown in Figure 5.4.2.2 (defined as a and b) are equivalent in dynamics and performance. The mechanical natural frequency in both the cases is:

$$\omega_m = \sqrt{\frac{\frac{K_S K_E}{K_E + K_S}}{M_E}} = \sqrt{\frac{K_L}{M_E}} \quad \text{Rad/Sec}$$

One difference should be noted. β_E , the load position, is the same in the two cases. However, β_{fb} piston position in Figure (a) is analogous to $\beta_p + \beta_a$ in Figure (b). Weston's load simulator is designed to provide the equivalent load spring as shown in Figure 5.4.2.3 - (b), where β_c = equivalent mechanical input with respect to the barrel.

FIGURE 5.4.2.3

FIGURE 5.4.2.2	CONFIGURATION (a)	CONFIGURATION (b)
To determine re- sponse of $\frac{\beta_{fb}}{\beta_c}$ ($\beta_{fb} = \beta_p + \beta_a$)	Monitor Response of $\frac{\beta_p}{\beta_c}$ ($\beta_a = 0$)	Monitor Response of $\frac{\beta_a + \beta_p}{\beta_c}$
To determine re- sponse of $\frac{\beta_L}{\beta_c}$	Monitor Response of $\frac{\beta_L}{\beta_c}$	Monitor Response of $\frac{\beta_L}{\beta_c}$



5. SYSTEM ANALYSIS: (Continued)

5.4 Dynamic Analysis: (Continued)

5.4.2 Equations: (Continued)

5.4.2.2 Kinematic Relations:

Referring to the power servo schematic, Figure 5.4.2.5, the motion of the summing point X_1 is given by:

$$X_1 = + \frac{b}{a+b} x_d - \frac{a}{a+b} \beta_{fb} \quad (1)$$

Ignoring the effects of the buffer (which limits the error to the control valve).

$$X_v = \frac{c+d}{d} X_1 - \frac{c}{d} X_f \quad (2)$$

5.4.2.3 Control Valve Characteristics:

Referring to Figure 5.3.1.4 and Section 5.3.1.6, the control valve characteristics are described by:

$$W_a = \frac{C_d U b_v}{\sqrt{T_s}} g \left[\left(1 + \frac{X_v}{U} \right) \sqrt{\frac{2k}{R(k-1)}} \sqrt{\left(\frac{P_a}{P_s} \right)^{2/k} - \left(\frac{P_a}{P_s} \right)^{(k+1)/k}} P_s - \left(1 - \frac{X_v}{U} \right) \sqrt{\frac{k}{\left(\frac{R(k+1)}{2} \right)^{(k+1)/(k-1)}}} P_a \right] \quad (3)$$

$$W_b = \frac{C_d U b_v}{\sqrt{T_s}} g \left[\left(1 + \frac{X_v}{U} \right) \sqrt{\frac{k}{\left(\frac{R(k+1)}{2} \right)^{(k+1)/(k-1)}}} P_b - \left(1 - \frac{X_v}{U} \right) \sqrt{\frac{2k}{R(k-1)}} \sqrt{\left(\frac{P_b}{P_s} \right)^{2/k} - \left(\frac{P_b}{P_s} \right)^{(k+1)/k}} P_s \right] \quad (4)$$

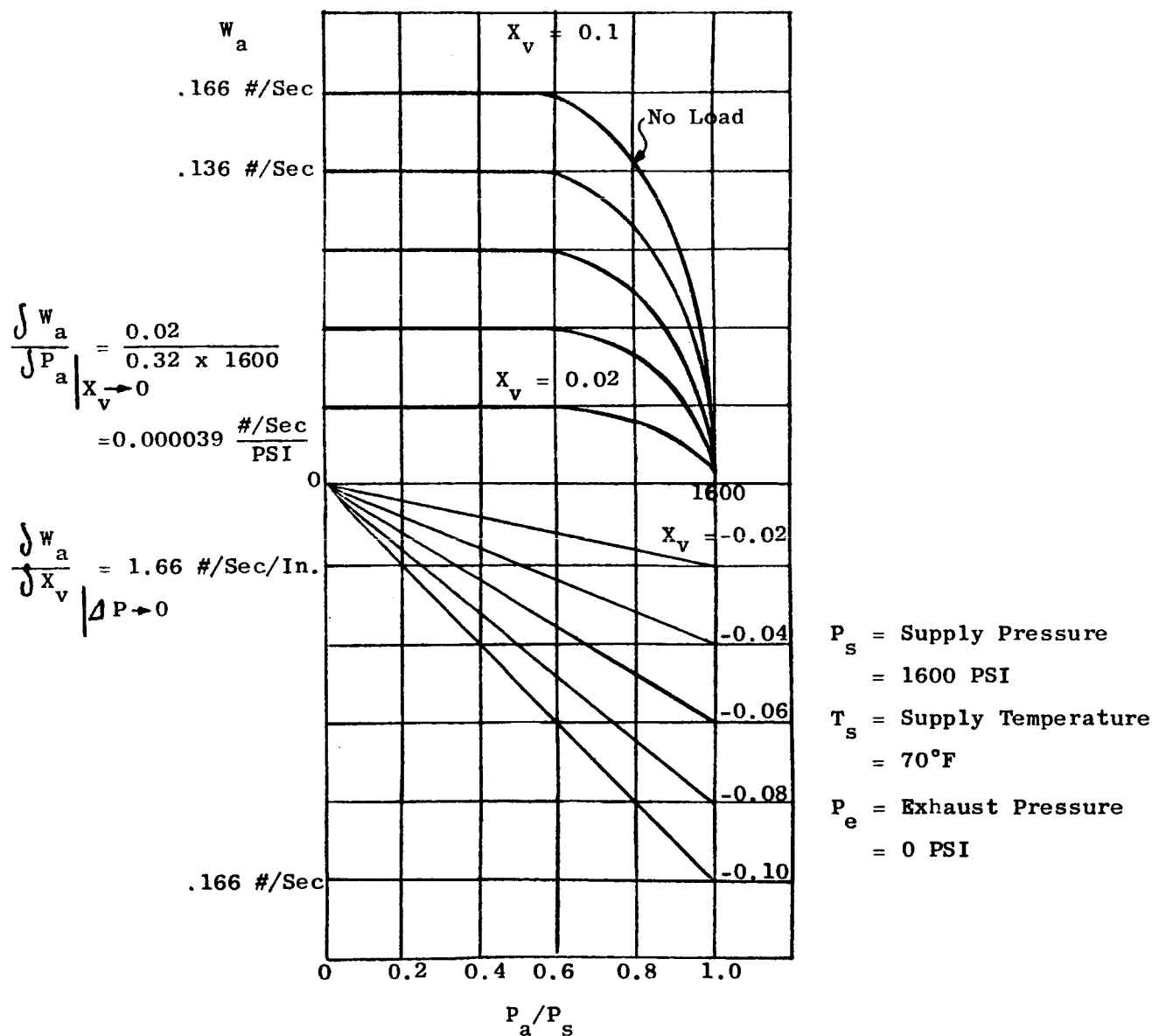


5. SYSTEM ANALYSIS: (Continued)

5.4 Dynamic Analysis: (Continued)

5.4.2 Equations: (Continued)

5.4.2.3 Control Valve Characteristics: (Continued)



THEORETICAL PNEUMATIC SPOOL SLEEVE VALVE CHARACTERISTICS

FIGURE 5.4.2.4

The non-linear curve shown in the figure can be linearized using the following technique.



5. SYSTEM ANALYSIS: (Continued)

5.4 Dynamic Analysis: (Continued)

5.4.2 Equations: (Continued)

5.4.2.3 Control Valve Characteristics: (Continued)

In simple terms:

$$W_a = f_v (X_v, P_a) \quad (5)$$

$$W_b = f_v (-X_v, P_b) \quad (6)$$

Where f_v is the functional relationship as shown in Figure 5.4.2.4.

At no load $P_a = 0.8 P_s$

$$\Delta W_a = \frac{\partial W_a}{\partial X_v} (\Delta X_v) + \frac{\partial W_a}{\partial P_a} (\Delta P_a) \quad (7)$$

$$\Delta W_b = \frac{\partial W_b}{\partial X_v} (-\Delta X_v) + \frac{\partial W_b}{\partial P_b} (\Delta P_b) \quad (8)$$

Denoting

$$\frac{\partial W}{\partial X_v} \text{ by } k_1$$

and

$$\frac{\partial W}{\partial P} \text{ by } k_2$$

$$\Delta W_a = k_{1a} (\Delta X_v) + k_{2a} (\Delta P_a) \quad (9)$$

$$\Delta W_b = k_{1b} (-\Delta X_v) + k_{2b} (\Delta P_b) \quad (10)$$



5. SYSTEM ANALYSIS: (Continued)

5.4 Dynamic Analysis: (Continued)

5.4.2 Equations: (Continued)

5.4.2.3 Control Valve Characteristics: (Continued)

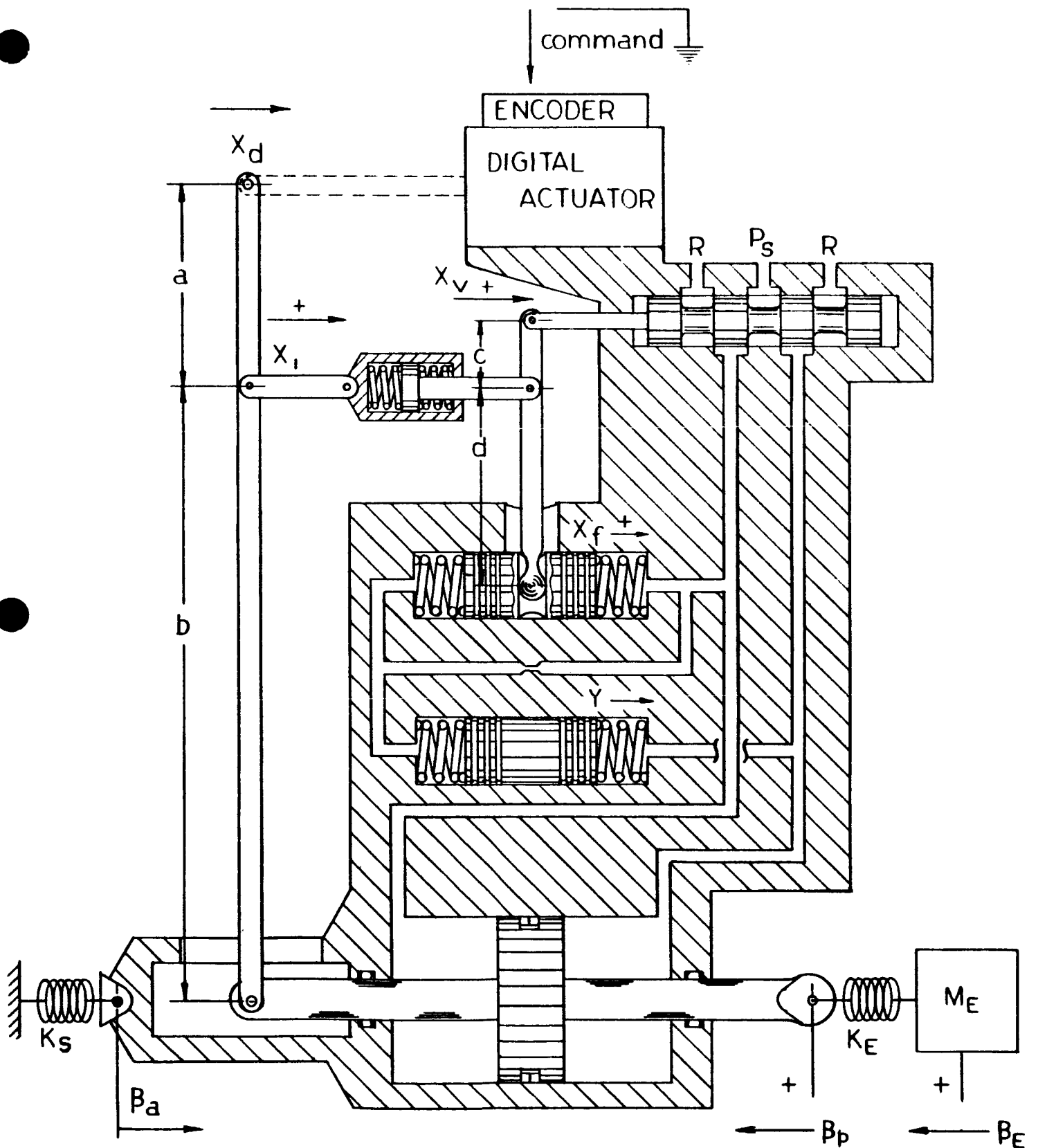
k_1 and k_2 are measured from the control valve pressure-flow curve in Figure 5.4.2.4

$$k_1 = \frac{\partial W}{\partial X_v} = 1.66 \text{ \#/sec/in} \quad (11)$$

$$k_2 = \frac{\partial W}{\partial P} = 0.000039 \text{ \#/sec/psi} \quad (12)$$

It may be noted that for a symmetrical valve and around neutral position

$$k_{1a} = k_{1b} \quad \text{and} \quad k_{2a} = k_{2b}$$



SCHEMATIC
POWER SERVO

FIG. 5.4.2.5

5. SYSTEM ANALYSIS: (Continued)

5.4 Dyanmic Analysis: (Continued)

5.4.2 Equations: (Continued)

5.4.2.4 Actuator:

Assuming adiabatic changes

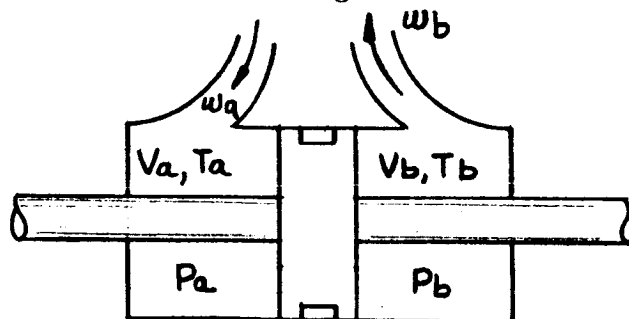


FIGURE 5.4.2.6

from the energy equation it can be shown that

$$w_a T_a - \frac{g P_a}{C_p} \frac{d V_a}{dt} = \frac{g}{kR} \frac{d}{dt} (P_a V_a) \quad (13)$$

$$w_b T_b - \frac{g P_b}{C_p} \frac{d V_b}{dt} = \frac{g}{kR} \frac{d}{dt} (P_b V_b) \quad (14)$$

If P_{a1} denotes initial values of P_a etc., the two equations (13) and (14) can be linearized to

$$T_a (\Delta w_a) - \frac{g P_{a1}}{C_p} \frac{d}{dt} (\Delta V_a) = \frac{g}{kR} \left[P_{a1} \frac{d(\Delta V_a)}{dt} + V_{a1} \frac{d}{dt} (\Delta P_a) \right] \quad (15)$$

$$T_b (\Delta w_b) - \frac{g P_{b1}}{C_p} \frac{d}{dt} (\Delta V_b) = \frac{g}{kR} \left[P_{b1} \frac{d(\Delta V_b)}{dt} + V_{b1} \frac{d}{dt} (\Delta P_b) \right] \quad (16)$$



5. SYSTEM ANALYSIS: (Continued)

5.4 Dynamic Analysis: (Continued)

5.4.2 Equations: (Continued)

5.4.2.4 Actuator: (Continued)

Assume $T_a = T_b = T_1$ and for small changes $P_{a1} = P_{b1} = P_1$, then subtracting (16) from (15) and rearranging:

$$(\Delta w_a - \Delta w_b) = \frac{g}{RT_1} \left[2 P_1 A \frac{d(\Delta \beta_{fb})}{dt} + \frac{V_1}{k} \frac{d}{dt} (\Delta P_a - \Delta P_b) \right] \quad (17)$$

From equations (9) and (10)

$$(\Delta w_a - \Delta w_b) = 2k_1 (\Delta X_v) - k_2 (\Delta P_a - \Delta P_b) \quad (18)$$

Equating the right hand sides of equation (17) and (18)

$$\begin{aligned} & \frac{g}{RT_1} \left[2 P_1 A \frac{d(\Delta \beta_{fb})}{dt} + \frac{V_1}{k} \frac{d}{dt} (\Delta P_a - \Delta P_b) \right] \\ &= 2k_1 (\Delta X_v) - k_2 (\Delta P_a - \Delta P_b) \end{aligned}$$

Rearranging and using Laplace notation to replace $\frac{d}{dt}$ by s

$$\begin{aligned} & \left(\frac{g V_1}{k RT_1} s + k_2 \right) (\Delta P_a - \Delta P_b) \\ &= 2k_1 (\Delta X_v) - \frac{2g P_1 A}{R T_1} s (\Delta \beta_{fb}) \end{aligned}$$

Multiplying throughout by $\frac{R T_1}{2g P_1}$



5. SYSTEM ANALYSIS: (Continued)

5.4 Dynamic Analysis: (Continued)

5.4.2 Equations: (Continued)

5.4.2.4 Actuator: (Continued)

$$As (\Delta \beta_{fb}) = \frac{k_1 R T_1}{g P_1} (\Delta x_v) - \left[\frac{V_1}{2k P_1} s + \frac{k_2 R T_1}{2g P_1} \right] (\Delta P_a - \Delta P_b) \quad (19)$$

Denoting

$$\frac{k_1 R T_1}{g P_1} = C_1 \frac{\text{sq. in.}}{\text{sec.}} \quad (\text{no load valve flow sensitivity or valve flow gain})$$

$$\frac{1.66 (2.47 \times 10^5) 530}{(386) 1280} = 440 \frac{\text{in.}^2}{\text{sec.}}$$

$$\frac{k_2 R T_1}{2g P_1} = C_2 \frac{\text{in.}^5}{\text{lb-sec}} \quad (\text{loss of valve flow per unit load pressure}) = 0.0052 \frac{\text{CIS}}{\text{psi}}$$

$$\frac{(3.9 \times 10^{-5}) (2.47 \times 10^5) (530)}{(2) (386) (1280)} = 52 \times 10^{-4}$$

and

$$\frac{V_1}{2k P_1} = C_3 \frac{\text{in.}^5}{\text{lb.}} \quad (\text{fluid compliance}) = 0.0034 \frac{\text{In.}^5}{\text{Lb.}}$$

$$\frac{(1.5) (6.75) (1.2)}{2 (1.4) (1280)} = 3.4 \times 10^{-3} = 0.0034 \frac{\text{In.}^5}{\text{Lb.}}$$

where the factor 1.2 includes the line volume of 20%.

5. SYSTEM ANALYSIS: (Continued)

5.4 Dynamic Analysis: (Continued)

5.4.2 Equations: (Continued)

5.4.2.4 Actuator: (Continued)

Equation (19) can be written as

$$\Delta S (\Delta \beta_{fb}) = C_1 (\Delta X_v) - (C_2 + C_3 S) (\Delta P_a - \Delta P_b) \quad (20)$$

5.4.2.5 Dynamic Pressure Feedback Network:

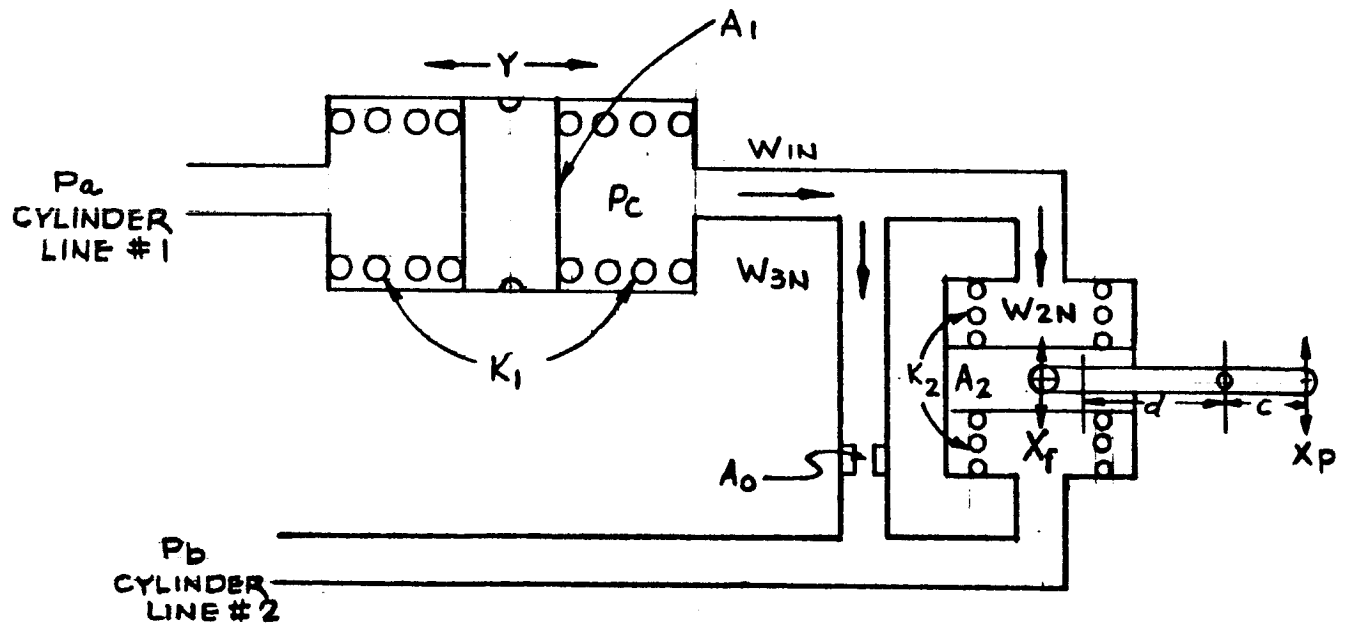


FIGURE 5.4.2.7



5. SYSTEM ANALYSIS: (Continued)

5.4 Dynamic Analysis: (Continued)

5.4.2 Equations: (Continued)

5.4.2.5 Dynamic Pressure Feedback Network: (Continued)

Referring to Figure 5.4.2.7, from the continuity equation:

$$W_{1N} = W_{2N} + W_{3N} \quad (21)$$

where

$$W_{1N} = \rho_c A_1 \frac{d}{dt} y \quad (22)$$

$$W_{2N} = \rho_c A_2 \frac{d}{dt} x_f \quad (23)$$

W_{3N} = flow through the orifice

$$= C_d A_o \sqrt{\frac{2k}{R(k-1)}} \sqrt{\left(\frac{P_b}{P_c}\right)^{2/k} - \left(\frac{P_b}{P_c}\right)^{(k+1)/k}} \frac{P_c}{\sqrt{T_u}} \quad (24)$$

for $P_b < P_c$

Previously it was shown that $P_{a1} = P_{b1} = 0.8 \times 1600 = 1280$ psi. And further, since the actuator area is fairly large, the ΔP across the actuator is small and therefore the instantaneous pressure values do not vary much from the steady state values. This operation also maintains the gas density ρ_c practically constant for the same reason.

With these approximations

$$W_{3N} = K_o A_o (P_c - P_b) \quad (25)$$

Where K_o = constant of proportionality.



5. SYSTEM ANALYSIS: (Continued)

5.4 Dynamic Analysis: (Continued)

5.4.2 Equations: (Continued)

5.4.2.5 Dynamic Pressure Feedback Network: (Continued)

Substituting (22), (23) and (25) in (21)

$$\rho_c A_1 \frac{d}{dt} Y = \rho_c A_2 \frac{d}{dt} X_f + K_o A_o (P_c - P_b) \quad (26)$$

Referring to Figure 5.4.2.7

$$(P_a - P_c) A_1 = K_1 Y \quad (27)$$

$$(P_c - P_b) A_2 = K_2 X_f \quad (28)$$

From equation (26), (27), and (28) using Laplace notation

$$\frac{X_f}{(P_a - P_b)} = \frac{\frac{A_2}{K_2} \left(\frac{A_1^2 \rho_c}{K_1 K_o A_o} \right) s}{\left(\frac{A_1^2}{K_1} + \frac{A_2^2}{K_2} \right) \frac{\rho_c}{K_o A_o} s + 1} \quad (29)$$

Since $A_1 = A_2$ and $K_1 = K_2$, equation (29) can be simplified to:

$$\frac{X_f}{P_a - P_b} = \frac{\frac{A_1}{K_1} \tau s}{2 \tau s + 1} \quad \text{where} \quad \tau = \frac{A_1^2}{K_1} \frac{\rho_c}{K_o A_o} \text{ Sec.} \quad (30)$$



5. SYSTEM ANALYSIS: (Continued)

5.4 Dynamic Analysis: (Continued)

5.4.2 Equations: (Continued)

5.4.2.6 Load:

The mass load and the springs diagram is shown in Figure 5.4.2.8.

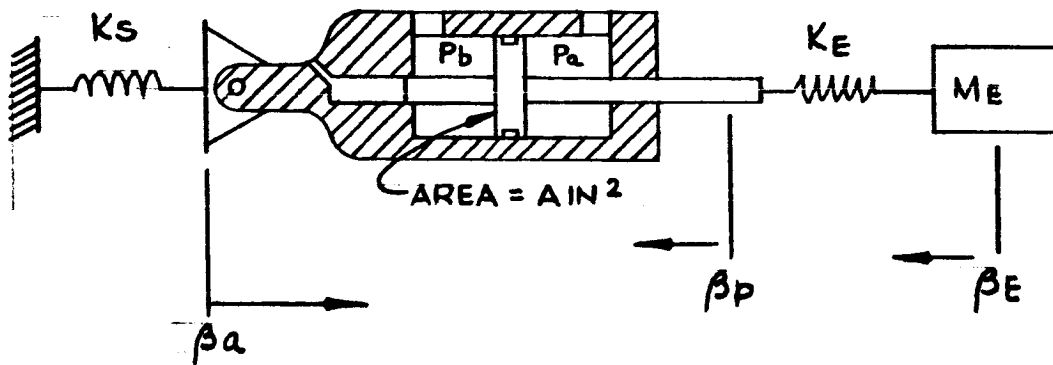


FIGURE 5.4.2.8

Referring to Figure 5.4.2.8, if P_a is greater than P_b , the actuator force F_a is

$$F_a = A (P_a - P_b) \quad (31)$$

$$F_a \text{ also equals } K_s \beta_a \quad (32)$$

further

$$K_E = (\beta_p - \beta_E) = \frac{M d^2}{dt^2} \beta_E \quad (33)$$

Net motion of the piston with respect to the frame ground is β_{fb} .

$$\beta_{fb} = \beta_p + \beta_a$$

where the directions of β 's are as shown in Figure 5.4.2.8.



5. SYSTEM ANALYSIS: (Continued)

5.4 Dynamic Analysis: (Continued)

5.4.3 Overall System Dynamics - Stability Consideration:

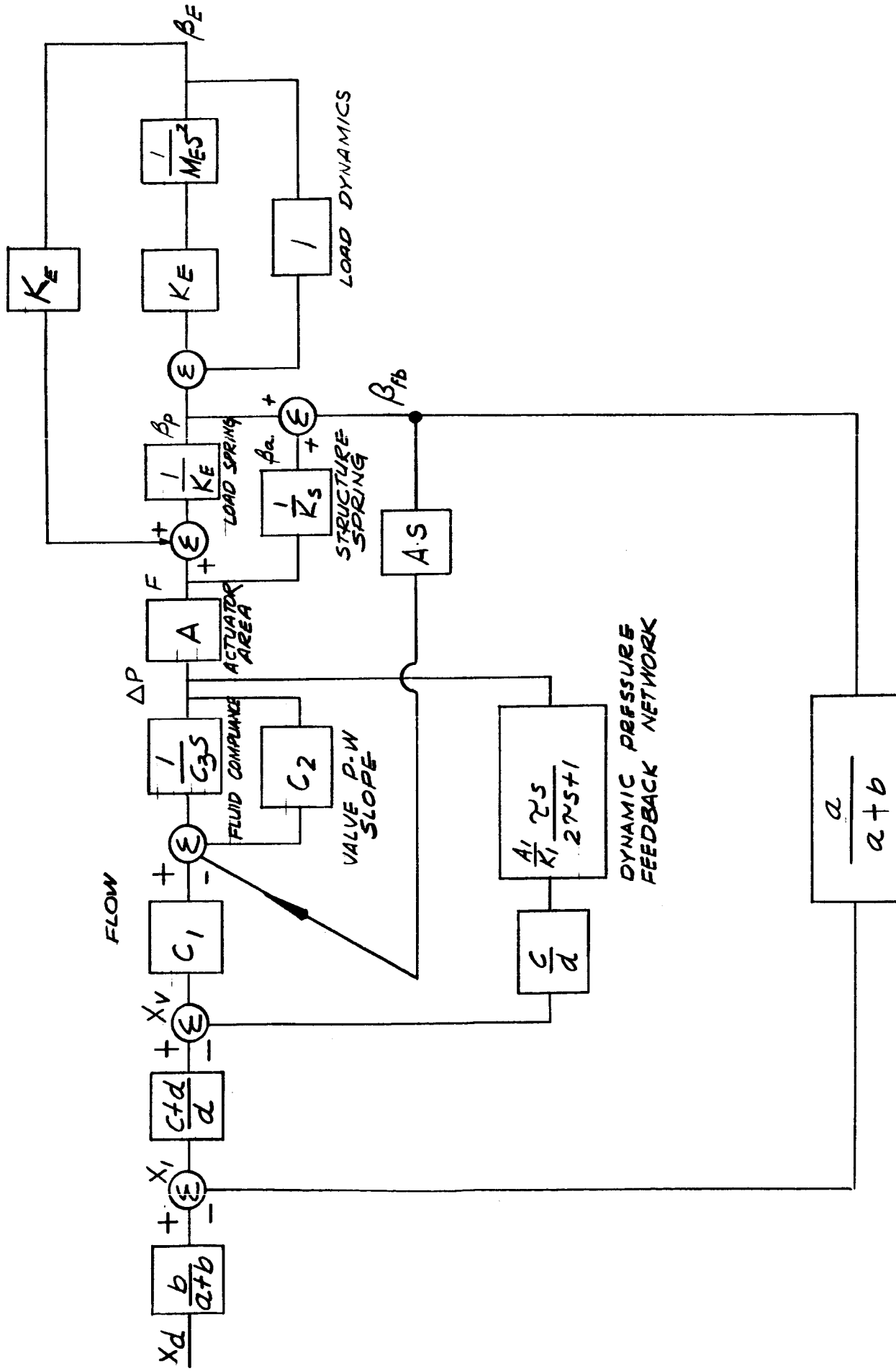
The preceeding section presented the equations and transfer functions of the various power servo elements. This section presents the linear dynamic analysis of the complete system. It is shown later that the ΔP across the power servo ram is small, hence the linear analysis based on constant gas density and linear valve characteristics provided results which were extremely close to the results obtained from the computer study using rigorous non-linear equations.

The following linear analysis assumes zero viscous load damping. The specified load damping of $\zeta_L = 0.05$ is so small that the load can be considered almost undamped.

Figure 5.4.3.1 presents the complete system block diagram including the kinematic relationships, valve characteristics, air compliance, resonant load, and the dynamic pressure feedback network. In order to simplify the analysis, the diagram is redrawn in a more convenient form as shown in Figure 5.4.3.2. The new transfer functions are derived as follows: From load equations 31, 32, and 33 it can be shown that

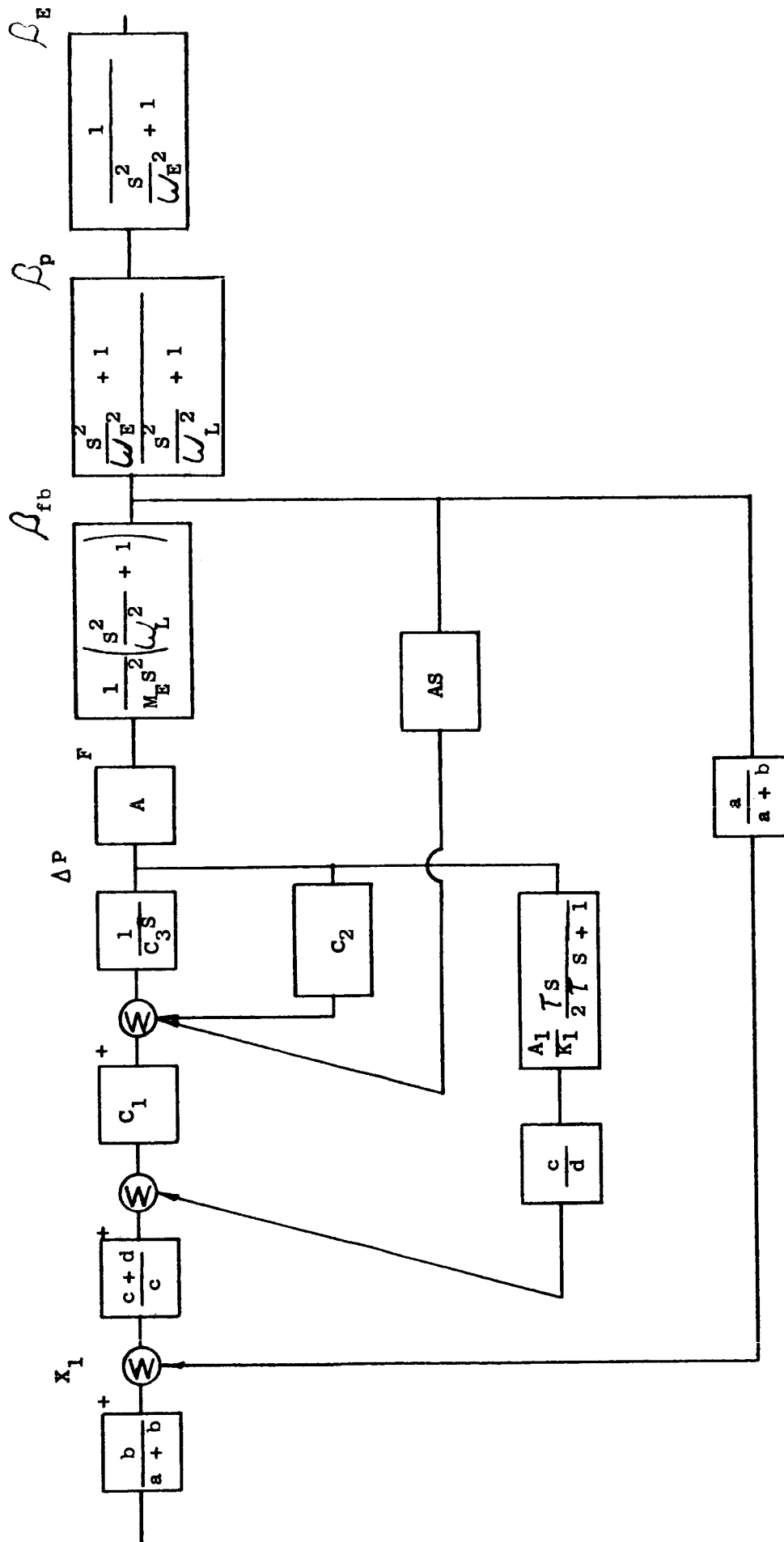
$$\frac{\beta_{fb}}{F_a} = \frac{\beta_a + \beta_p}{F_a} = \frac{1}{M_E S^2} \left[\left(\frac{M_E}{K_E} + \frac{M_E}{K_S} \right) S^2 + 1 \right] \quad (1)$$

$$\frac{\beta_p}{\beta_{fb}} = \frac{\frac{M_E}{K_E} S^2 + 1}{\left(\frac{M_E}{K_E} + \frac{M_E}{K_S} \right) S^2 + 1} \quad (2)$$



POWER SERVO - TRANSFER FUNCTION
BLOCK DIAGRAM

FIG. 5.4.3.1



MODIFIED TRANSFER FUNCTION BLOCK DIAGRAM

FIGURE 5.4.3.2



5. SYSTEM ANALYSIS: (Continued)

5.4 Dynamic Analysis: (Continued)

5.4.3 Overall System Dynamics - Stability Consideration: (Continued)

and

$$\frac{\beta_E}{\beta_p} = \frac{1}{\left[\frac{M_E}{K_E} s^2 + 1 \right]} \quad (3)$$

Denoting

$$\frac{1}{\sqrt{\frac{M_E}{K_E}}} \quad \text{by } \omega_E \dots \text{Engine Resonance Frequency} \quad (4)$$

and

$$\frac{1}{\sqrt{\frac{M_E}{K_S} + \frac{M_E}{K_E}}} \quad \text{by } \omega_L \dots \text{Load Resonance Frequency Comprising of Engine and Structure Spring} \quad (5)$$

The transfer function diagram is redrawn as shown in Figure 5.4.3.2.

Referring to Figure 5.4.3.2, the transfer function relating β_{fb} to X_1 without the D.P.F. network is given by:

$$\frac{\beta_{fb}}{X_1} = \frac{\left(\frac{c+d}{c} \right) \left(\frac{C_1 A}{C_3 s} \right) \left(\frac{1}{M_E s^2} \right) \left(\frac{s^2}{\omega_L^2} + 1 \right)}{1 + \frac{C_2}{C_3 s} + \frac{A^2}{C_3 M_E s^2} \left(\frac{s^2}{\omega_L^2} + 1 \right)}$$



5. SYSTEM ANALYSIS: (Continued)

5.4 Dynamic Analysis: (Continued)

5.4.3 Overall System Dynamics Stability Consideration: (Continued)

$$\frac{\beta_{fb}}{x_1} = \frac{\left(\frac{c+d}{c}\right) \left(\frac{C_1}{A s}\right) \left(\frac{s^2}{\omega_L^2} + 1\right)}{\left(\frac{1}{\omega_L^2} + \frac{C_3 M_E}{A^2}\right) s^2 + \frac{C_2 M_E}{A^2} s + 1} \quad (6)$$

Denoting

$$\frac{1}{\sqrt{\frac{1}{\omega_L^2} + \frac{C_3 M_E}{A^2}}} \quad \text{by } \omega_{PL} \dots \text{Pneumatic and Load Natural Frequency} \quad (7)$$

and

$$\frac{1}{2} \frac{C_2 M_E}{A^2} \frac{1}{\sqrt{\frac{1}{\omega_L^2} + \frac{C_3 M_E}{A^2}}} \quad \text{by } \zeta_{PL} \dots \text{Damping Factor} \quad (8)$$

Equation (6) can be rewritten as

$$\frac{\beta_{fb}}{x_1} = \frac{\left(\frac{c+d}{c}\right) C_1 \left(\frac{s^2}{\omega_L^2} + 1\right)}{A s \left(\frac{s^2}{\omega_{PL}^2} + \frac{2 \zeta_{PL}}{\omega_{PL}} s + 1\right)} \quad (9)$$



5. SYSTEM ANALYSIS: (Continued)

5.4 Dynamic Analysis: (Continued)

5.4.3 Overall System Dynamics Stability Consideration: (Continued)

Referring to Figure 5.3.1, from the open loop plot of the power servo, the open loop natural frequency should be 6 cps with ζ of 0.85. Preliminary calculations showed that with the given mass, mechanical natural frequency and the air compliance at 0.8×1600 psi (steady state ram pressure), the actuator area required to provide $\frac{\omega_{PL}}{2\pi}$ of 6 cps is in excess of 6.5 in.^2 .

However, the damping ζ is very low. The need for some sort of pressure feedback was therefore apparent. Use of direct load pressure feedback results in loss of static system stiffness. If the load pressure is fed through a network with the transfer function of $\frac{K_T S}{2\tau S+1}$ then for transients and step inputs the pressure feedback is significant, but for slow inputs there is no pressure feedback.

Referring to Figure 5.4.3.2, the transfer function relating β_{fb} and X_1 with the D.P.F. network is

$$\frac{\beta_{fb}}{X_1} = \frac{\left(\frac{c+d}{c}\right) \left(\frac{C_1 A}{C_3 M_E S^3}\right) \left(\frac{S^2}{\omega_L^2} + 1\right)}{1 + \frac{C_2}{C_3 S} + \frac{A^2}{C_3 M_E S^2} \left(\frac{S^2}{\omega_L^2} + 1\right) + \frac{c C_1 \tau A_1 / K_1}{d C_3 (2\tau S+1)}} \quad (10)$$

In the above equation C_2 represents $\frac{\Delta \text{ Volumetric Flow}}{\Delta P - \text{Load}}$ and as such is the reciprocal of the valve output impedance, taking into account the leakage. The larger the value of C_2 , the greater is the system damping. If C_2 and the friction are assumed zero, then the system damping without the artificial



5. SYSTEM ANALYSIS: (Continued)

5.4 Dynamic Analysis: (Continued)

5.4.3 Overall System Dynamics Stability Consideration: (Continued)

damping circuit is zero. Since the primary purpose of the D.P.F. network is to introduce artificial damping, if C_2 be assumed zero (to simplify the following analysis) then the above analysis would be the worst case. The network parameters obtained from the following calculations would provide a degree of damping greater than actually required. The system design permits easy modification of the D.P.F. network gain and time constant to complement the actual friction and practical P - W slope of the valve.

In equation (10) setting $C_2 = 0$ and multiplying numerator and denominator by $\frac{M_E C_3 (2\tau S + 1) S^2}{A^2}$

$$\frac{\beta_{fb}}{X_1} = \frac{\left(\frac{c+d}{c}\right) \left(\frac{C_1}{A S}\right) \left(\frac{S^2}{\omega_L^2} + 1\right) (2\tau S + 1)}{\frac{M_E C_3}{A^2} (2\tau S + 1) S^2 + \frac{C_1 c A_1 M_E}{d K_1 A^2} \tau S^2 + \left(\frac{S^2}{\omega_L^2} + 1\right) (2\tau S + 1)} \quad (11)$$

Simplifying equation (11)

$$\frac{\beta_{fb}}{X_1} = \frac{\left(\frac{c+d}{c}\right) \left(\frac{C_1}{A S}\right) \left(\frac{S^2}{\omega_L^2} + 1\right) (2\tau S + 1)}{\left(2\tau \frac{M_E C_3}{A^2} + \frac{2\tau}{\omega_L^2}\right) S^3 + \left(\frac{1}{\omega_L^2} + \frac{\tau C_1 A_1 M_E c}{K_1 A^2 d} + \frac{M_E C_3}{A^2}\right) S^2 + 2\tau S + 1} \quad (12)$$



5. SYSTEM ANALYSIS: (Continued)

5.4 Dynamic Analysis: (Continued)

5.4.3 Overall System Dynamics Stability Consideration: (Continued)

Now $\frac{1}{\omega_L^2} + \frac{C_3 M_E}{A^2} = \frac{1}{\omega_{PL}^2}$ as defined in (7). Therefore,

(12) can be written as

$$\frac{\beta_{fb}}{x_1} = \frac{\left(\frac{c+d}{c}\right) \left(\frac{C_1}{A s}\right) \left(\frac{s^2}{\omega_L^2} + 1\right) (2\tau_{S+1})}{\frac{2\tau}{\omega_{PL}^2} s^3 + \left(\frac{1}{\omega_{PL}^2} + \frac{\tau C_1 A_1 M_E c}{K_1 A^2 d}\right) s^2 + 2\tau_{S+1}} \quad (13)$$

The characteristic equation of (13) is a third order equation and can be expressed as

$$(\tau'_{S+1}) \left(\frac{s^2}{\omega'_{PL}{}^2} + \frac{2\zeta'_{PL}}{\omega'_{PL}} s + 1 \right) \quad (14)$$

Or multiplying the two bracketed terms, equation (14) can be rewritten as

$$\frac{\tau'}{\omega'_{PL}{}^2} s^3 + \left(\frac{1}{\omega'_{PL}{}^2} + \frac{2\zeta'_{PL} \tau'}{\omega'_{PL}} \right) s^2 + \left(\tau' + \frac{2\zeta'_{PL}}{\omega'_{PL}} \right) s + 1 \quad (15)$$

Comparing (15) to the denominator of (13)

$$\frac{2\tau}{\omega_{PL}^2} = \frac{\tau'}{\omega'_{PL}{}^2} \quad (16)$$



5. SYSTEM ANALYSIS: (Continued)

5.4 Dynamic Analysis: (Continued)

5.4.3 Overall System Dynamics Stability Consideration: (Continued)

$$\frac{1}{\omega_{PL}^2} + \frac{\tau_{C_1 A_1 M_E}^c}{K_1 A^2 d} = \frac{1}{\omega_{PL}'^2} + \frac{2\zeta_{PL}' \tau'}{\omega_{PL}'} \quad (17)$$

$$2\tau = \tau' + \frac{2\zeta_{PL}' \tau'}{\omega_{PL}'} \quad (18)$$

Referring to open loop plot on Figure 5.3.1,

$$\omega_{PL}' = 2\pi \times 6 \text{ Rad/Sec} \quad \text{with} \quad \zeta_{PL}' = 0.85$$

Further note that

- 1) ω_{PL}' , the natural frequency with D.P.F. is less than ω_{PL} , the natural frequency without D.P.F. From equation (18), 2τ should be greater than τ' for ζ_{PL}' to be positive and finite. From equation (16), therefore, ω_{PL} should be greater than ω_{PL}' .
- 2) ω_{PL} is a function of the effective actuator area and should be as small as required to meet the dynamic response.

After a number of trial and error solutions, ω_{PL} was selected as $2\pi \times 6.25$ cps. Desired $\omega_{PL}' = 2\pi \times 6$ cps and desired $\zeta_{PL}' = 0.85$.

Solving equations (16), (17), and (18) with

$$\omega_{PL} = 2\pi \times 6.25$$

$$\omega_{PL}' = 2\pi \times 6$$

$$\zeta_{PL}' = 0.85$$



5. SYSTEM ANALYSIS: (Continued)

5.4 Dynamic Analysis: (Continued)

5.4.3 Overall System Dynamics Stability Consideration: (Continued)

$$2\tau = 0.607 \text{ Sec.} \quad (19)$$

$$\tau' = 0.562 \text{ Sec.} \quad (20)$$

and

$$\frac{\tau C_1 A_1 M_E c}{K_1 A^2 d} = 0.025 \quad (21)$$

Actuator Area for Dynamic Performance

In order to provide $\omega_{PL} = 2\pi \times 6.25 = 39.3 \text{ cps}$ from equation (7)

$$\frac{1}{\omega_{PL}^2} = \frac{1}{\omega_L^2} + \frac{C_3 M_E}{A^2}$$

$$\left(\frac{1}{39.3} \right)^2 = \left(\frac{1}{\omega_L} \right)^2 + \left(\frac{C_3 M_E}{A^2} \right) \quad (22)$$

Where

$$\omega_L = \frac{1}{\sqrt{\frac{M_E}{K_S} + \frac{M_E}{K_E}}} = 2\pi \times 8 \text{ Rad/Sec.} = 50 \text{ Rad/Sec.}$$

as given in Figure 5.1.2.

C_3 is calculated from equation (20) in Section 5.4.2

$$C_3 = \frac{V_1}{2k P_1} = \frac{A (\beta_p \text{ max}) + (20\% \text{ for lines})}{2k P_1}$$

$$= \frac{A \times 1.5 \times 1.2}{2 \times 1.4 \times (0.8 \times 1600)}$$



5. SYSTEM ANALYSIS: (Continued)

5.4 Dynamic Analysis: (Continued)

5.4.3 Overall System Dynamics Stability Consideration: (Continued)

$$M_E = 3.337 \frac{\text{lb. sec}^2}{\text{in}}$$

Substituting numerical values in equation (22)

$$\frac{A \times 1.5 \times 1.2}{2 \times 1.4 \times (0.8 \times 1600)} \times \frac{3.337}{A^2} = \left(\frac{1}{39.3} \right)^2 - \left(\frac{1}{50} \right)^2 \quad (23)$$

Solving for the actuator area A from equation (23)

$$\underline{A = 6.75 \text{ In.}^2} \quad (24)$$

D.P.F. Network Design

From equation (21)

$$\frac{\tau_{11}^{C_1 A_1 M_E c}}{K_1 A^2 d} = 0.025$$

Where τ = D.P.F. Time Constant

$$\begin{aligned} &= \frac{A_1^2}{K_1} \frac{\rho_c}{K_o A_o} \quad \text{Sec. Equation (30) Sec. 5.4.2} \\ &= \frac{.607}{2} \quad \text{Sec. Equation (19) Sec. 5.4.3} \end{aligned}$$

$$\frac{c}{d} = \text{Link Ratio} = \frac{1}{3}$$

$$A = \text{Actuator Area} = 6.75 \text{ In.}^2$$

$$C_1 = \text{Control Valve Flow Gain} = 440 \text{ In}^3/\text{Sec}/\text{In.}$$

$$\begin{aligned} \rho_c &= \text{Air density at Ram Pressures of } 0.8 \times 1600 \text{ and} \\ &\quad \text{Room Temperature of } 70^\circ\text{F.} \\ &= 0.00376 \text{ Lbs}/\text{In}^3 \end{aligned}$$

$$K_o = \text{Linear Constant of Proportionality for the D.P.F. Orifice in } \frac{1}{\text{sec.}}$$



5. SYSTEM ANALYSIS: (Continued)

5.4 Dynamic Analysis: (Continued)

5.4.3 Overall System Dynamics Stability Consideration: (Continued)

$$\frac{K_o A_o}{\rho_c} = \frac{\delta_Q}{\delta_P} \text{ of the D.P.F. orifice}$$

Rewriting the above equation (21) with numerical substitutions

$$\frac{A_1}{K_1} = \frac{(.025) A^2 d}{\tau^c_{c1} M_E c} = \frac{(.025) (45.56) (3)}{(.303) (440) (3.337)} = 0.0077$$

$$\frac{A_1^2}{K_1} \frac{\delta_P}{\delta_Q} = 0.303$$

Selecting $A_1 = 0.585 \text{ in}^2$ and solving above equations

$$K_1 = \frac{A_1}{0.0077} = \frac{0.585}{0.007} = 76 \text{ lbs/in}$$

$$\frac{\delta_P}{\delta_Q} = \frac{\tau^K_{c1}}{A_1^2} = \frac{(.303) 76}{0.342} = 67 \frac{\text{lbs-sec}}{\text{in}^5}$$

The orifice sizing is computed from $\frac{\delta_P}{\delta_Q}$ of the orifice. The next paragraph shows that $(\Delta P_a - \Delta P_b)_{\text{max.}}$ is normally 100 psi. The steady state pressure on the two sides of the piston is 1280 psi.

$$\therefore P_{a \text{ max.}} = 1330 \text{ psi}$$

$$P_{b \text{ min.}} = 1230 \text{ psi}$$

Volumetric flow through the orifice is

$$\begin{aligned} Q_{\text{max.}} &= \frac{(\Delta P_a - \Delta P_b)_{\text{max.}}}{\frac{\delta_P}{\delta_Q}} \\ &= \frac{100}{67} = 1.5 \text{ in}^3/\text{Sec.} \end{aligned}$$



5. SYSTEM ANALYSIS: (Continued)

5.4 Dynamic Analysis: (Continued)

5.4.3 Overall System Dynamics Stability Consideration: (Continued)

The air density at 1280 psi is 0.00376 \#/In^3 . Assuming the density does not change much for $\pm 50 \text{ psi}$, the weight flow through the orifice is

$$\begin{aligned} \dot{W} &= 1.5 \times 0.00376 \text{ \#/In}^3 \\ &= 0.0056 \text{ \#/Sec.} \end{aligned}$$

The orifice size for

$$P_u = 1330 \text{ psi}$$

$$P_d = 1230 \text{ psi}$$

$$\frac{P_d}{P_u} = 0.925$$

$$\dot{W} = 0.0056$$

$$k = 1.4$$

$$C_d = 0.65$$

$$T = 530^\circ$$

is 0.026 Inches Diameter.

Actuator ΔP

The dynamic force on the actuator is calculated as follows.

Assuming maximum of 15% input at 5 cycles/sec., the maximum output acceleration is

$$\begin{aligned} \alpha_{\text{max.}} &= 0.15 \times (1.5) (2\pi \times 5)^2 \\ &= 222 \text{ In/Sec.}^2 \end{aligned}$$



5. SYSTEM ANALYSIS: (Continued)

5.4 Dynamic Analysis: (Continued)

5.4.3 Overall System Dynamics Stability Consideration: (Continued)

$$\begin{aligned}\text{The maximum force} &= 222 \times M_E \\ &= 222 \times 3.337 \\ &= 740 \text{ Lbs.}\end{aligned}$$

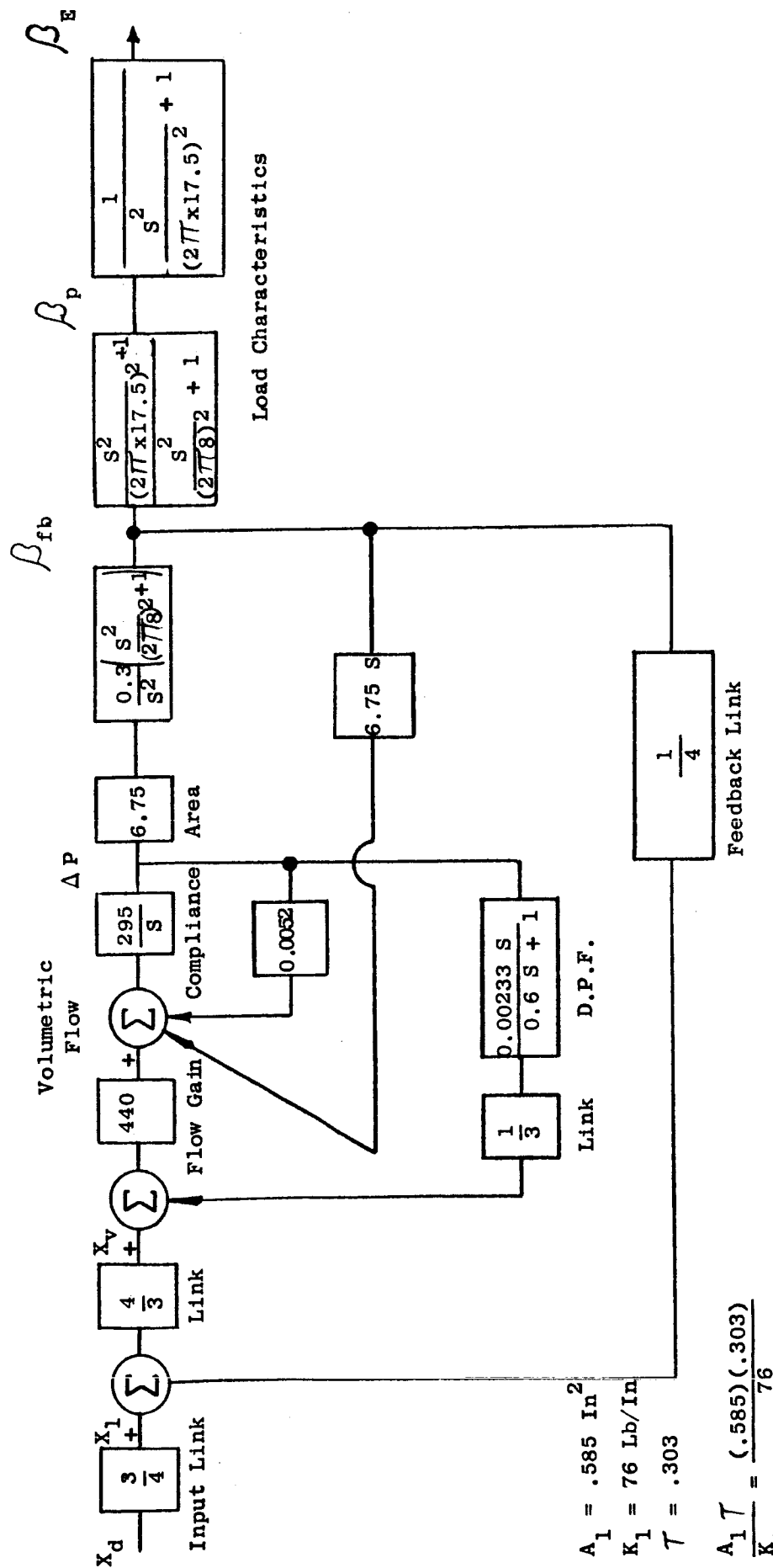
$$\text{The actuator area} = 6.75 \text{ In.}^2$$

$$\text{Therefore the maximum } P = \frac{740}{6.75} = 110 \text{ psi}$$

This simple analysis shows that because of the large actuator area, the load ΔP is fairly small compared to the available 1600 psi. It may be recalled that the actuator area was closer to a 6.75 In.², to meet dynamic requirements. Because the pressure on the two sides of the piston varies by a maximum of ± 50 psi, the gas density is more or less constant (change = $\frac{50}{1280} \times 100 = 3.9\%$). This behavior of the system permits linear analysis to yield very accurate results.

System Block Diagram With Numerical Values

Figure 5.4.3.3 shows the transfer function block diagram of Figure 5.4.3.2 with numerical values.



TRANSFER FUNCTION BLOCK DIAGRAM

FIGURE 5.4.3. 3



5. SYSTEM ANALYSIS: (Continued)

5.5 Computer Analysis: (Power Servo)

5.5.1 General:

The power servo was analyzed on the 150 amplifier pace computer.

The following presentation of the computer study was performed on the assumption of hydrogen as the working fluids at -260°F. The kinematic relationships also were slightly different than presently incorporated in the system. However, the loop gain and the dynamics were the same. The prime purpose of the computer study was to investigate the effects of the non-linearities and the optimum D.P.F. network gain and time constant.

5.5.2 Terminology:

K_1	Input Linkage Ratio = $\frac{X_v}{X_d}$	=	0.2 In/In.
K_v	Valve Flow Gain = $\frac{W_a}{X_v}$	=	$\frac{0.04 \text{ \#/Sec.}}{0.02 \text{ -- nominal}}$
W_a	Mass Flow Into Chamber (a)		\#/Sec.
W_b	Mass Flow Into Chamber (b)		\#/Sec.
T_s	Gas -- Supply Temperature		200° R
k	Ratio of Specific Heats		$\frac{C_p}{C_v} = 1.7$
C_p	Specific Heat of Gas at Constant Pr.		$1.135 \times 10^7 \frac{\text{In.}}{\text{Sec}^2 \text{ } ^\circ \text{R}}$
R	Gas Constant for Hydrogen		$3.5 \times 10^6 \frac{\text{In.}}{\text{Sec}^2 \text{ } ^\circ \text{R}}$
A	Actuator Area		6.75 In^2
P_a	Pressure In Chamber (a)		psi
P_b	Pressure In Chamber (b)		psi



5. SYSTEM ANALYSIS: (Continued)

5.5 Computer Analysis: (Continued)

5.5.2 Terminology: (Continued)

P_s	Supply Pressure	1600 psi
P_R	Return Pressure	0
K_E	Engine/Load Spring	40,000 #/In.
K_s	Structure Spring	10,418 #/In.
M_E	Engine/Load Mass	3.337 # $\frac{\text{Sec.}^2}{\text{In.}}$
β_a	Actuator Housing Motion	In.
β_E	Load Motion	In.
β_p	Actuator Piston Motion	In.
D	Load Viscous Damping	16.65 Lbs/In/Sec.
F_{CL}	Friction - Coulomb	200 Lbs.
τ	Compensation Network Time Constant	0.1 Sec. Nominal
K_{f1}	Position Feedback $\frac{X_v}{\beta_a + \beta_b}$	0.066 $\frac{\text{In.}}{\text{In.}}$
K_{f2}	Dynamic Pressure Feedback = $\frac{X_v}{\text{psi across piston \#2}}$	0.00045 $\frac{\text{In.}}{\text{psi}}$
X_v	Valve Spool Travel	Nominal
		In.

5.5.3 Basic Equations:

(1) Control Valve

$$W_a = f_v (X_v, P_a)$$

$$W_b = f_v (-X_v, P_b)$$



5. SYSTEM ANALYSIS: (Continued)

5.5 Computer Analysis: (Continued)

5.5.3 Basic Equations: (Continued)

(2) Actuator Chambers

$$W_a T_s - \frac{g P_a}{C_p} \frac{d V_a}{dt} = \frac{g}{k R} \frac{d}{dt} (P_a V_a)$$

$$W_b T_s - \frac{g P_b}{C_p} \frac{d V_b}{dt} = \frac{g}{k R} \frac{d}{dt} (P_b V_b)$$

(3) Load

$$F = (P_a - P_b) A$$

$$\begin{aligned} F &= K_s \beta_a \\ &= K_E (\beta_p - \beta_E) \\ &= \frac{d^2 X_E}{dt^2} + D \frac{d X_E}{dt} + F_c \end{aligned}$$

$$F_c = \text{Friction Force}$$

$$\begin{aligned} &\frac{d \beta_E}{dt} \\ &= \frac{\left(\frac{d \beta_E}{dt} \right)}{\left(\frac{d \beta_E}{dt} \right)} F_{CL} ; \quad F_{CL} = \text{Constant} \end{aligned}$$

(4) Actuator Volumes

$$V_a = V_1 + A(\beta_a + \beta_p)$$

$$V_b = V_1 - A(\beta_a + \beta_p)$$

(5) Valve Motion

$$X_v = k_1 X_d - k_{f1} (\beta_a + \beta_p) - K_{f2} \frac{(\tau_s)}{(2\tau_s + 1)} (P_a - P_b)$$

Weston Hydraulics Limited



5.5.4 Variables - Scale Factors:

<u>VARIABLE</u>	<u>SYMBOL</u>	<u>UNITS</u>	<u>MAX. ANTICIPATED VALUE</u>	<u>SCALE FACTOR</u>
Input	X_d	Inches	0.5"	100 V/In.
Output	β_p	Inches	1.5"	40 V/In.
Output Velocity	$\dot{\beta}_p$	Inches/Sec.	6 In/Sec	5 V/In/Sec.
Output Acceleration	$\ddot{\beta}_p$	Inches/Sec. ²	150 In/Sec	-----
Output Force	F	Lbs.	10,800 Max. (Working Force 2000 Lbs.)	0.01 V/#
Spool Travel	X_1	Inches	0.1" Flow Saturation at 0.02"	500 V/In.
Gas Flow	W_a, W_b	Lbs/Sec.	0.04 #/Sec.	1000 V/#/Sec.
Flow x Temperature	$W_a T_s$	$\frac{\text{Lbs. } ^\circ\text{R}}{\text{Sec.}}$	8 $\frac{\text{# } ^\circ\text{R}}{\text{Sec.}}$	5 V $\frac{\text{# } ^\circ\text{R}}{\text{Sec.}}$
Pressure	P_a, P_b	Lbs/In^2	1600 psi	.05 V/#/In ²
Volume	V_a, V_b	In ³	25 In ³	2 V/In ³
Pressure x Volume	$P_a V_a, P_b V_b$	Lb-In.	40,000	0.001 V/# In.



5. SYSTEM ANALYSIS: (Continued)

5.5 Computer Analysis: (Continued)

5.5.5 Computer Results:

- (1) The power servo was unstable without D.P.F. network.
- (2) The response is a function of the loop gain and the D.P.F. gain.
- (3) The relative change in response was greater for the D.P.F. gain variation.
- (4) The D.P.F. time constant variations produced very slight changes in the response. The servo response was nearly the same for time constant changes from 0.05 to 0.5 sec.

- (5) The desired response was achieved with

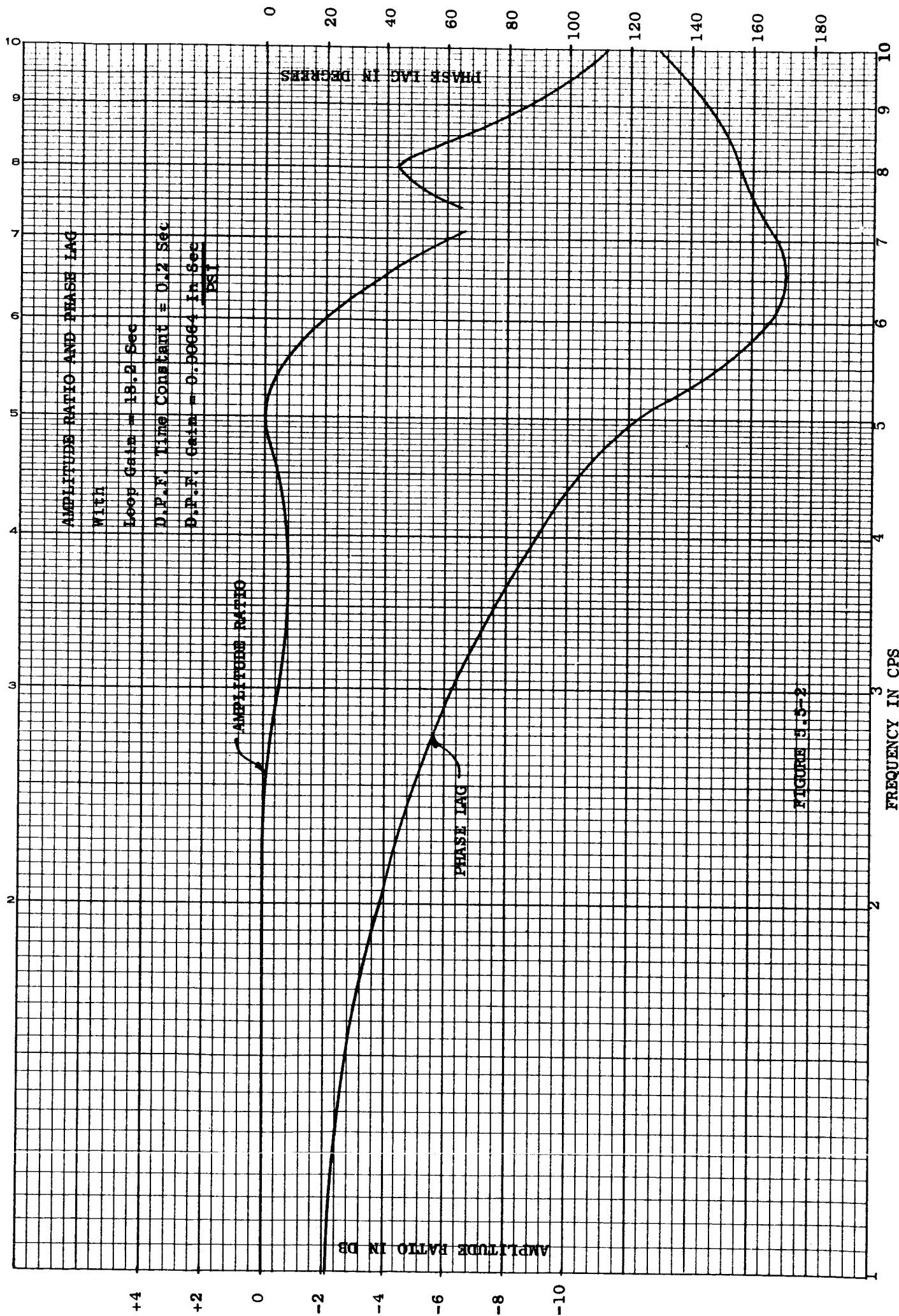
Loop Gain = 18.2 Sec.^{-1}

D.P.F. Time Constant = 0.2 Sec.

D.P.F. Gain = $0.00064 \frac{\text{In. Sec.}}{\text{psi}}$

Figure 5.5.1 and 5.5.2 shows the step response and the frequency response results of the computer study.

- (6) The ΔP across the actuator, under worst dynamic conditions, approached 150 psi.



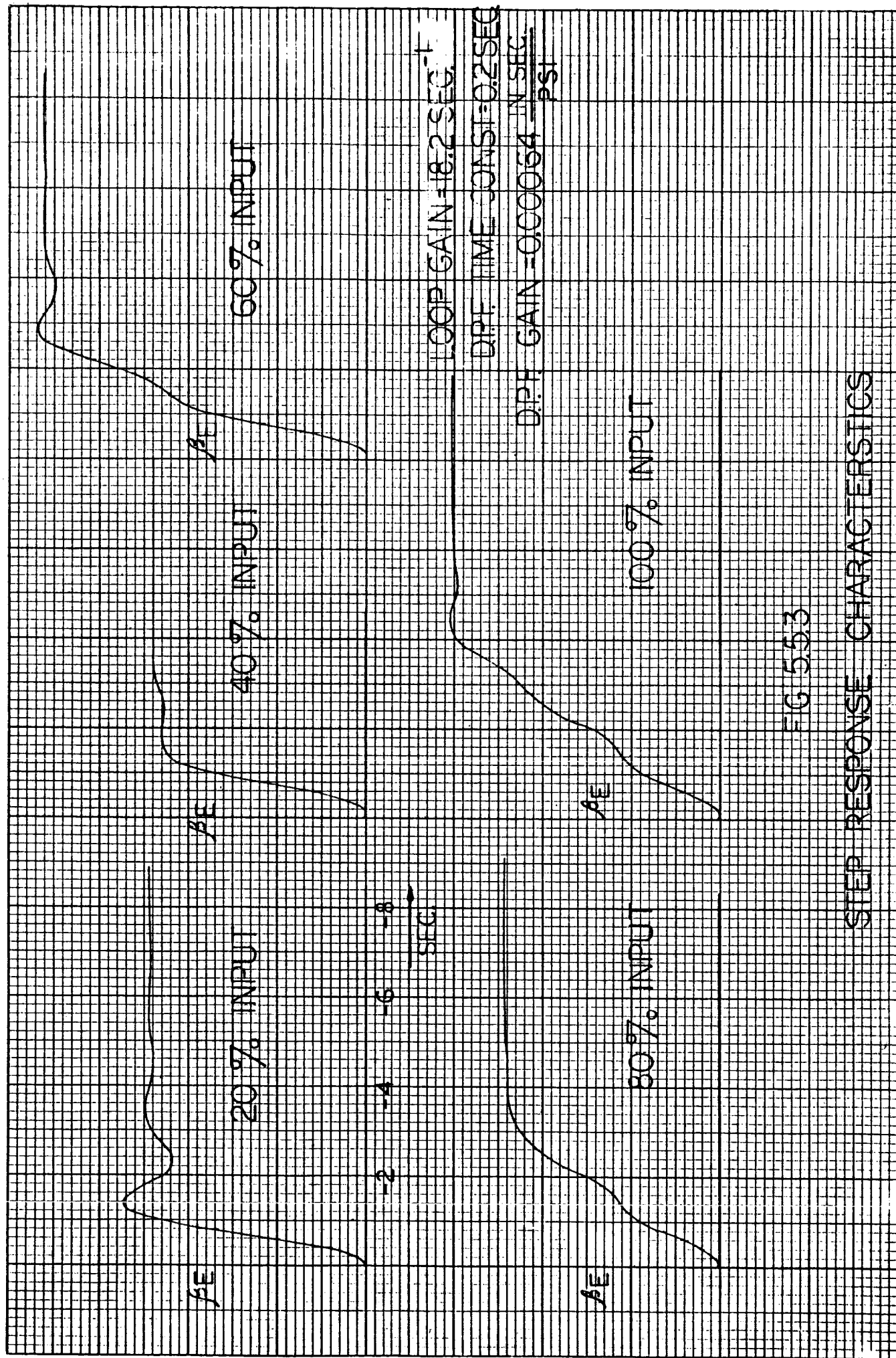


FIG 553

STEP RESPONSE CHARACTERISTICS



6. COMPONENT DESCRIPTION:

6.1 Stepper Motor:

The Stepper Motor is an "IMC Magnetics Corporation" variable reluctance three phase motor. The step angle is 15° per pulse and is capable of pulse rates exceeding 300 pps bi-directionally under required encoder loading. The motor operates at 28 VDC with an input power rating of 10 watts.

The Stepper Motor is mounted to one housing section of the encoder assembly. The output pinion gear vs the binary code gear ratio was selected to convert the 15° step output of the motor to 10° steps of the binary disk.

The motor and the controller schematic is shown in Figure 6.1.1. The schematic shows six diodes and two resistors. The diodes function to energize two windings of the motor at a time. This feature is necessary to obtain smooth motor performance in the 0 - 100 pps range. The resistors are included to balance the windings so that the motor may take equal steps.

6.2 Encoder:

The Encoder assembly consists of the binary disk and spacer plate sandwiched between two housing sections. Each housing is a sub-assembly containing 4 pilot valves and 4 orifice assemblies. Each pilot valve is a dome operated 3 way, 2 position valve. The housings are aluminum alloy anodized and are internally ported. The spacer plate is CRES and is lap finished to minimize external leakage and to control the gap of the binary disk running between the two housings. The binary disk is 303 CRES and is fabricated from a purchased precision gear. One half of the twin 4 channel binary code is milled .020 inches deep on each side of the gear disk. The disk is final lapped to obtain size and finish necessary for proper operation. The binary disk pivots on a teflon bushing which is mounted in one housing section.

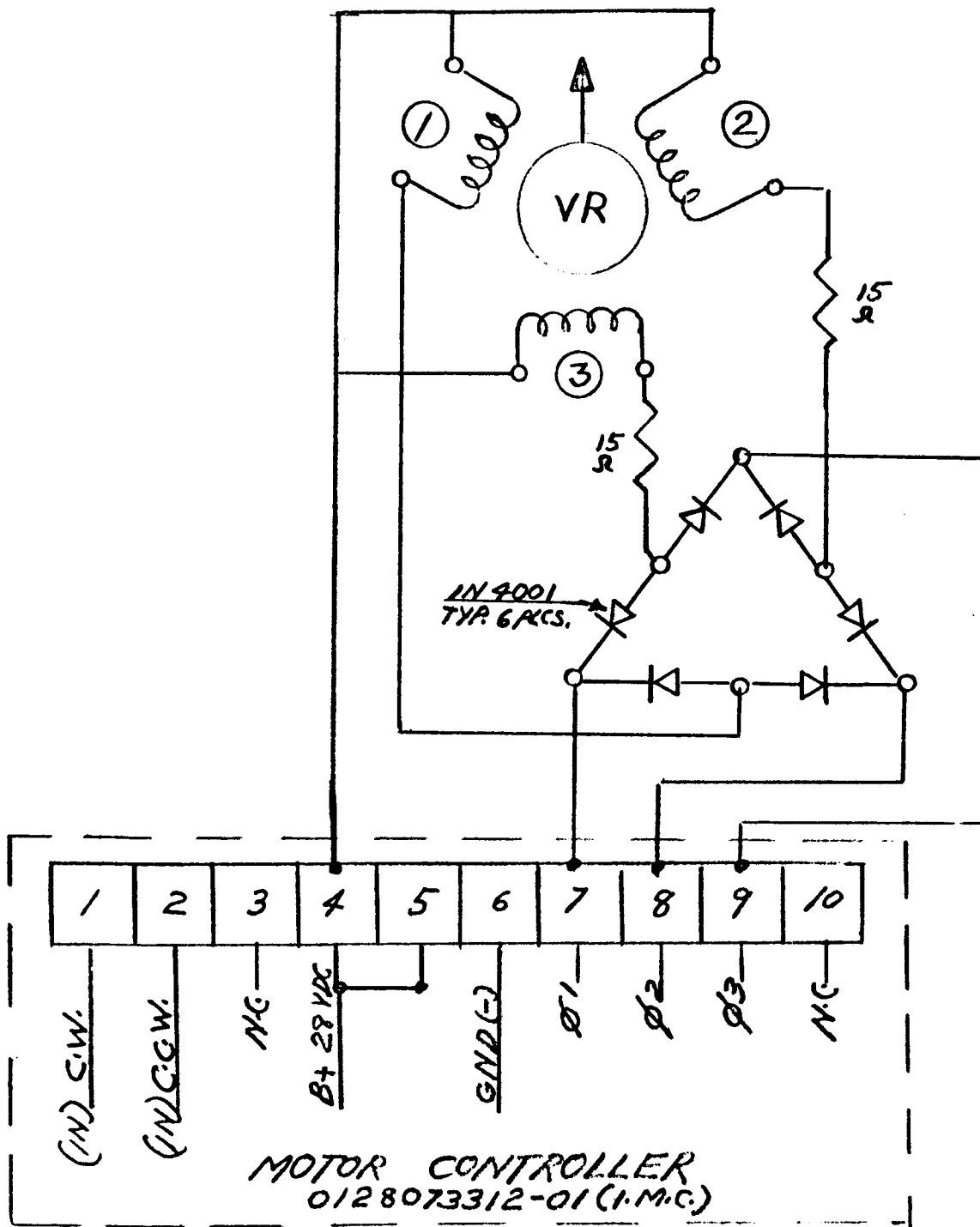


FIG. 6.1.1



6. COMPONENT DESCRIPTION: (Continued)

6.2 Encoder: (Continued)

The pilot valves are CRES throughout, the spring being 17-7 PH CRES. The seats are hardened 17-4 PH with hardened balls which function as poppets. The valves incorporate one dynamic seal which is teflon.

The primary orifices are easily removable for any orifice diameter adjustments to obtain optimum operation during prototype testing. Both the disk pressure inlet and the pilot valve pressure inlet in each housing are fitted with filters rated at 2 micron nominal, 10 micron absolute.

6.3 P.B.D.A.:

The Digital Actuator is composed of an anodized aluminum housing containing individual adders corresponding to each 4 channels of both twin codes, making a total of 8. The adders are made of 17-4 PH CRES heat treated to 190,000 psi tensile strength. The adders are linked to each other in a hook and groove manner. Each adder incorporates two "shrink-fit" teflon riding lands which provide low friction and some sealing in addition to teflon piston rings. The output adder (last in the chain) has link pivot provisions for attaching to the power servo package.

6.4 Power Servo Package:

The Power Servo unit consists of two main housings which are anodized aluminum. One contains the control valve, the dynamic power feedback (D.P.F.), and the input bungee assembly. The other housing contains the main ram and is bolted to the control valve housing using "O" ring face seals for interconnection.

Weston Hydraulics Limited



6. COMPONENT DESCRIPTION: (Continued)

6.4 Power Servo Package: (Continued)

6.4.1 Control Valve:

The Control Valve is a typical spool-sleeve type fabricated as a mating lapped assembly from 440 C CRES. Spool to sleeve diametral clearance is held to .000150 - .000200 inches on all lands. Eccentricity and/or out of roundness does not exceed .000025 tir. The control valve input features a unique ball joint connection which eliminates misalignment.

6.4.2 D.P.F.:

The Dynamic Pressure Feedback damping network is composed of 2 spring balanced pistons and a pivot arm which provides feedback to the control valve input linkage system. One piston has an orifice which is removable to facilitate testing. The pistons are anodized aluminum and incorporate two "shrink fit" teflon riding lands identical to those on each adder of the digital actuator. The pivot arm is CRES and has a highly polished ball end pivoting in a nylon bushing contained in one of the pistons. The springs are 17-7 PH CRES.

6.4.3 Main Ram:

The main actuator piston is 17-4 PH CRES heat treated to 190,000 psi tensile strength. The piston uses standard "O" ring with teflon channel seal combination for dynamic seals. The output end is a standard ball type rod end bearing. The opposite end of the piston provides a roller bearing pivot for direct connection to feedback linkages.

Weston Hydraulics Limited



6. COMPONENT DESCRIPTION: (Continued)

6.4 Power Servo Package: (Continued)

6.4.4 Bungee Assembly:

The Bungee Assembly is contained in an anodized aluminum housing connected in series with the control valve input linkages and provides damping in both direction. The spring is 17-7 PH CRES.

6.4.5 Linkages:

All connecting linkages are made of anodized aluminum and are fitted with bronze bushings to provide maintenance-free operation.

6.5 Instrument Servo:

Because of the added expense of acquiring an analog to digital converter to drive the stepper motor, an alternate method was chosen. This alternate drive is the instrument servo. It consists of an "Inland" DC amplifier with matching DC torque motor with feedback accomplished through a gear reduction and rotary potentiometer. Sinusoidal input is supplied by a function generator. The instrument servo output is directly coupled to the stepper motor shaft which is free-running (not energized). This type of drive does not provide discrete positioning of the binary disk as would the stepper motor, however the simulation is comparable enough to obtain necessary data.

A schematic of the entire actuator, with both input systems, is shown on Figure 6.

SCHEMATIC - NASA P27160 ACTUATOR & TEST EQUIPMENT

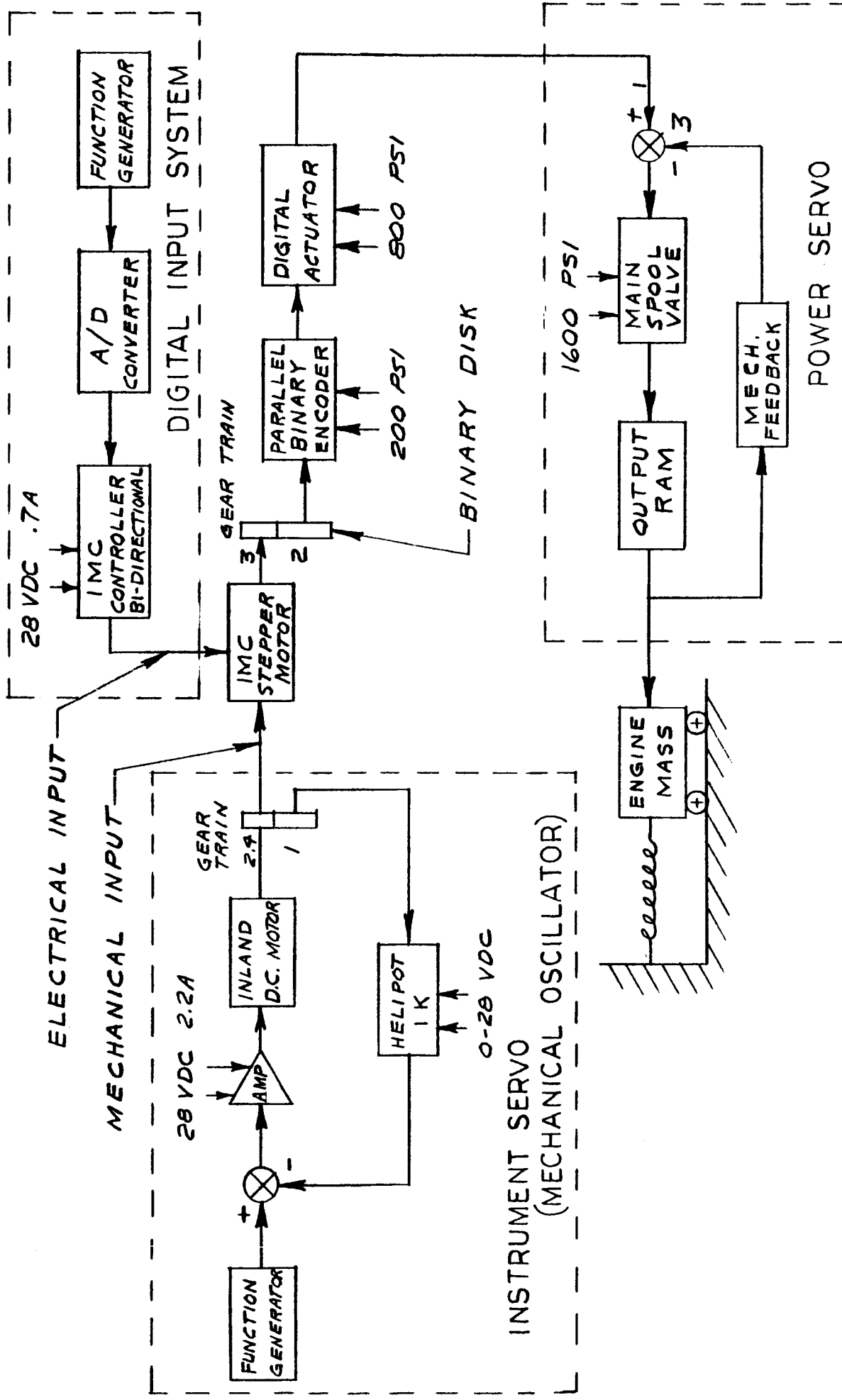


FIG. 6.



6. COMPONENT DESCRIPTION: (Continued)

6.6 Load Simulator Fixture:

The purpose of the load simulator fixture was to allow dynamic performance testing of the digital actuator assembly under conditions simulating the spring-mass characteristics, i.e. natural frequency, of a gimballed engine, the moment arm of the actuator, and system damping. Specifically, the requirements were:

$$\text{Engine Mass} = M_e = 3.337 \text{ lb-sec}^2/\text{in}$$

$$\text{Engine Spring} = K_e = 40,000 \text{ lbs/in}$$

$$\text{Structural Spring} = K_s = 10,418 \text{ lbs/in}$$

$$\text{Equivalent Load Spring} = K_L = \underline{8290} \text{ lbs/in}$$

$$\text{Moment Arm of Engine Pivot} = L_e = 20.6 \text{ in}$$

$$\text{Load Natural Frequency} = f_m = 7.95 \text{ cps}$$

$$\text{Load Damping} = \zeta = 0.05 \text{ (20 DB Minimum Overshoot)}$$

Weston's load simulator fixture was basically an "A-Frame" supporting a simple pendulum to simulate the engine; the actuator was rigidly attached to the pendulum a distance L_e down from the pendulum pivot point and attached to the structure (ground) via a plate spring that simulates K_L . The pendulum was a 8 x 6 1/2 WF beam, 60 inch long, with about 118 lbs of "point mass" located 60 inch from the pivot point. The calculated equivalent mass of the pendulum was 3.53 lb-sec²/in. The spring rate of the pendulum was in excess of 600,000 lbs/in. The equivalent load spring was a fixed-fixed beam plate having a calculated spring rate of about 9000 lbs/in.

The rotation of the simulated engine about null was measured with a rotary potentiometer attached via a pulley to the pivot point of the pendulum. Displacement of the Actuator piston relative to the Actuator was measured with a linear potentiometer attached to the Actuator.



6. COMPONENT DESCRIPTION: (Continued)

6.6 Load Simulator Fixture: (Continued)

Figure 6.6.1 is a sketch showing schematically how the system was installed.

Tests were conducted to measure the natural frequency and damping of the load simulator. The actuator was replaced with a bar having a spring rate in excess of 1,500,000 lbs/in. A linear potentiometer was attached to the bottom of the simulated load. The load was then struck with a soft mallet and allowed to vibrate at the spring-mass system natural frequency. From the displacement versus time trace, the parameters of interest were measured. The curve of Figure 6.6.2 is a representative trace. From this trace, the natural frequency was measured as:

$$f_m = \frac{5 \text{ cycle}}{.62 \text{ secs}} = 8.05 \text{ cps}$$

The damping ratio was computed from the equation:

$$\zeta = \frac{\frac{1}{2\pi} \ln A_1/A_2}{\sqrt{1 + (1/2\pi \ln A_1/A_2)^2}}$$

A_1 = Magnitude of first overshoot

A_2 = Magnitude of second overshoot

$$= \frac{\frac{1}{2\pi} \ln 13/7.5}{\sqrt{1 + (1/2\pi \ln 13/7.5)^2}}$$

= .0875 (Equivalent to about 15 DB overshoot.)

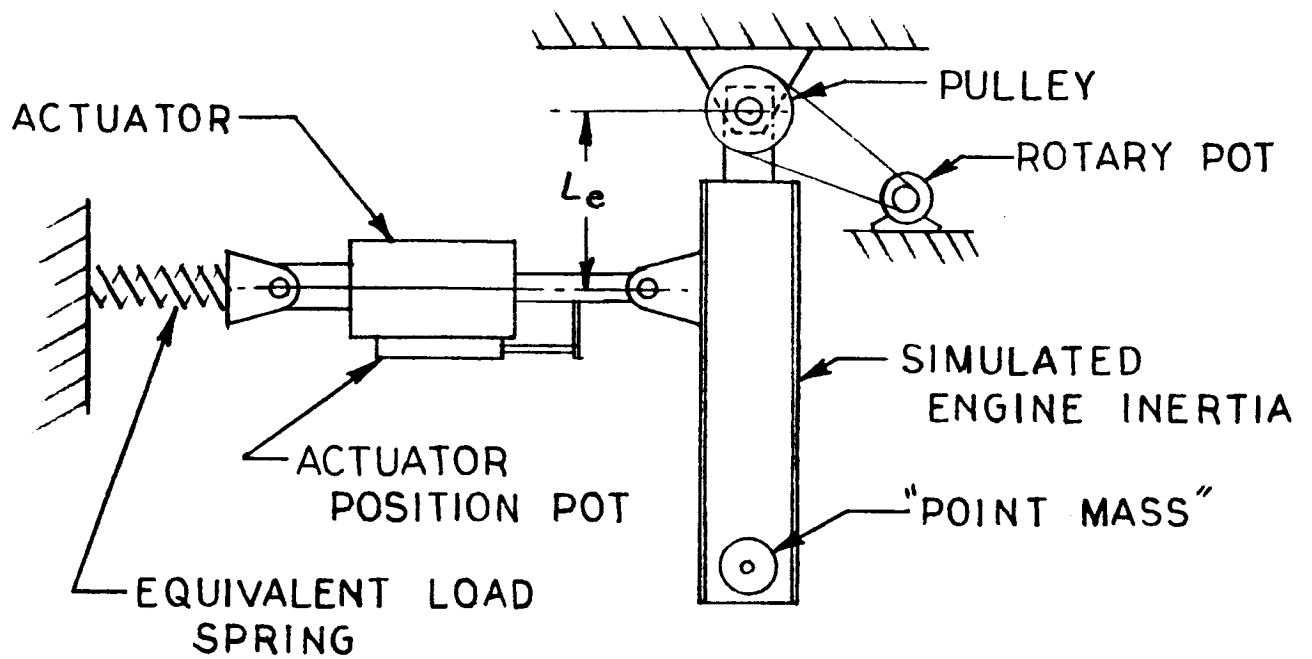


FIG. 6.6.1

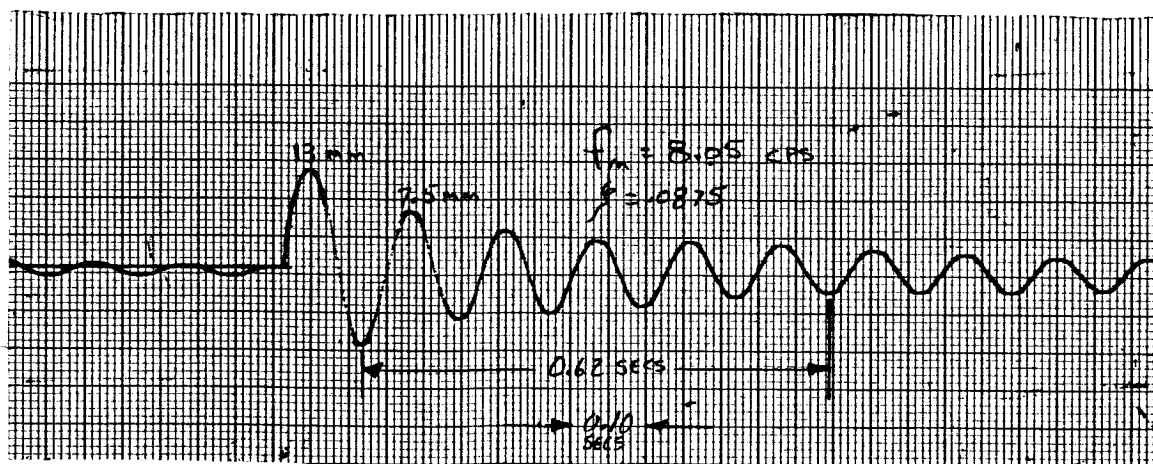


FIG. 6.6.2



7. TEST RESULTS:

7.1 General:

Initial testing was conducted on a component basis. This was necessary because of the unique and original design of most components and also the complexity of the total system. Upon completion of satisfactory performance by each component, step by step combining and testing of sub-assemblies was performed. Position transducers and pressure transducers were used in conjunction with a Sanborn 4 track oscillograph and a Hewlett-Packard oscilloscope with a Polaroid scope camera to observe and record data. A light beam oscillograph was used to record the step input response.

7.2 Power Servo:

All testing of the power servo was conducted installed in the load simulator fixture (See Section 6.6). Before final testing of the complete system, preliminary tests were performed with the power servo using an electro-mechanical sinusoidal input which consisted of a variable speed motor driving a cam linkage.

The dynamic performance of the system was established by frequency response tests conducted upon the analog portion (power servo) of the unit. The tests were performed with the digital actuator and pneumatic encoder removed to facilitate the imposition of the sinusoidal command to the system.

Position transducers were attached to the input, the actuator output, and the load. The load transducer was a rotary potentiometer which monitored the swing of the load about its pivot. The phase and amplitude relationship between these three variables was recorded with input frequencies ranging from 0.75 cps to 6.0 cps. The input supply pressure was 1600 psi.



7. TEST RESULTS: (Continued)

7.2 Power Servo: (Continued)

Figures 7.2.1 and 7.2.2 present frequency response and phase lag curves which were reduced from the data taken. Figure 7.2.2 is the no load condition. Typical samples of this data are shown in Figures 7.2.3 and 7.2.4.

Several sets of data were recorded using different orifice and spring rate combinations in the D.P.F. piston network. The most desirable combination was a .031 diameter orifice with 30 lb/in. springs which very closely approximates the analytical results.

Changing spring rates from 30 lb/in. to 38 lb/in. to 45 lb/in. resulted in no appreciable change. However, any variance in orifice diameter larger or smaller by more than .005 produced less damping, therefore resulting in increasing degrees of instability of the system.

An attempt was made to operate the power servo by blocking the D.P.F. network mechanically and also pneumatically. In either case, with the application of any input to the control valve, the load (and actuator) instantaneously began to oscillate violently requiring immediate shutdown by dumping the supply pressure. This very vividly demonstrated the need for the D.P.F. network in this system.

7.3 Encoder:

Prior to assembly into the encoder, each pilot valve was tested to assure its performance. Individual data and installation position is shown in Figure 7.3.1. This was accomplished in a separate test fixture. The operation of the binary disk assembled between the encoder housings was verified by monitoring signal

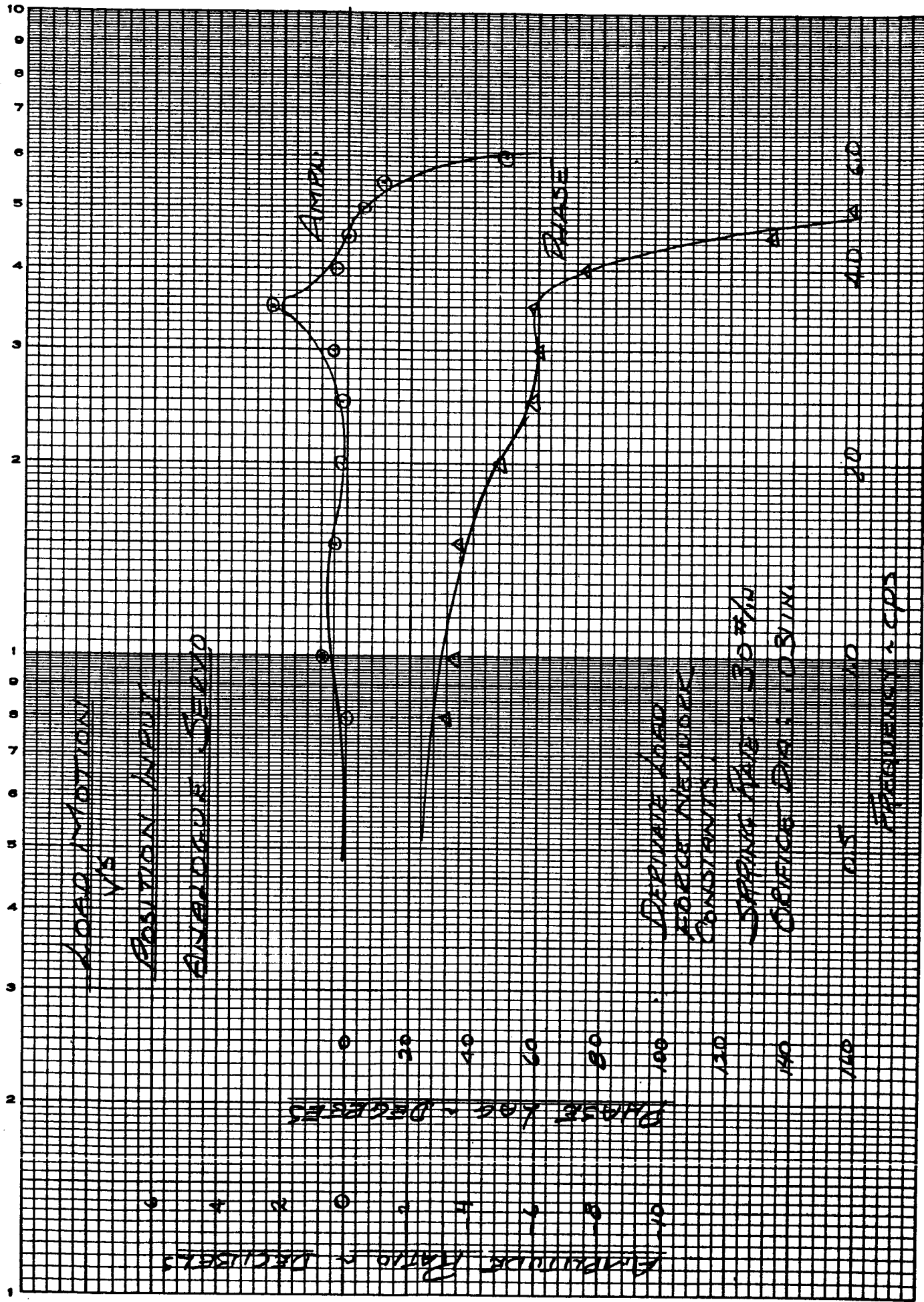


FIG. 7.2.1

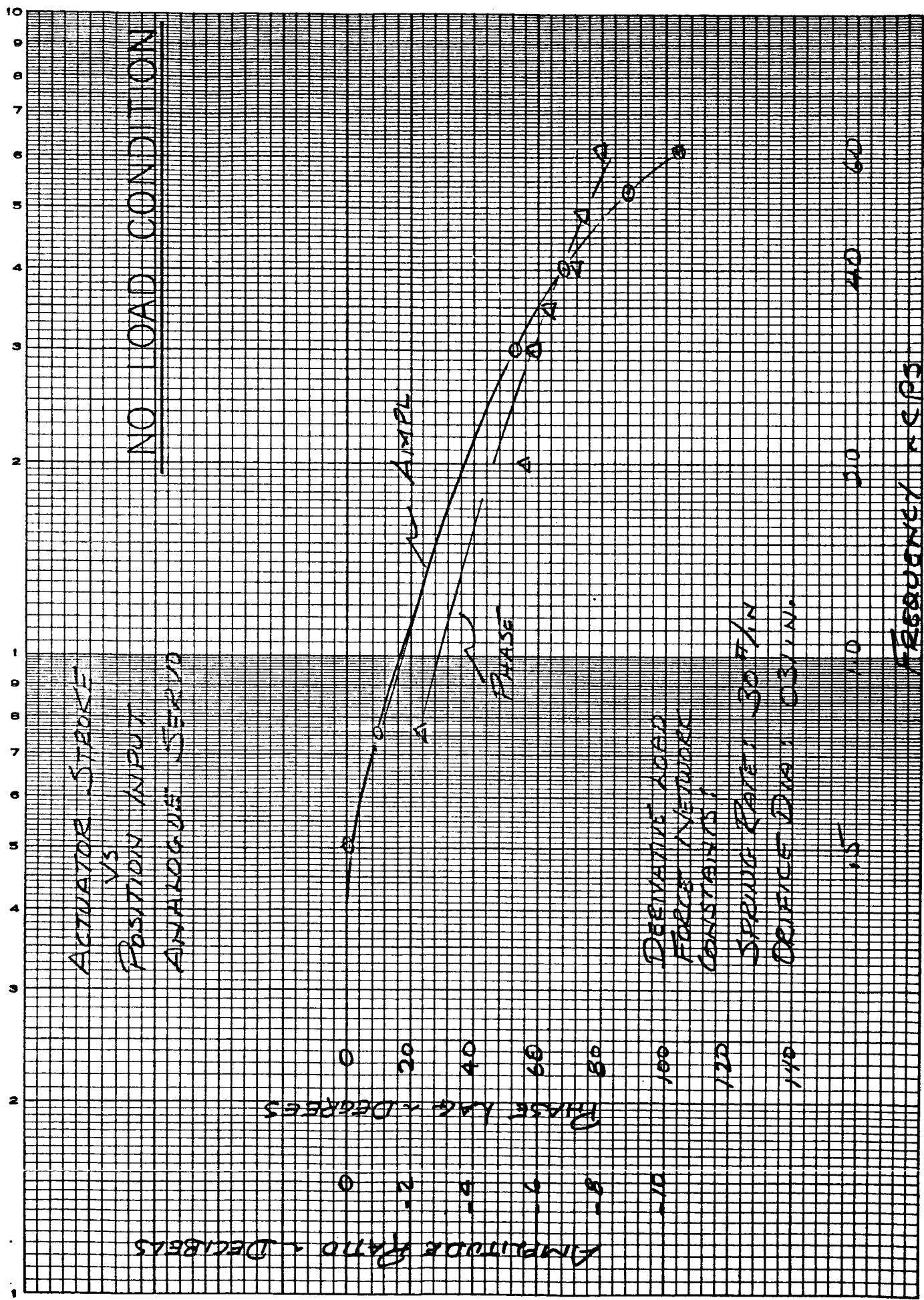
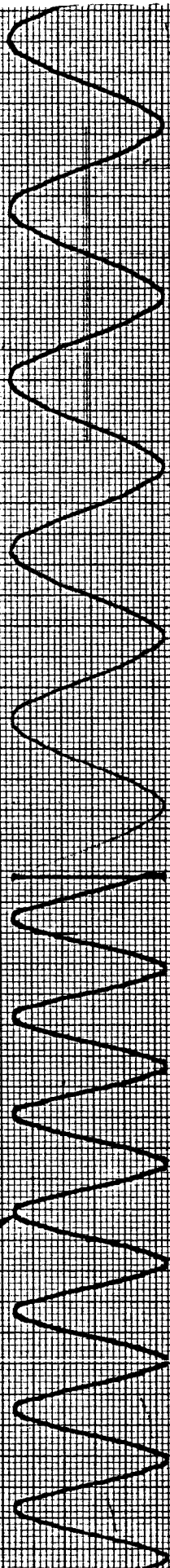
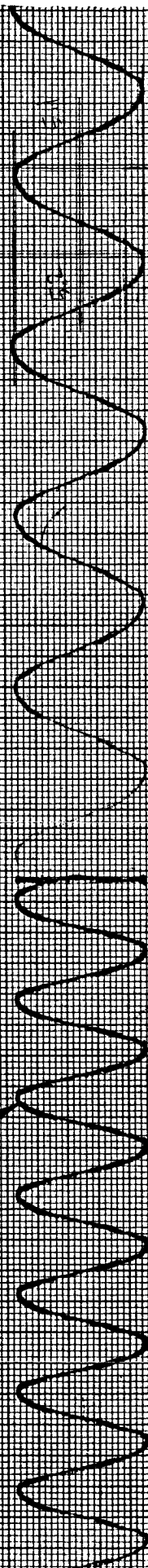


FIG. 7.2.2.

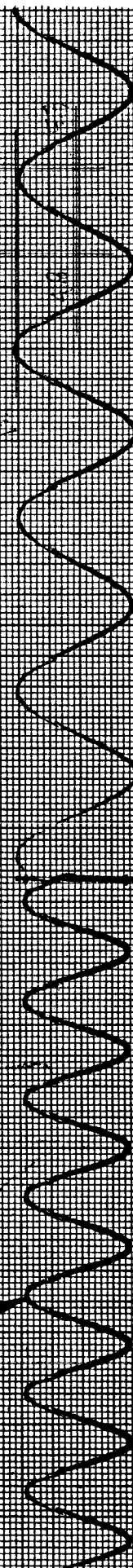
INPUT



ACTUATOR



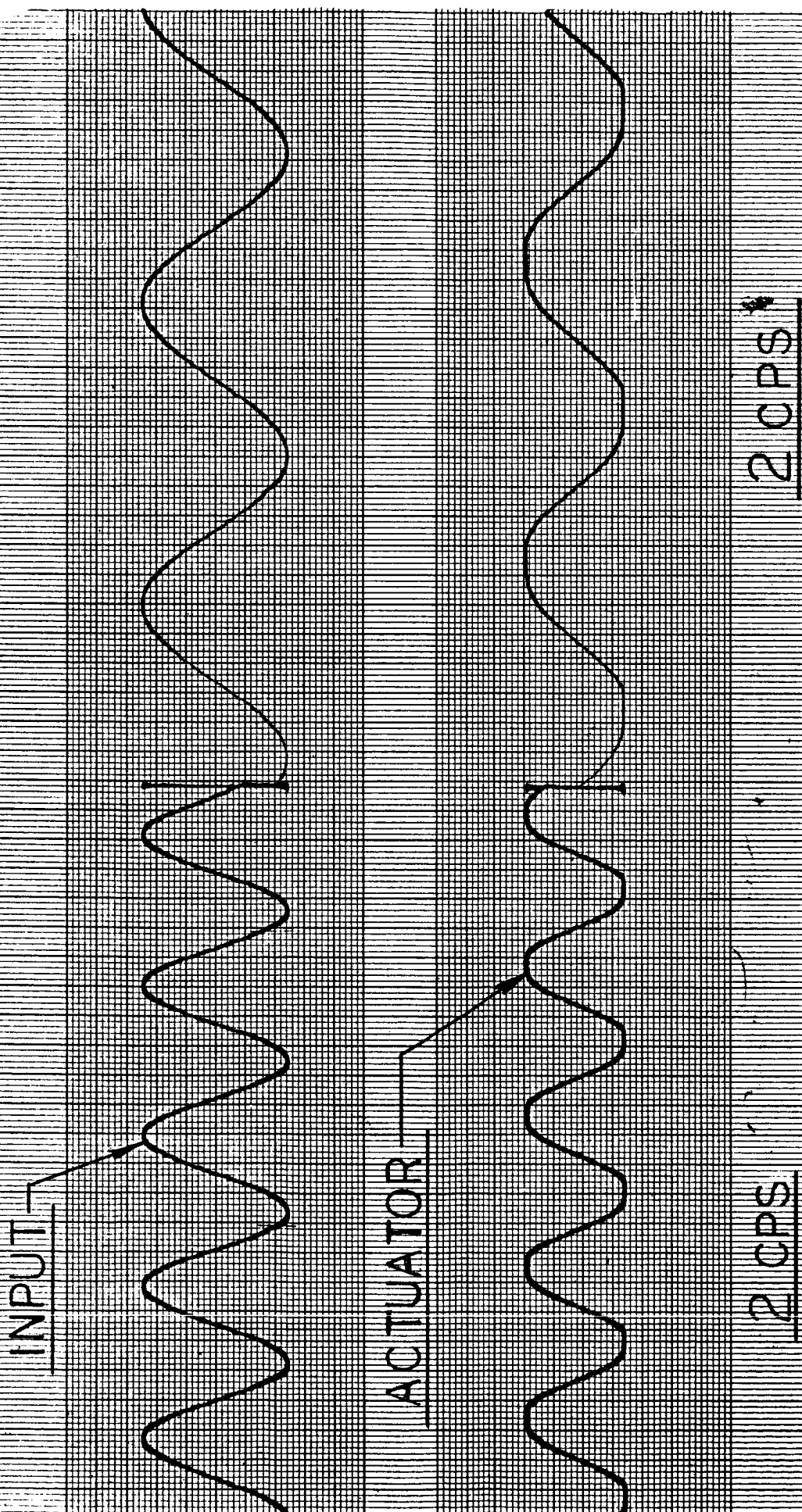
LOAD



3.3 CPS

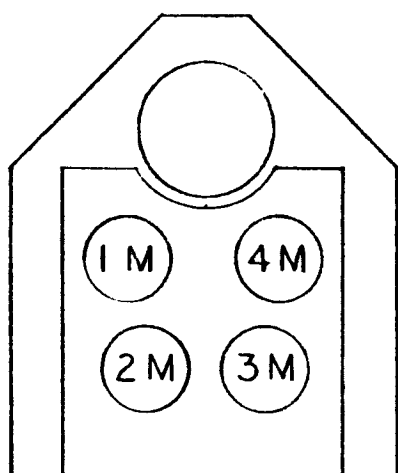
3.6 CPS

FIG. 7.2.3



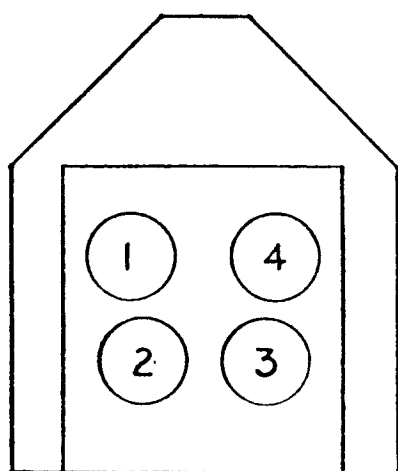
NO LOAD CONDITION

FIG. 7.2.4



HOUSING, LEFT
(MOTOR)
NORMALLY OPEN

VALVE NO.	ACTUATION P.S.I.	DE-ACTUATION P.S.I.
1 M	115	80
2 M	110	75
3 M	115	80
4 M	115	75

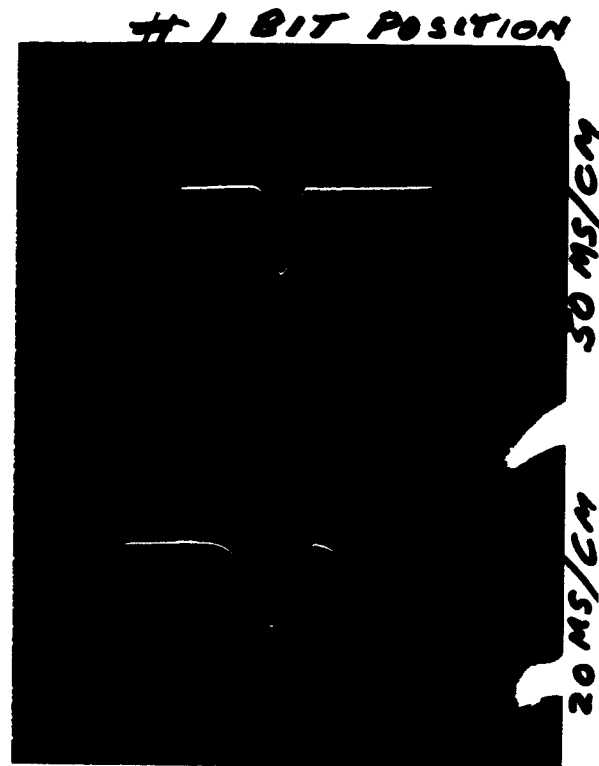


HOUSING RIGHT
NORMALLY CLOSED

1	125	90
2	120	85
3	115	85
4	120	90

PILOT VALVE INSTALLATION

FIG. 7.3.1.

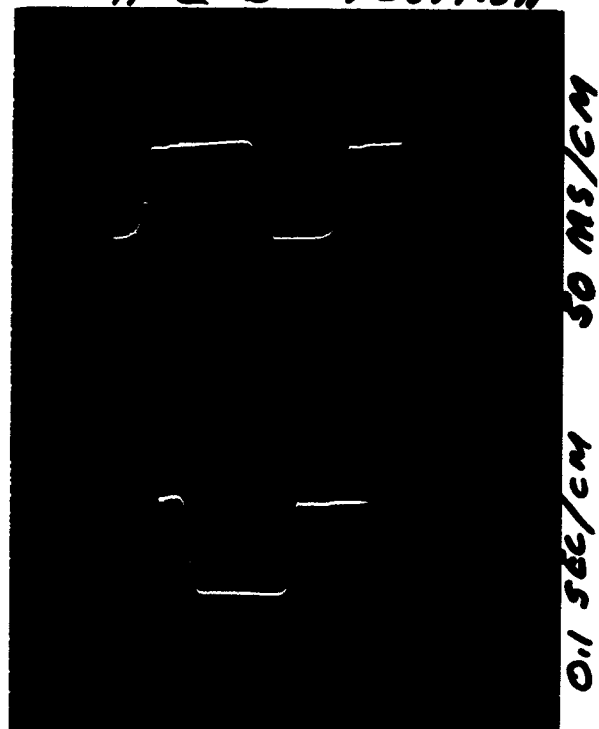


ENCODER
RESPONSE

50 PSI/CM

SWEEP

#2 BIT POSITION



POLAROID
PHOTOS
SIGNAL PRESSURE
VS
TIME

50 PSI/CM

FIG. 7.3.2



7. TEST RESULTS: (Continued)

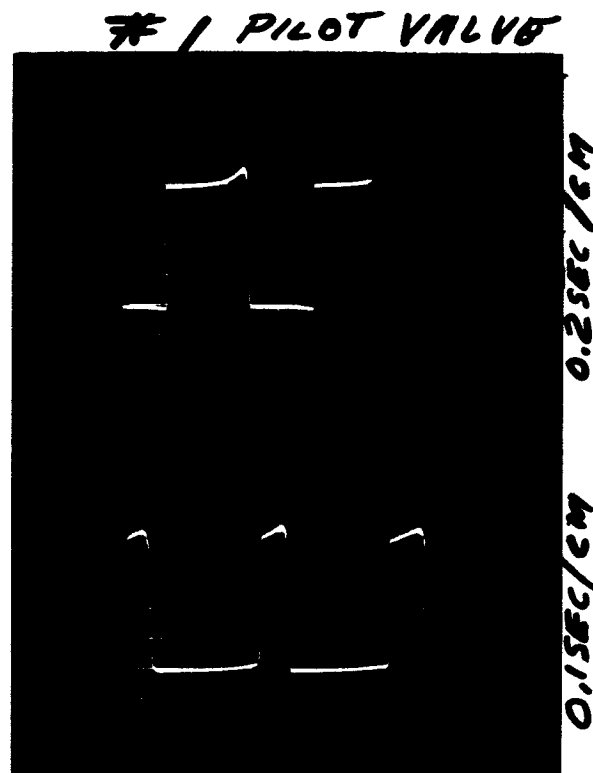
7.3 Encoder: (Continued)

pressures through dummy plugs installed in the pilot valve cavities. Figure 7.3.2 presents Polaroid photographs of scope traces of signal pressure versus time. The encoder supply pressure was 200 psi, which was dictated by the actuation requirements of the pilot valves. Testing was conducted using the stepper motor.

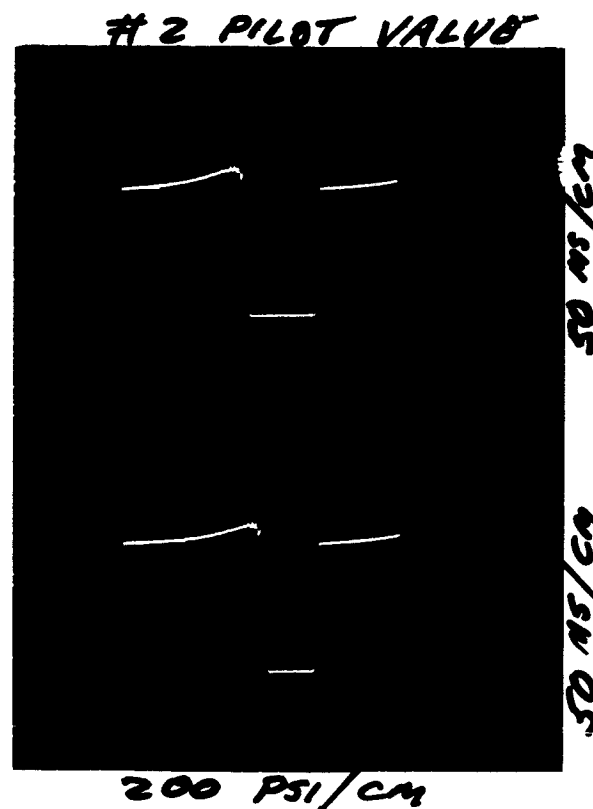
Preliminary testing of the encoder was conducted with a 650 psi supply pressure. Flow forces on the disk, even though reduced greatly by modifications to the housings and spacer plate, still caused peak torques in the order of 5 oz-inch. Reducing the adder and pilot valve supply pressure from 1600 to 800 psi and removing the springs from the pilot valves resulted in lower actuation of the pilot valves. This permitted reducing of the encoder supply pressure to 200 psi which in turn minimized the flow forces. Quite satisfactory performance of the encoder was then attained by using either the instrument servo or the stepper motor. (See Section 7.3.1)

The average pressure signal time constant was observed to be approximately 20 milliseconds. However, this is a 200 psi to 50 psi signal. Actuation of the pilot valves occurs between 125 psi and 75 psi. The actual useable pressure signal time constant is in the order of 8 milliseconds.

The pilot valves were then assembled into the encoder housings. By use of a fixture which simulated the digital actuator, but had provisions for a pressure transducer in each adder port, response data of the pilot valves was taken. The pilot valve supply pressure was 800 psi. The frequency range was again 1 cps to 5 cps.



PILOT VALVE
RESPONSE



POLAROID
PHOTOS
COMMAND PRESS.
VS
TIME

FIG. 7.3.3.



7. TEST RESULTS: (Continued)

7.3 Encoder: (Continued)

The time constant was approximately 5 milliseconds. The valves generate a 800 psi to 0 psi command signal to the adders in the digital actuator. Polaroid photos of scope traces of adder command pressure versus time are shown on Figure 7.3.3. The encoder assembly was driven by the stepper motor for these tests.

7.3.1 Stepper Motor Versus Instrument Servo:

Preliminary testing of the encoder, and later the entire system, was performed using the instrument servo as described in Section 6.5. The fact that this type of drive does not assume discrete positions and travels at a constant velocity, coupled with the disk code groove mismatch due to manufacturing tolerances, creates undue retrograde problems in the digital actuator.

Powered by a function generator through the controller, the stepper motor is very capable of running continuously in either CW or CCW direction. With the addition of a SPDT switch to accomplish reversing, the stepper motor becomes a much more desirable drive. The only drawback is that the input frequency, which is a square wave or pulse input, is limited by the ability of the operator to reverse the switch. Automatic electro-mechanical reversing could be added, again in lieu of an analog to digital converter, but it is not within the scope of the present budget.



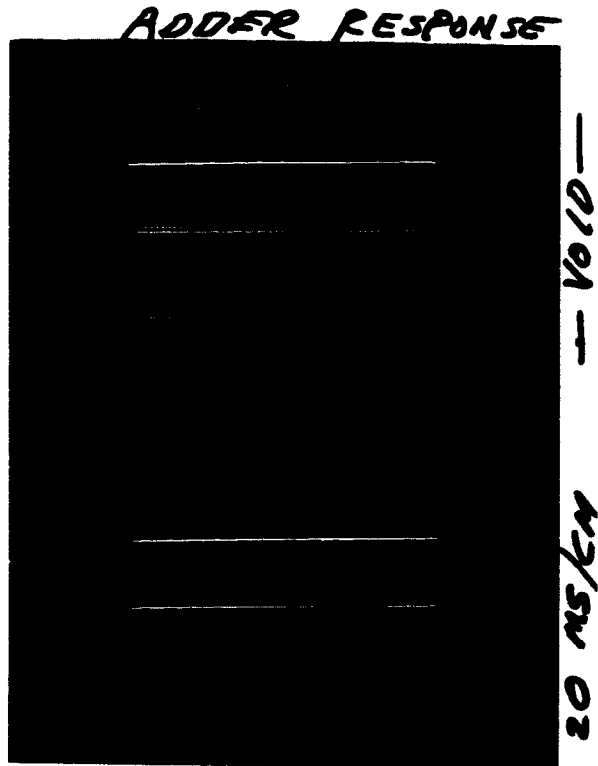
7. TEST RESULTS: (Continued)

7.4 Digital Actuator:

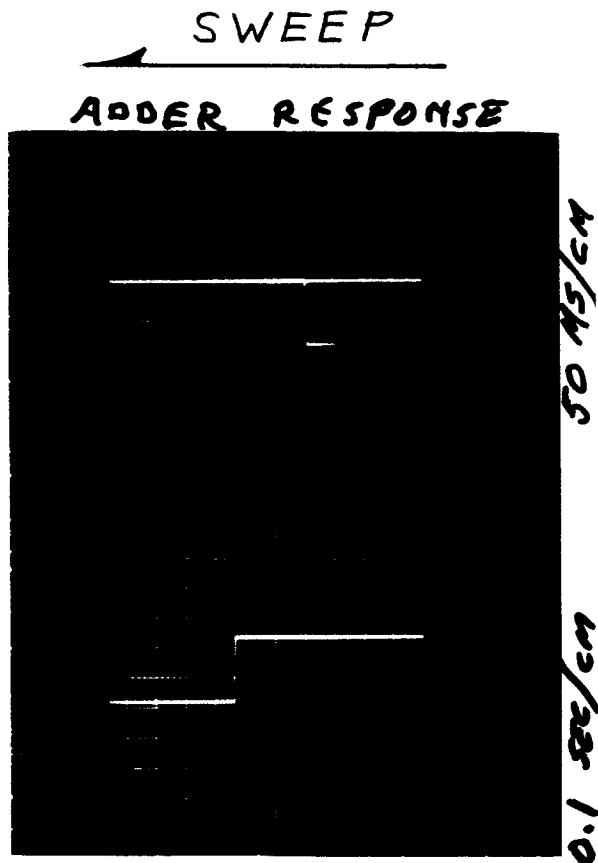
No preliminary testing of the digital actuator was performed prior to mating with the encoder. This was due primarily to the confidence warranted the design because of its simplicity coupled with previous Weston experience with this type of actuator. Another consideration was the cost and complexity of a solenoid valve bank or similar setup necessary to command each adder simultaneously. Actual testing of the digital actuator was conducted using the encoder, thus continuing the step by step test plan. Digital actuator response was determined by using a position transducer connected to the adder stack output with input to the encoder from the stepper motor.

A slope trace of change of position versus time was observed and photographed. This data, which varifies a time constant of less than 5 milliseconds, is shown on Figure 7.4.1.

After continued cycling of the entire system, disassembly of the digital actuator did disclose a loosening of the shrink fit teflon bands or riding lands. A new set of adders was installed for further testing. A re-evaluation of this area dictated that a more positive groove to teflon relationship be incorporated in the adders. This rework was completed and the digital actuator retested to assure satisfactory performance.



ADDER
RESPONSE



POLAROID
PHOTOS
POSITION CHANGE
VS
TIME

FIG. 7.4.1



7. TEST RESULTS: (Continued)

7.5 Entire System:

Testing of the entire system was limited because of the lack of a suitable input source, namely an A/D converter. A digital command input was achieved by using a function generator with a square wave output and a SPDT switch to stop, start, and reverse the stepper motor. Although the stepper motor will respond to inputs in excess of 500 pulses per second (pps), testing was limited to the ability of the operator to flip the SPDT switch or about 30 pps.

A step input-response test was conducted on the complete system including the stepper motor, encoder and digital actuator. The actuator and load positions versus time are shown in Figure 7.5.1. As shown, a significant degree of underdamping is evident in the transient behavior of the load. This oscillatory condition is attributed to the threshold characteristics of the feedback linkage and derivative force network and could be minimized by additional effort. It should be noted, however, that the frequency response tests indicated a higher degree of effective damping which is due to the higher levels of load acceleration and thus greater excursions of the damping mechanism.

7.6 Miscellaneous Data:

7.6.1 Control Valve - Load Flow Curves:

A plot of weight flow versus cylinder pressure at various control valve stroke positions is shown on Figure 7.6.1. The P_2 to P_1 pressure ratio values at the bottom of Figure 7.6.1 apply only to the supply to cylinder portion of the graph. Cylinder to return (atmosphere) is always sonic flow.

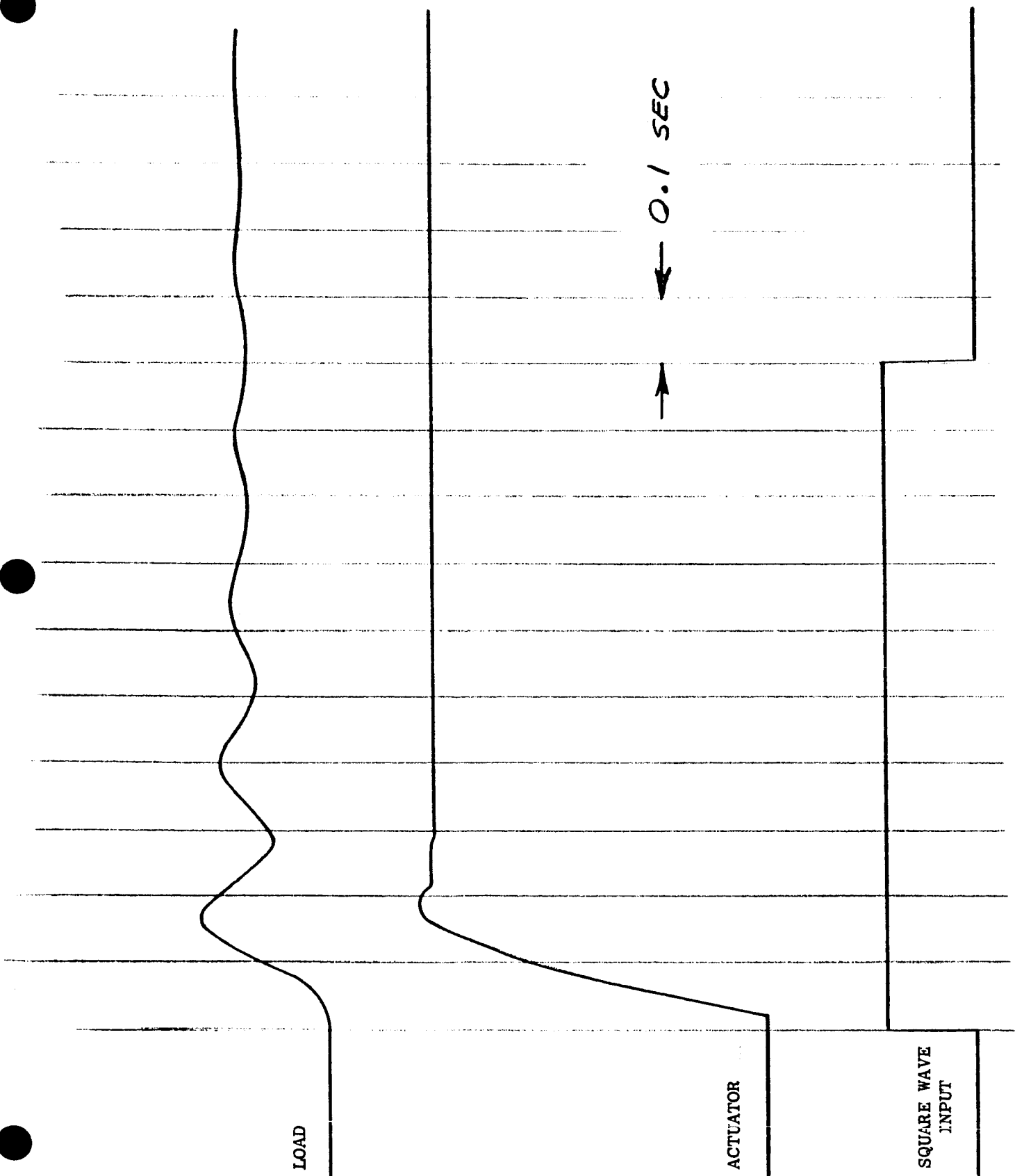


FIG. 7.5.1

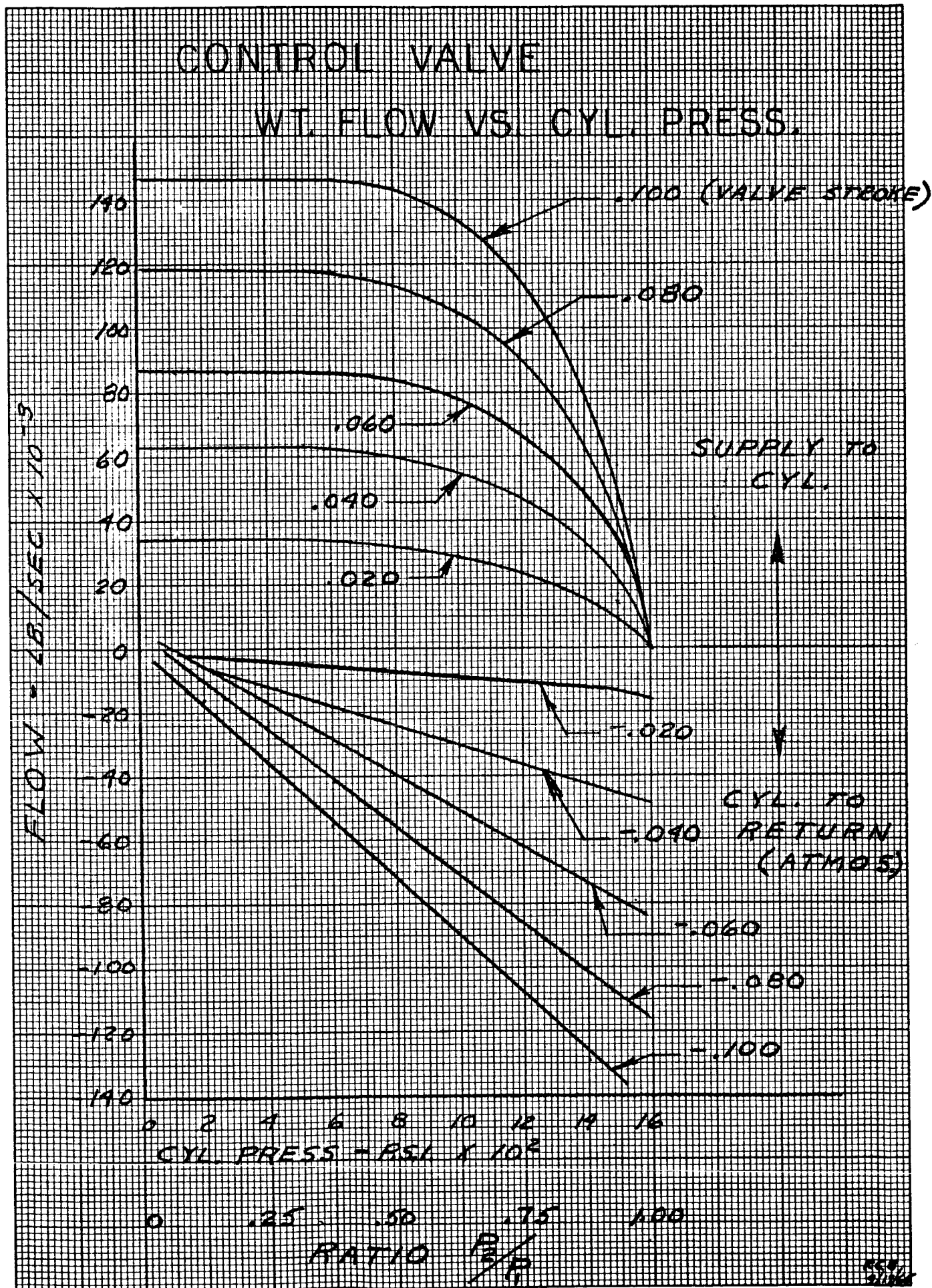


FIG. 7.6.1.

Weston Hydraulics Limited



7. TEST RESULTS: (Continued)

7.6 Miscellaneous Data: (Continued)

7.6.2 Ram Pressure:

With the control valve in null position, the pressure on each side of the ram was observed to be 1050 psi. The inlet supply pressure was 1600 psi.

7.6.3 Steady State Leakage:

Leakage was measured by tying both return lines together and recording total leakage using a flowmeter. The measured leakage flow was approximately 1.0 scfm (.0013 #/Sec.).

7.6.4 Friction Load:

The friction load of the actuator main ram and the simulated engine load was recorded. The force reading was taken at the attach point of the load to the actuator. Break out friction was measured to be 24 pounds minimum to 32 pounds maximum. Running friction was less than 20 pounds. These tests were performed with no pressure applied.

Weston Hydraulics Limited



7. TEST RESULTS: (Continued)

7.7 Gas Properties and System Performance:

Properties and System Performance	Air at 70°F and 1600 psi	N ₂ at 70°F and 1600 psi	Helium at 70°F and 1600 psi	H ₂ -260°F and 1600 psi
-----------------------------------	--------------------------	-------------------------------------	-----------------------------	------------------------------------

I. Gas Properties

Density ₃ (Lbs/In ³)	0.0047	0.00484	0.00065	0.00088
Ratio of specific heat	1.4	1.4	1.66	1.71
Viscosity Lb Ft.-Sec	12 x 10 ⁻⁶	12 x 10 ⁻⁶	12.5 x 10 ⁻⁶	3.54 x 10 ⁻⁶
Speed of Sound (Ft/Sec)	1088	1250	3500	3250
Gas Constant	53	55	386	766

II. System Performance

Metering Area (In ²)	0.00342	0.00342	0.00342	0.00342
Max. Gas Flow (Lb/Sec)	0.068	0.068	0.0255	0.0284
Max. Gas Flow (In ³ /Sec.)	14.5	14.5	39.2	40
No Load (Max.) Velocity (In/Sec.)	2.15	2.15	6	6
Pneumatic + Mechanical Natural Frequency (cps)	5.75	5.75	6	6
Power Servo Response (closed loop)	Flat up to 4 cps + 1 db peak	Flat up to 4 cps + 1 db peak	Flat up to 4.4 cps + 1 db peak	Flat up to 4.4 cps + 1 db peak

Weston Hydraulics Limited



7. TEST RESULTS: (Continued)

7.7 Gas Properties and System Performance: (Continued)

Properties and System Performance	Air at 70°F and 1600 psi	N ₂ at 70°F and 1600 psi	Helium at 70°F and 1600 psi	H ₂ -260°F and 1600 psi
--------------------------------------	-----------------------------	--	--------------------------------	---------------------------------------

II. System Performance (Cont.)

General Response
based on speed of
sound in medium -
referred to H₂
(Units)

0.335	0.385	1.08	1
-------	-------	------	---

Friction Based
on Viscosity
referred to
Hydrogen
(Units)

0.29	0.29	0.29	1
------	------	------	---

Price per
bottle of
gas

Free supply
available at
Weston

\$2.14 per 100
cu. ft. stored
at 2200 psi

\$10.80 per
100 cu. ft.

\$2.20 per
100 cu. ft.

Conclusions and Recommendations:

- 1.) Air and nitrogen will give very nearly the same performance characteristics.
- 2.) Helium at room temperature will give the same performance characteristics as hydrogen at -260°F.
- 3.) A system designed for hydrogen gas at -260°F will have approximately 1/3 loop gain when worked with air or nitrogen and hence will produce poorer response.
- 4.) A system designed for air or nitrogen when worked with hydrogen will have three times the loop gain and will definitely be unstable.



7. TEST RESULTS: (Continued)

7.7 Gas Properties and System Performance: (Continued)

Conclusions and Recommendations: (Continued)

- 5.) The basic design/hardware change necessary for the system designed for H_2 to work on air or nitrogen is to increase all the fluid metering areas by a factor of three.
- 6.) The conclusion is to design the system for air or nitrogen. The system is designed to meet the dynamic response required by NASA. The system will give identical performance with H_2 if all the metering areas are reduced by a factor of three.



8. WEIGHT COMPARISON WITH ANALOG:

A meaningful weight comparison of the digital actuation system versus an equivalent analog system cannot be made now. Definitely, at this time, an analog system does have a weight advantage. However, any realistic comparison would have to take into consideration the current "state of the art" positions of the two systems. As previously noted, the digital system as described in this report was primarily designed as a test unit with little emphasis placed on weight. It is certain that any further development of digital systems will result in weight reduction along with other advancements.



9. RELIABILITY COMPARISON:

9.1 Scope:

Weston presents in this section of the report, a preliminary reliability study and comparison of the digital actuation system developed under this contract vs a typical analog actuation system.

9.2 Introduction:

9.2.1 This study shall be limited to analysis of each system (analog and digital) at a component level, rather than an "in depth" analysis of detail parts comprising the two systems. Since the Digital Actuator Assembly, Weston P/N 27160, was designed as a "breadboard" type unit in order to verify the results of the analytical study, reliability assessment at a detail level would not be valid. However, certain conclusions may be drawn at this time regarding the comparative system inherent reliabilities based on a component evaluation.

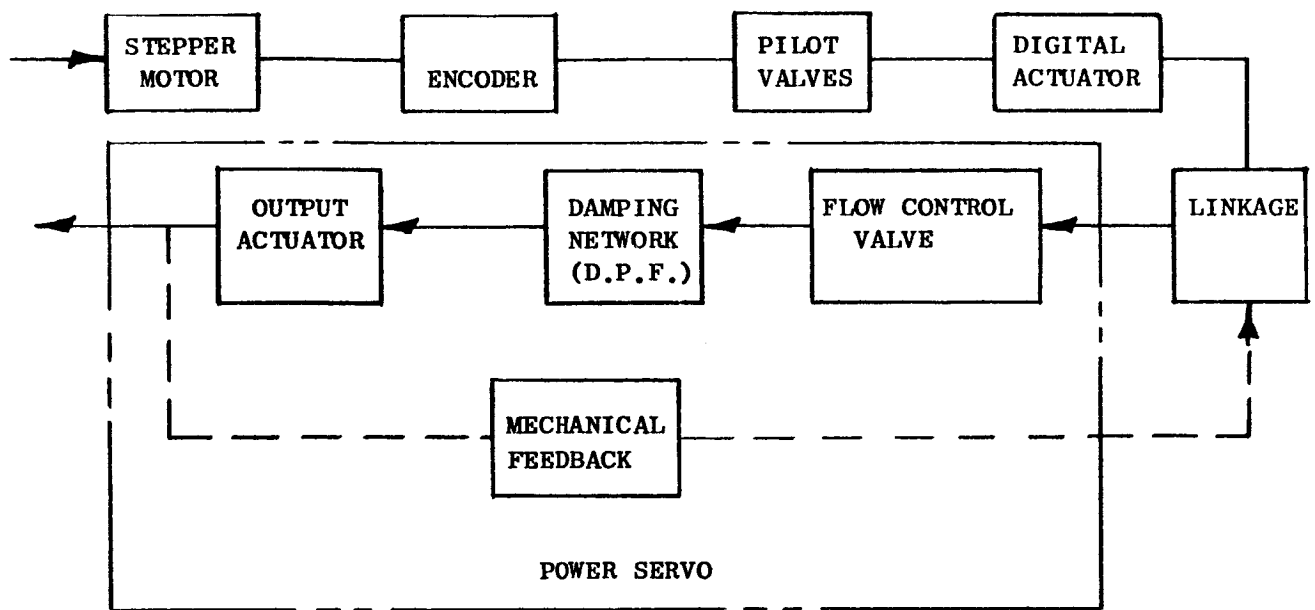
9.2.2 The analog actuator to be used as a comparison in this analysis is a conventional flight control actuator that receives an electrical signal proportional to the required output displacement. The electrical signal is received by an electro-pneumatic servo-valve, which converts it into a pneumatic flow. This flow is then applied to a small servo ram, which drives the power servo flow control valve through mechanical linkage. We have assumed mechanical feedback from the servo ram to the electro-pneumatic servo-valves.

9.2.3 Functional block diagrams of the digital actuation system and the equivalent analog input system are included as Figure 9.2.3-1 and 9.2.3-2. It will be observed from the diagrams that the power servo, consisting of the main flow control valve, damping network (D.P.F.), output actuator, and linkage, are identical in both the digital and analog input systems. Therefore, the reliability comparison reduces itself to a comparison of the method used to convert the input electrical signal into the displacement output signal that drives the mechanical input linkage to the main flow control valve.

9.3 Reliability Analysis:

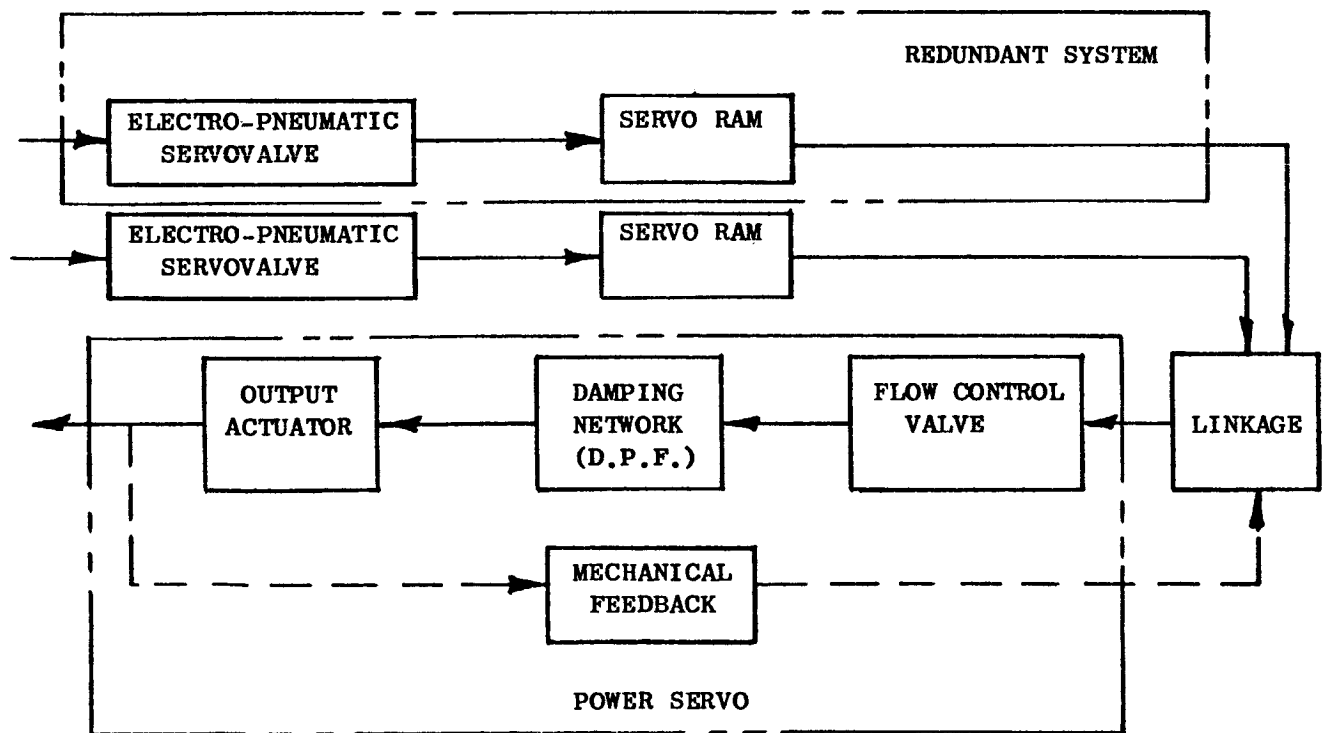
9.3.1 Discussion of This Analysis:

The reliability of an equipment is the ability of that equipment to produce the required output for the time the output is desired in service. The measurement of reliability, then, is a study of the performance of the equipment, after all members of the population have performed. This type of study will yield a typical statement, such as, "From the population of 100 samples, 90 survived the full life requirement in service. The reliability of the equipment was 90 percent." This reliability



DIGITAL SYSTEM

FIGURE 9.2.3-1



ANALOG SYSTEM

FIGURE 9.2.3-2



9.3 Reliability Analysis: (Continued)

9.3.1 Discussion of This Analysis: (Continued)

statement is authoritative, because it reports actual observed occurrences. It does not project to future predictions.

A reliability study, such as this report, is, on the other hand, a prediction of the anticipated reliability of an equipment. The study precedes the performance demonstration of any of the equipment. Therefore, a preliminary study is not fully authoritative, but rather is an estimate, or synthesis, of the reliability.

The growing emphasis on reliability predictions is causing a refinement of methods for establishing and collecting pertinent data that will, in time, lead to accurate predictions. The current "state-of-the-art" is not one of high accuracy. However, it is sufficiently advanced to permit an assessment of components. The most valid part of a reliability study is separate component evaluation, which generates a comparative scale of reliabilities, permitting the detection of "weak links" in advance of fabrication and test.

This report is in two sections. The first section discusses the inherent reliability of the proposed Digital Flight Control Actuator. The second section discusses the reliability of an equivalent Analog Flight Control Actuator. Thus, it is possible to get a direct comparison of the potential of each type of system.

9.3.2 Component Reliability Analysis:

The concept of reliability used in this report is the assumption that all failures are purely "random" in nature, that all "infant mortality" shall be detected during the acceptance tests, and that "wear out" failures shall be detected during routine maintenance.

The "random failure" approach to the analysis takes the mathematical form:

$$R = e^{-ft}$$

R = Reliability, or probability of survival

f = Constant random failure rate

t = Operating time (mission life)

e = 2.718 (natural logarithm base)

Note: If the product "ft" is less than 0.01 then the equation will reduce to $R = 1 - ft$, as a good approximation.

When a group of components operate in series, this is, if anyone should fail, then the group will fail, then the total reliability of that group is the mathematical product of the reliabilities of the individual components.



9.3 Reliability Analysis: (Continued)

9.3.2 Component Reliability Analysis: (Continued)

$$R_T = R_1 \times R_2 \times R_3 \times \dots \times R_n$$

The following failure rates used are derived from Report M-60-47, published by the Martin Denver Company, Denver, Colorado, and from Weston historical data, where pertinent.

The following analysis is based on a mission life (t) of 1.0 hour.

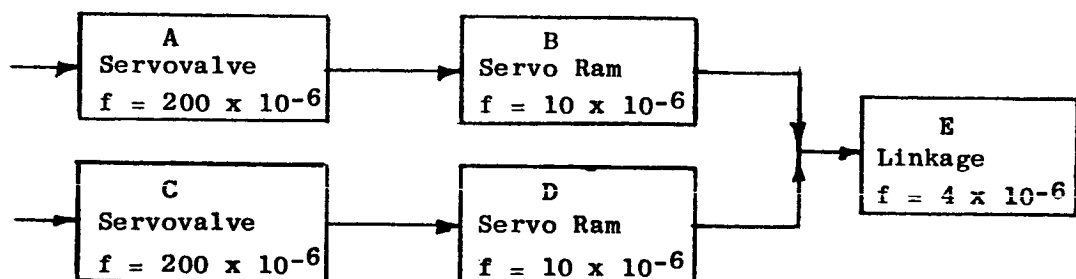
9.3.3 Reliability Calculation - Digital System:

Component	Quantity	f (per hour)	t (hours)	R (1 - ft)
Stepper Motor	1	0.71×10^{-6}	1	
Encoder	1	2.0×10^{-6}	1	
Pilot Valve	8	1.0×10^{-6}	1	
Digital Actuator	1	10.0×10^{-6}	1	
Linkage	1	2.0×10^{-6}	1	
System		22.71×10^{-6}	x 1	0.999978

9.3.4 Reliability Calculation - Analog System (Non-redundant):

Component	Quantity	f (per hour)	t (hours)	R (1 - ft)
Servo valve	1	200.0×10^{-6}	1	
Servo Ram	1	10.0×10^{-6}	1	
Linkage	1	4.0×10^{-6}	1	
System		214.0×10^{-6}	x 1	0.999786

9.3.5 Reliability Calculation - Analog System (Redundant):





9.3 Reliability Analysis: (Continued)

9.3.5 Reliability Calculation - Analog System (Redundant): (Continued)

To combine failure rates in a parallel redundant system:

$$(f_A + f_B) (f_C + f_D) + f_E = f_T \text{ (Total device failure rate)}$$

$$\begin{aligned} f_T &= (210 \times 10^{-6})^2 + 4 \times 10^{-6} \\ &= (44100 \times 10^{-12}) + 4 \times 10^{-6} \\ &= (0.0441 \times 10^{-6}) + 4 \times 10^{-6} \\ &= 4.0441 \times 10^{-6} \end{aligned}$$

$$R = 1 - f_T$$

$$t = 1$$

$$R = 1 - (4 \times 10^{-6})$$

$$R = .999996$$

9.4 Summary:

9.4.1 This analysis compares the inherent reliability of the digital input actuator, Weston P/N 27160, with an equivalent actuator that receives an analog input signal. The power servo components are common to both types of actuator and are therefore not considered in the analysis. The fundamental difference between the two units lies in the form of the electrical input signal and in the method used to convert the electrical signal into a displacement signal that can be used to drive the power servo flow control valve.

9.4.2 The digital actuator uses a "binary" bit type signal to drive the flow control valve. Valve motion is in finite steps, the magnitude and direction are a direct function of the input code. The analog actuator receives a current signal that is infinitely variable between the maximum bounds in each direction. The actuator output is directly proportional to, and in phase with, the input.



9.4 Summary: : (Continued)

- 9.4.3 A comparison of the reliability calculations for each system demonstrate that (1) the digital actuation system is inherently more reliable than the equivalent analog system, (2) an analog system with a redundant servovalve and servo ram assembly has a greater inherent reliability than a non-redundant digital system and (3) the optimum system from a reliability point of view would be a redundant digital system.
- 9.4.4 The analog actuator is basically less reliable than the digital actuator. This is due primarily to the extreme complexity of the servovalve.
- 9.4.5 Not considered in this analysis is the fact that the "adder piston" type of digital actuator contains a "built in" characteristic which is very similar to parallel redundancy. This is, if any one of the series of adder pistons should fail due to a loss of input, it would not result in a catastrophic failure since the remaining adders would continue to operate. In addition, the digital actuator would not require a digital to analog converter. This would necessarily improve the overall system reliability.

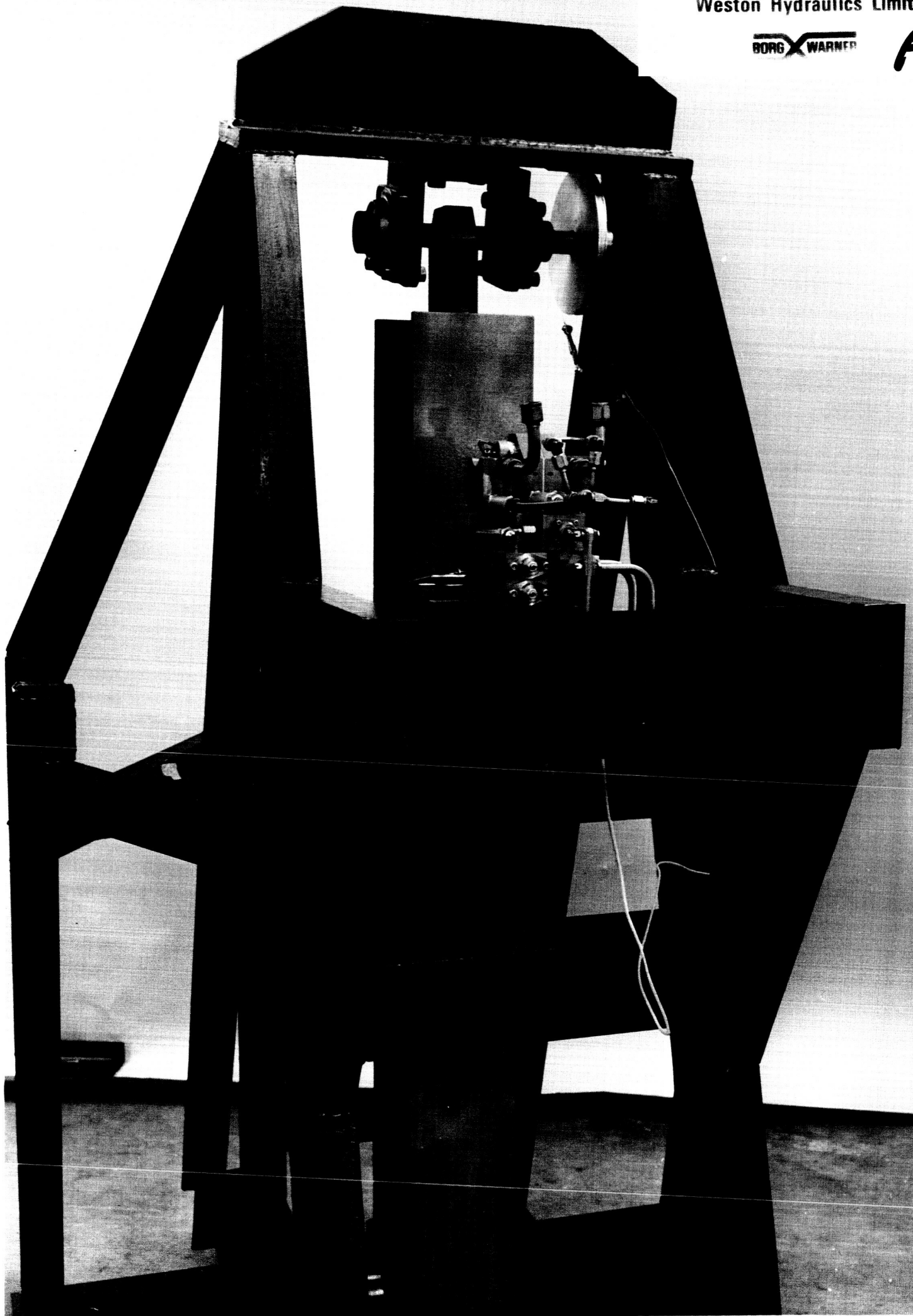
Weston Hydraulics Limited

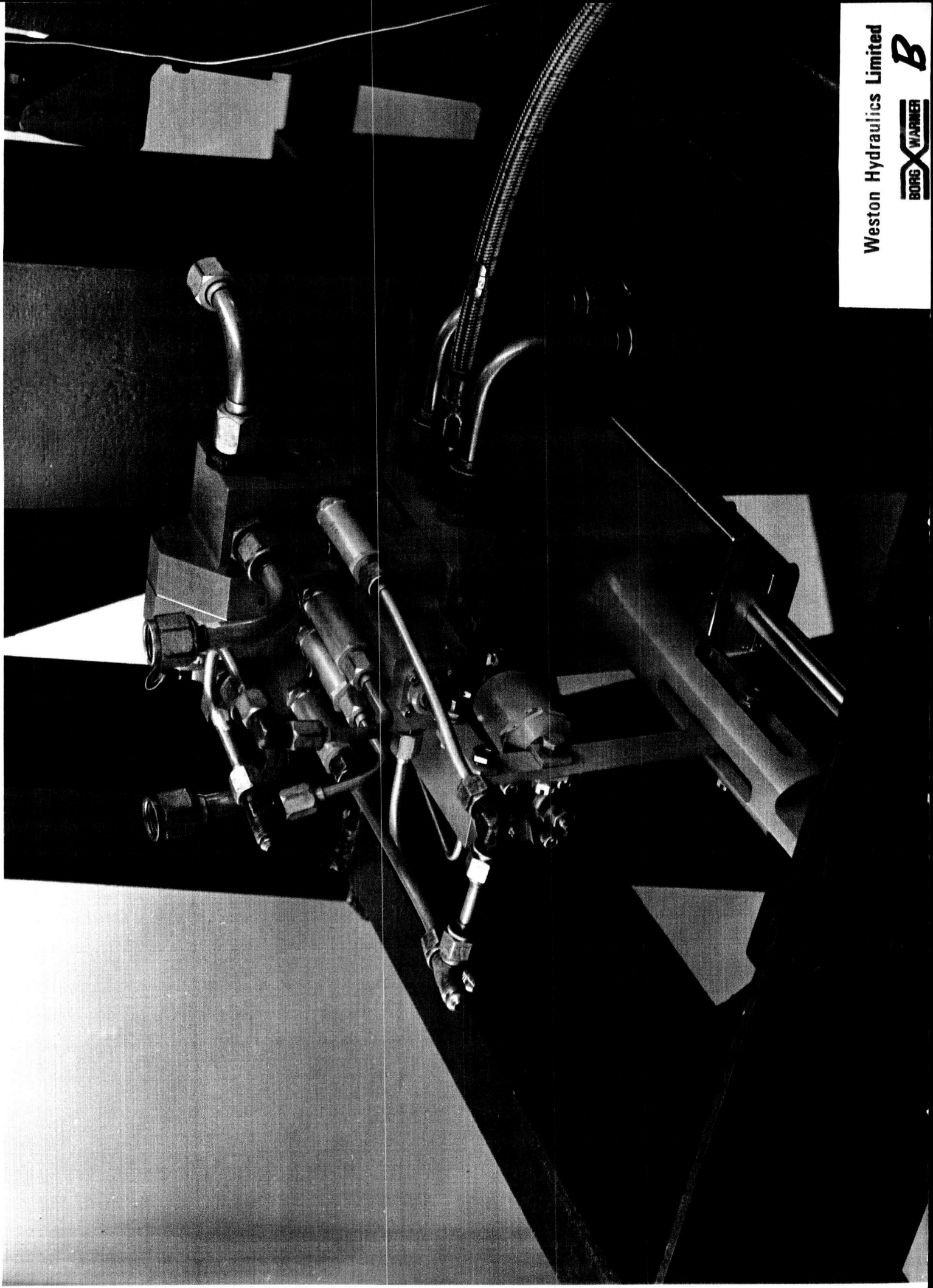


10. PHOTOGRAPHS:

PHOTO NO.

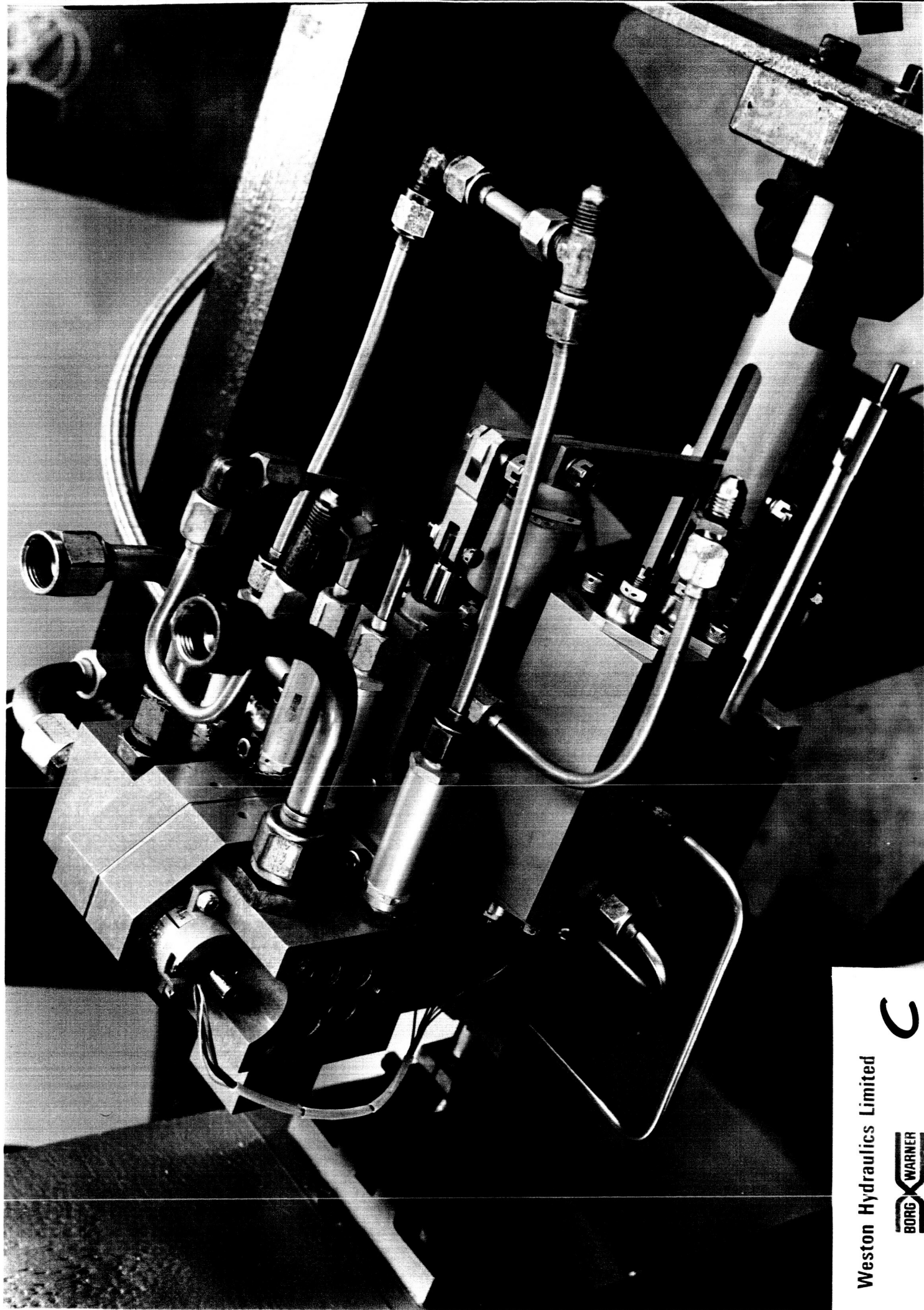
- A. Test Stand, Load, and Actuator
- B. Actuator In Test Stand
- C. Actuator Showing Attach Points
- D. Assembled Actuator
- E. Power Servo, Digital Actuator, and Encoder
- F. Control Valve, D.P.F. Mechanism, and Housing
- G. Encoder Internal View
- H. Encoder Face Showing Orifices
- I. Pilot Valve (Exploded View)
- J. Binary Disk
- K. Digital Actuator Adder Stack
- L. Individual Adder





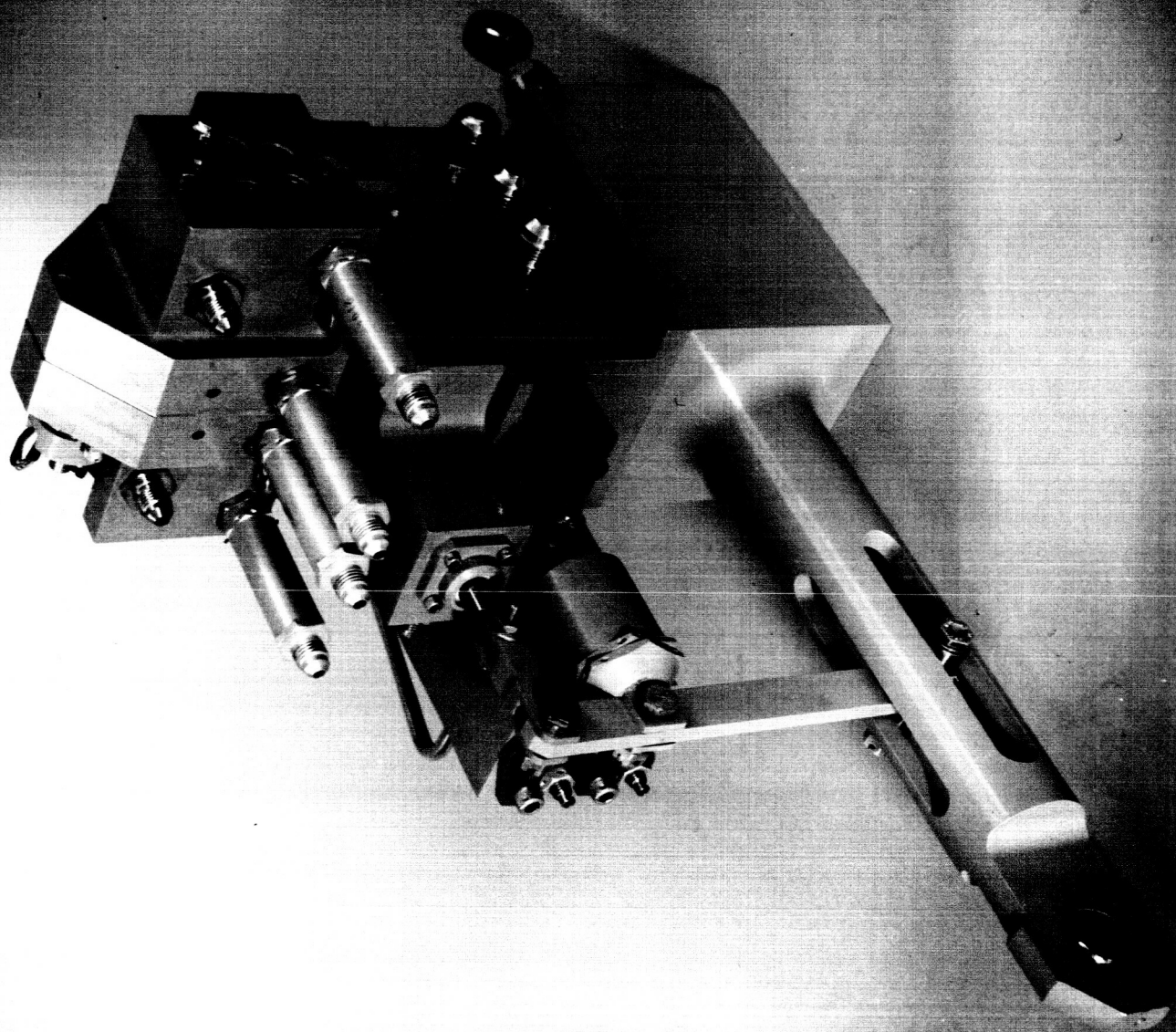
Weston Hydraulics Limited





Weston Hydraulics Limited

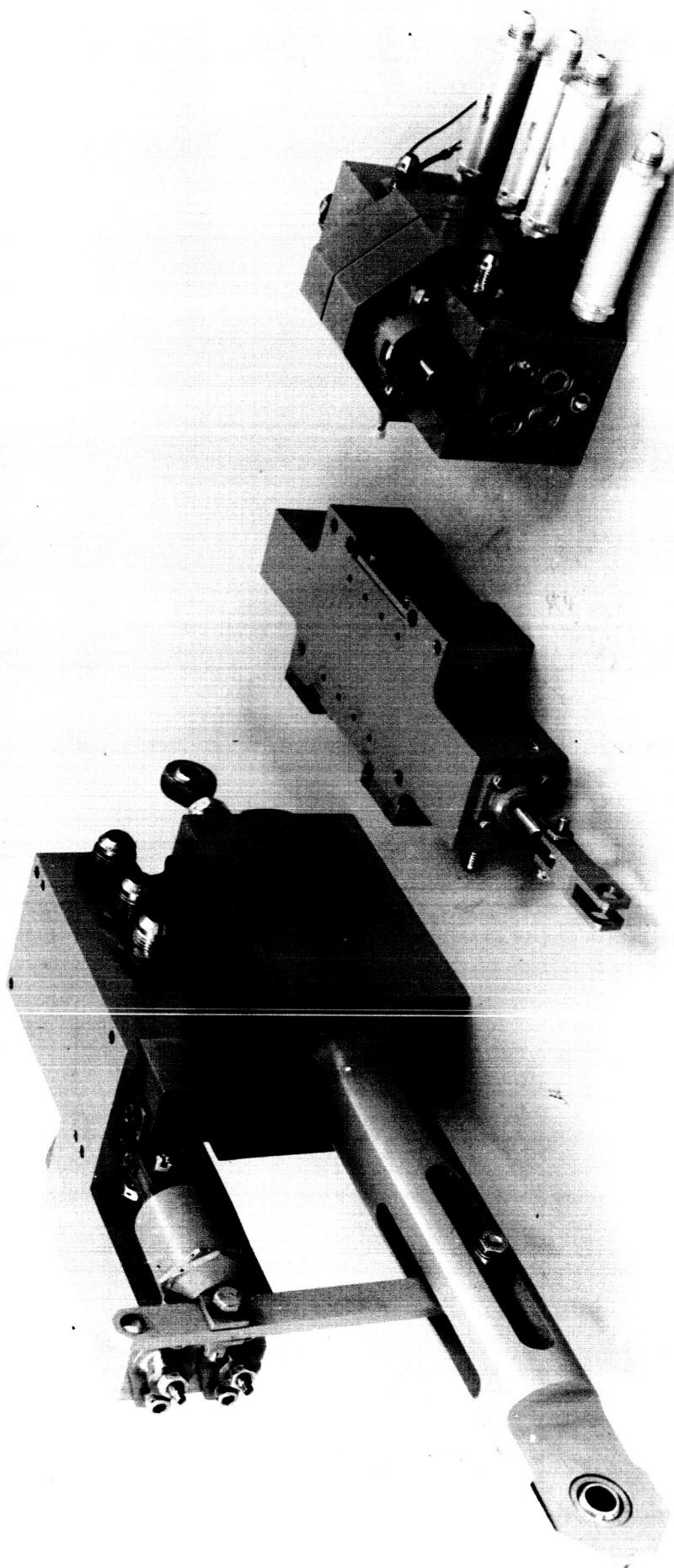


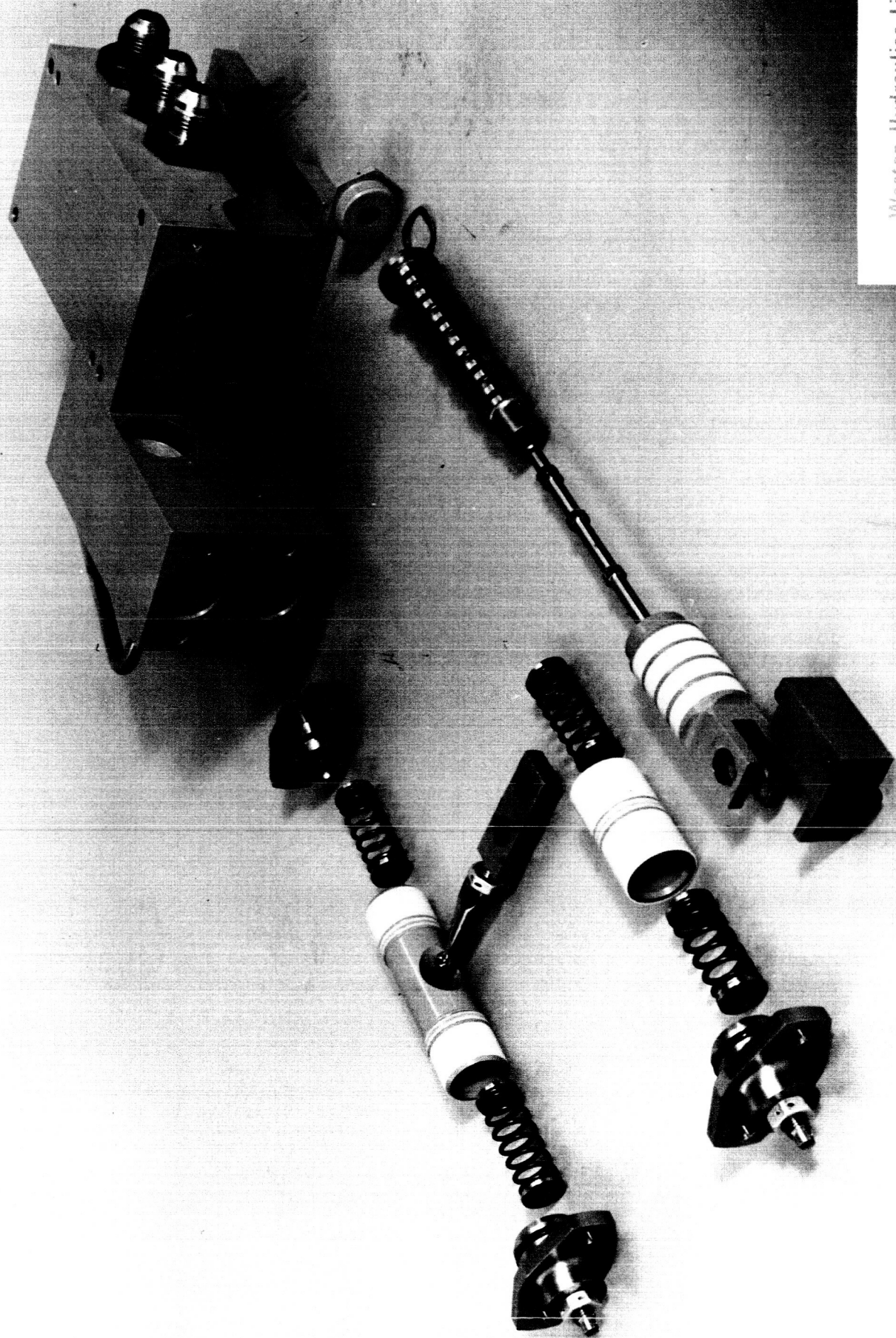


Weston Hydraulics Limited



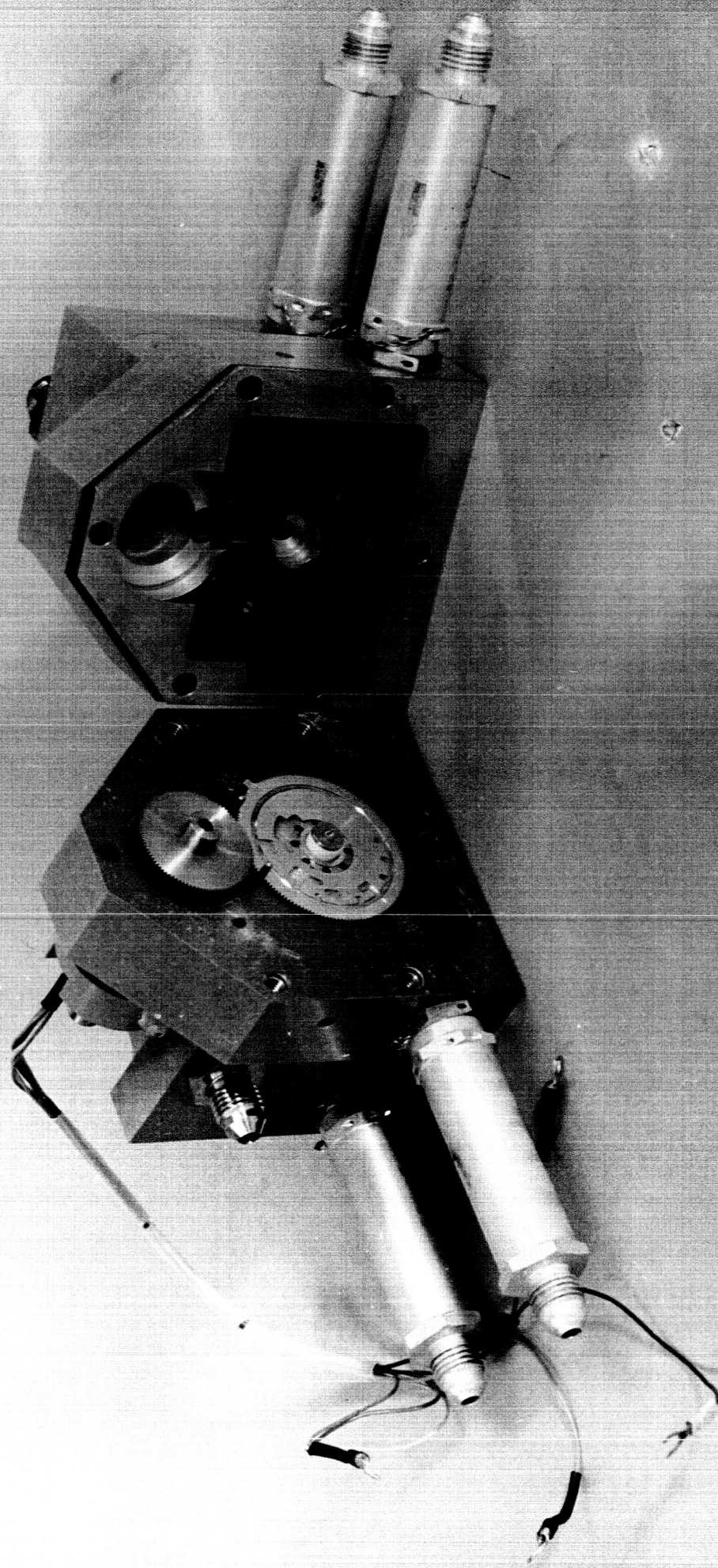
D





Weston Hydraulics Limited

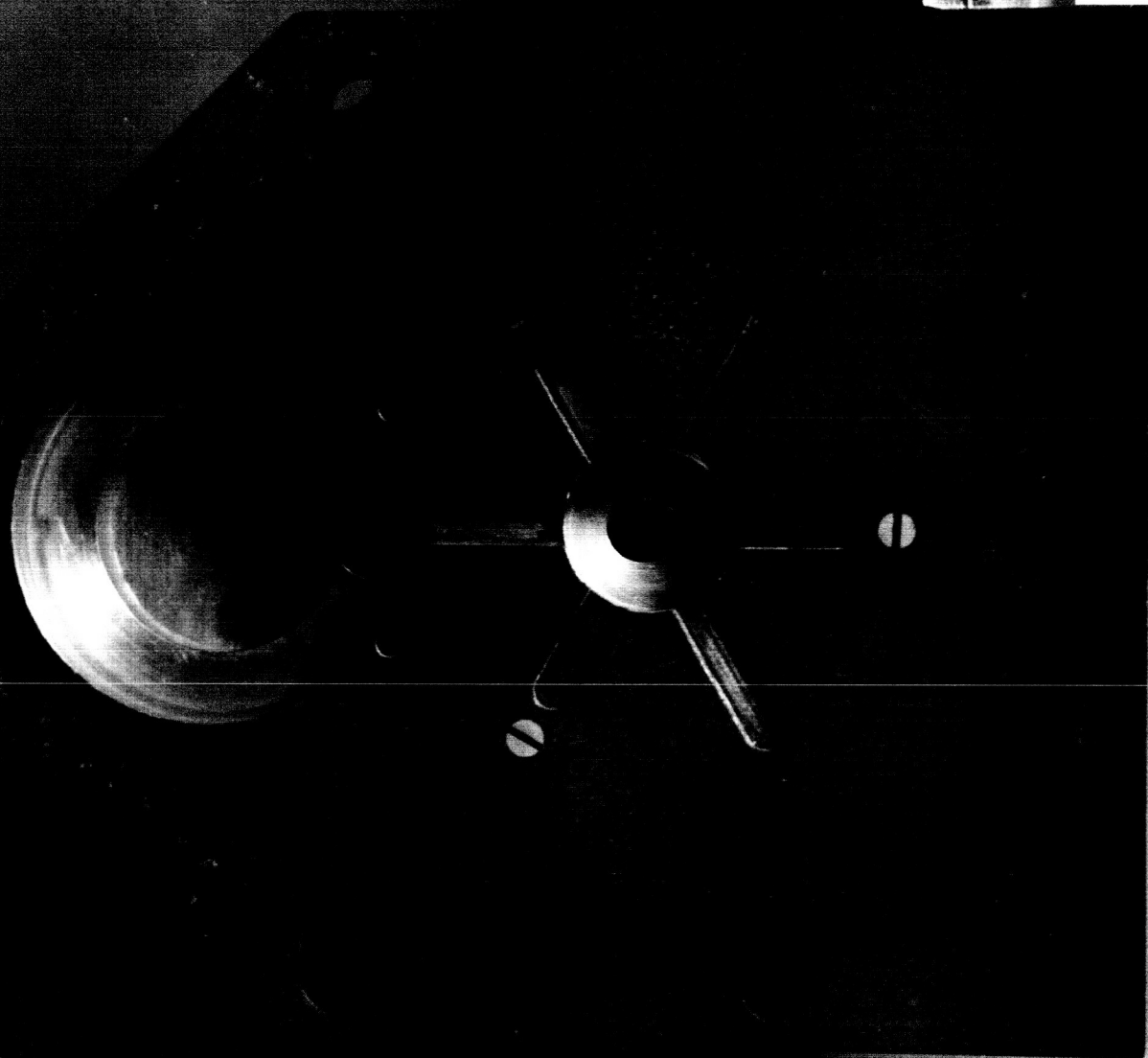


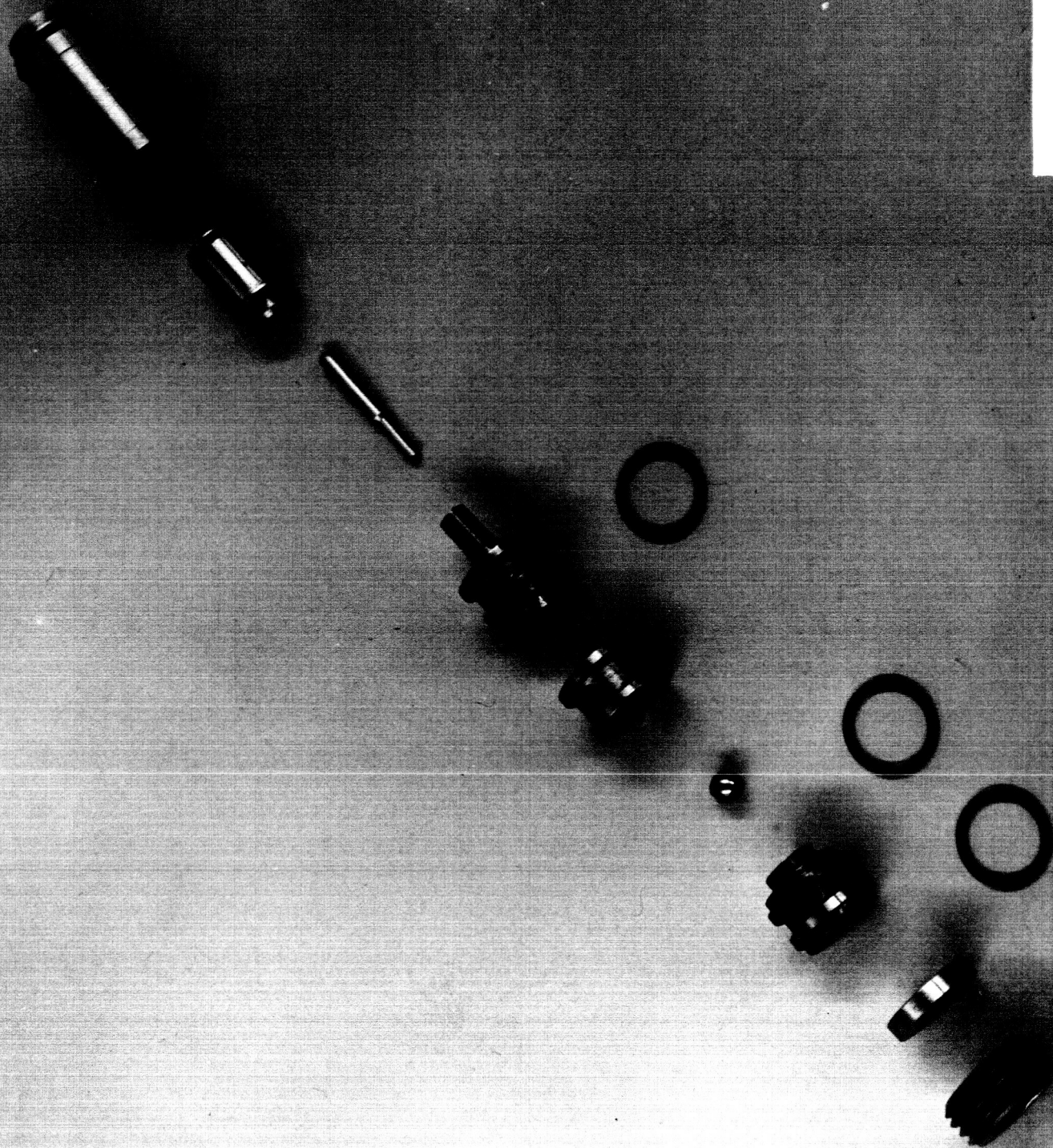


Weston Hydraulics Limited



H

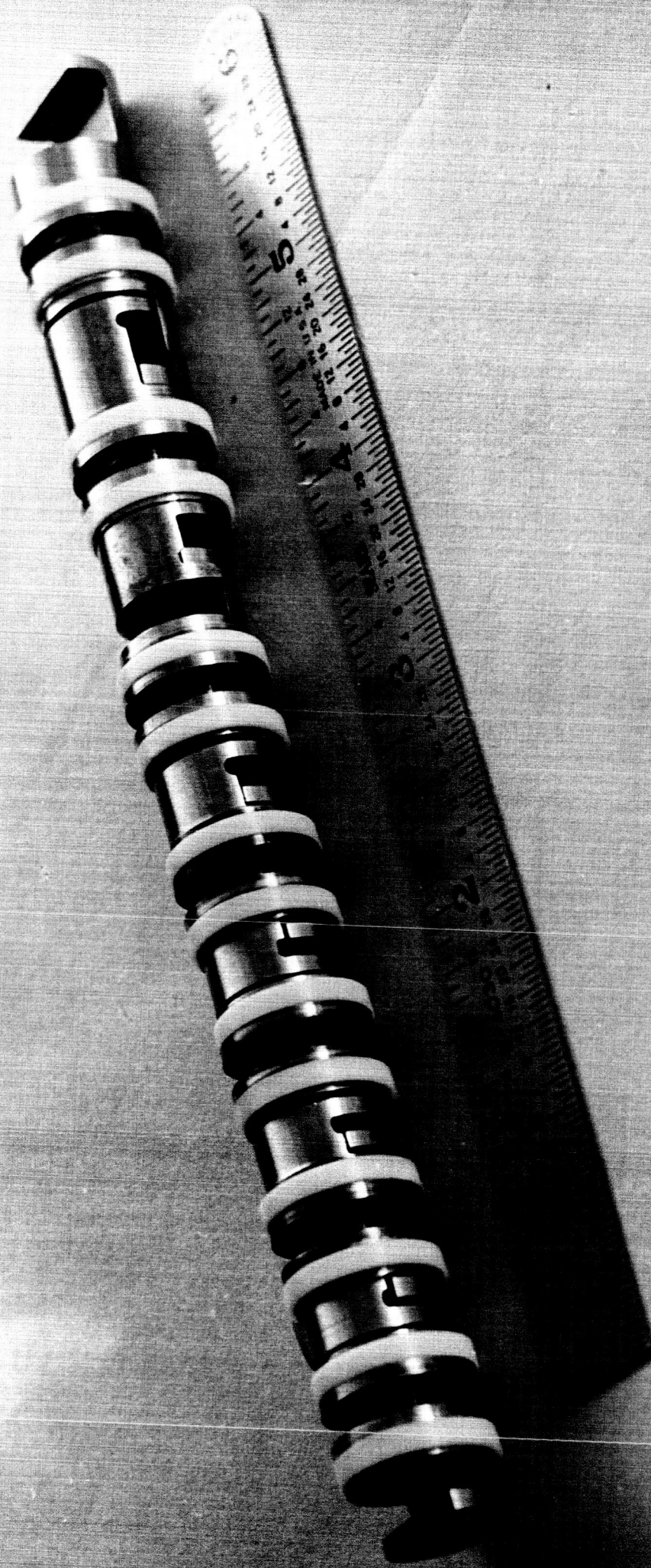






Weston Hydraulics Limited

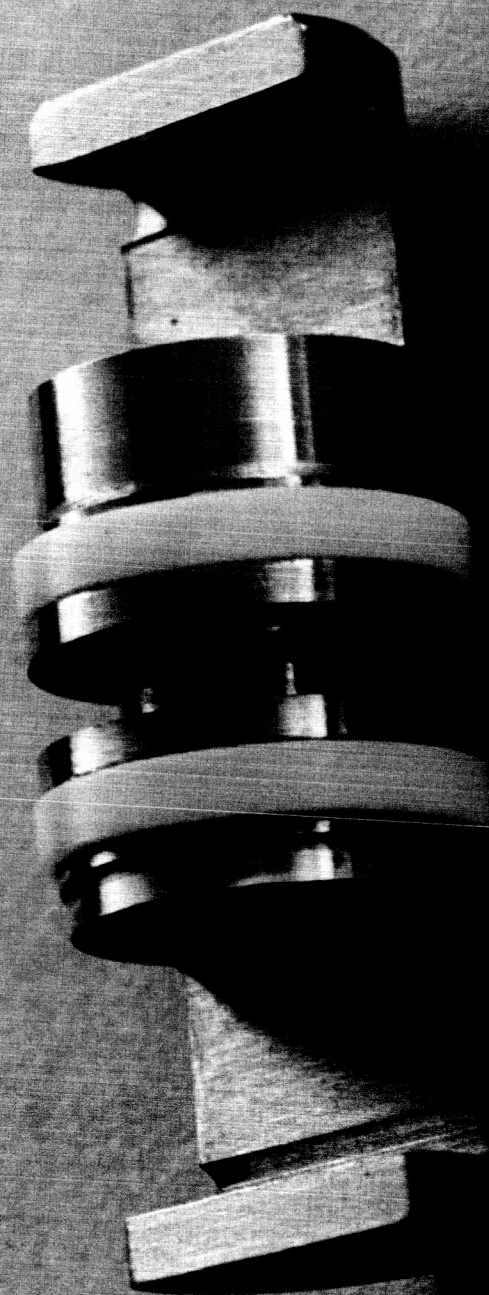




Weston Hydraulics Limited



K



Weston Hydraulics Limited



APPENDIX I

Per Cent Input (Open Loop) for Velocity Saturation

All the flight control actuation systems are generally limited to a maximum piston velocity. This requirement is imposed to avoid large reaction forces on the vehicle resulting from fast rates of the thrust vector control. Following analysis shows the relationship between the output stroke, maximum velocity, loop gain and the per cent inputs for velocity saturation.

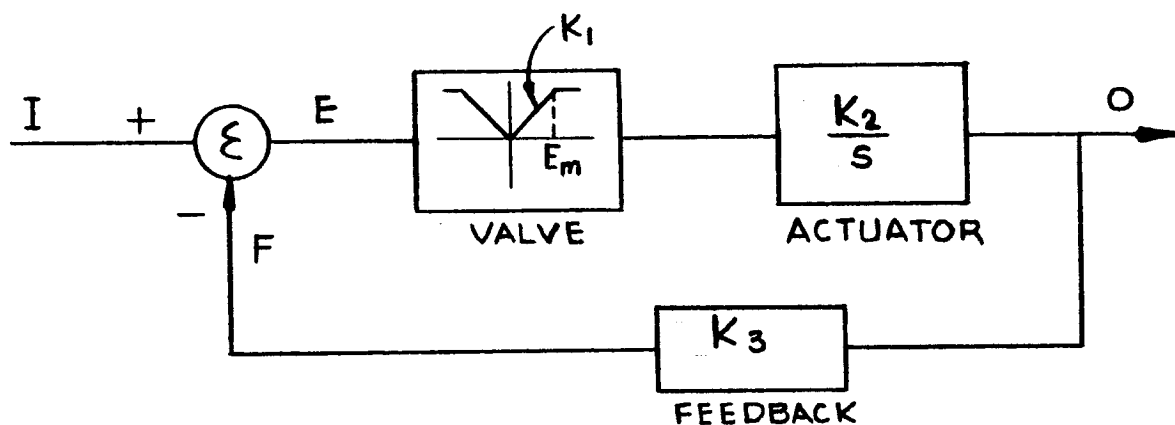


FIGURE I.1

- I = Input
- O = Output
- F = Feedback
- E = Error
- K_1 = Valve Gain
- K_2 = Actuator Gain
- K_3 = Feedback Gain
- S = Laplace Operator Sec^{-1}

Figure I.1 shows a simplified servo block diagram. The diagram excludes the dynamics of valve and actuator. Only velocity to position integration term is included.



With the loop open,

$$\text{Maximum velocity} = \dot{O}_m = K_1 K_2 E_m \quad \text{I.1}$$

Where E_m = Error required to saturate the valve open loop.

$$\text{Feedback Gain } K_3 = \frac{\text{Feedback}}{\text{Output}} = \frac{F}{O}$$

After the transients feedback equals input, therefore, $F = I$ or

$$\begin{aligned} K_3 &= \frac{I}{O} \quad \text{Steady State} \\ &= \frac{\text{Maximum Input}}{\text{Maximum Output}} \quad \left| \quad \text{Steady State} \right. \\ &= \frac{I_m}{O_m} \quad \left| \quad \text{Steady State} \right. \end{aligned} \quad \text{I.2}$$

From equation I.1

$$K_1 K_2 = \frac{O_m}{O_m} \quad \text{I.3}$$

From I.2 and I.3

$$K_1 K_2 K_3 = \frac{O_m I_m}{O_m E_m} \quad \text{I.4}$$

$$\text{Now } \frac{E_m}{I_m} \times 100 = p = \text{Percent input required to saturate the valve} \quad \text{I.5}$$

$$\text{And } K_1 K_2 K_3 = K_{O.L.} = \text{Open loop gain} \quad \text{I.6}$$

Substituting I.5 and I.6 in I.4

$$K_{O.L.} = \frac{100 O_m}{p O_m}$$

i.e. Open Loop Gain =

$$\frac{100 \text{ (Maximum output velocity)}}{\text{(Per cent input required to saturate the valve) (Maximum stroke from neutral)}}$$



APPENDIX II

Low Pressure Instability

One of the phenomenon observed during the testing of the power servo was the instability at low pressures. This phenomenon can be explained by the low pneumatic + structure + load resonance frequency at low pressures. At low pressures, the pneumatic spring rate is low.

$$\frac{1}{\omega_{PL}^2} = \frac{1}{\omega_{PL}^2} + \frac{V_1 M_E}{2k P_1 A^2}$$

Everything else being constant and P_1 variable, ω_{PL} can be expressed as

$$\frac{1}{\omega_{PL}^2} = K_1 + \frac{K_2}{P_1}$$

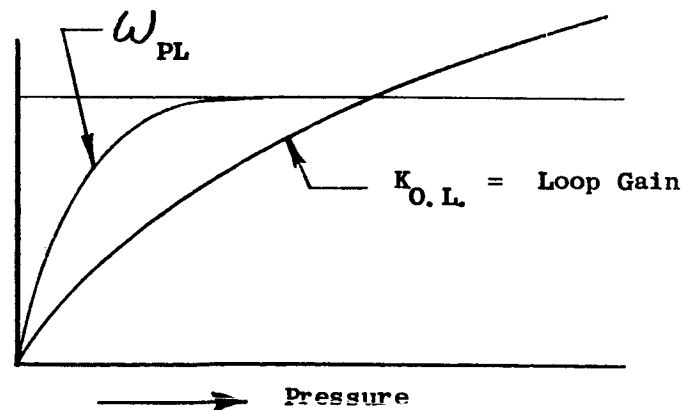
or

$$\omega_{PL} = \frac{P_1}{K_1 P_1 + K_2} = \frac{1}{K_1 + \frac{K_2}{P_1}}$$

In simplified terms, the loop gain is a function of the flow gain.

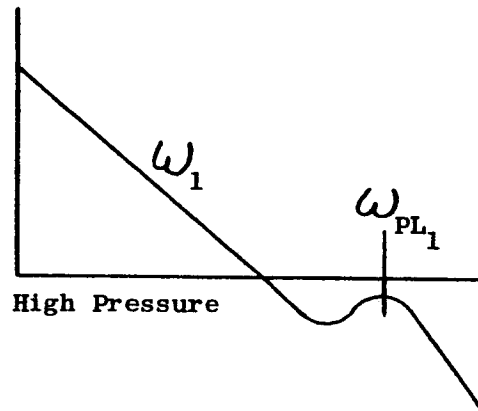
Approximating

$$Q = K_3 \sqrt{P}$$

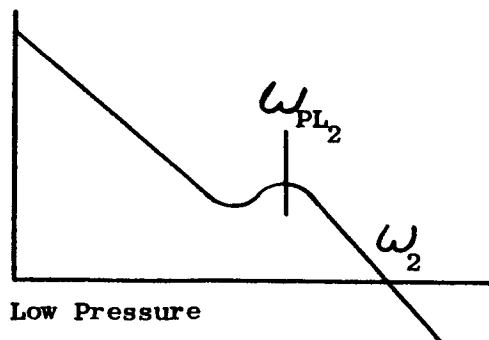


Around zero, the rate of change of ω_{PL} is more rapid than $K_{O.L.}$. Hence, if the system is designed for a certain pressure, at lower pressures $\Delta\omega_{PL}$ is far greater than $\Delta K_{O.L.}$ and instability occurs.

Frequency Response



Frequency Response



$$\omega_2 < \omega_1$$

$$\omega_{PL_2} < \omega_{PL_1}$$